Disruption of Chromosome Territories in Multiple Myeloma

by

Matheus Fabião de Lima

A Thesis submitted to the Faculty of Graduate Studies of
The University of Manitoba
in partial fulfilment of the requirements of the degree of

MASTER OF SCIENCE

Department of Physiology and Pathophysiology
University of Manitoba
Winnipeg

ABSTRACT

Background: Multiple Myeloma (MM) is an oligoclonal cancer of plasma cells. Currently, MM is an incurable disease. MM displays altered gene expression, chromosome aberrations and altered chromosome position, which contributes to high genomic instability of MM cells. Lamin A/C is a nuclear protein that plays a critical role in the maintenance of genomic stability and nuclear architecture. Recently, our group observed that expression of lamin A/C was upregulated in MM patient samples compared to normal B-lymphocytes. Therefore, our objective was to investigate the role of lamin A/C on genome organization in MM. **Methods and Results:** The expression of lamin A/C in MM cell line (RPMI-8226) was confirmed by western-blot (WB) and immunofluorescence analysis. Downregulation of lamin A/C was performed using two different small interfering RNAs (siRNA), for two different regions of lamin A/C mRNA, as well as scrambled siRNA (scrRNA), used as a control. siRNA reduced the levels of lamin A/C in ~80% in RPMI-8226 after 72-96 hours of transfection compared to scrRNA (both siRNAs). The impact of lamin A/C downregulation on chromosome territories (CT) and cell viability in MM was further analysed. The CT analysis revealed changes in CT 4,9,11,14,16,18, and 22. These chromosomes moved from the nuclear periphery to the nuclear center in RPMI 8226 after lamin A/C downregulation, compared to the scrRNA. Gene expression varies according to CT position. Analysis of siRNA lamin A/C treatment (RPMI-8226, 72 hours - quantitative PCR) shows upregulation of genes related to cell proliferation and cell survival. However, no changes in proliferation were observed. Analysis of chromatin changes using super resolution microscopy shows that downregulation of lamin A/C induces chromatin condensation (in 24 to 48 hours), followed by chromatin de-condensation (72 to 96 hours) in compared to scrRNA. **Summary and Conclusion:** Lamin A/C protein levels and their impact on MM cells is poorly understood. Lamin A/C plays a role in genome organization and chromosome positioning in MM. Its disruption alters chromosome positions and the

expression of genes involved in MM pathogenesis. This study addresses the role of nuclear architecture in MM and highlight new insights of targeting genome organization for cancer treatment.

Acknowledgements

I wish to express my sincere gratitude to my supervisor and co-supervisor Dr. Sabine Mai and Dr. Aline Rangel-Pozzo, for all support and guidance during this project. This work would not have been possible without mentorship and hard work.

I would also like to thank my laboratory members Monique Oliveira, Mohammad K. Hamedani, Darryl Dyck, Fabio Contu for all training and support in the lab. I would like to thank you my summer students Deesha Nayar and Tyler Lussier, with them I was able to develop teaching skills and get help in my bench experiments.

I wish to express my gratitude to Dr. Yvonne Myal, Dr. Barbara Nickel, and MSc Lucas Lima for your laboratory support.

I am also immensely grateful to my family and for their support and encouragement.

I would like to thank you Research Manitoba, Cancer Care Manitoba, and University of Manitoba and the Canada Research Chair (Tier 1) (S. Mai), for financial support during the execution of this project.

TABLE OF CONTENTS

LIST OF TABLES

LIST OF FIGURES

1. INTRODUCTION

1.1. Multiple Myeloma Epidemiology

According to the Global Cancer Statistics of 2020, Multiple Myeloma (MM) accounts for approximately 1% of all cancer diagnoses worldwide (Sung et al., 2021). A total of 176,000 new cases were observed in 2020, which 9,000 of cases being male and 77.000 being females (Sung et al., 2021). The mortality rate for the same period was 117,000, mostly occurring in males (Padala et el., 2021, Sung et al., 2021). Developed countries, such as Australia, Western Europe, and the USA display highest MM incidence rates, especially in African American population compared to other ethnicities (Padala et el., 2021). The average age of MM diagnosis is 70 years, characterizing it as a disease of older adults (Kaweme et al., 2021). In Canada, more than 4000 new diagnoses are expected for 2022, being the 3rd most frequent hematological cancer (Brenner et al., 2022). Furthermore, according to the Canadian Cancer Society, the incidence of MM still trends to increase overtime, especially with population aging. In 2022, more than 1600 lives are expected to be lost to MM, with mostly affected males (Brenner et al., 2022).

1.2. Multiple Myeloma Pathophysiology

Multiple Myeloma is an incurable oligoclonal cancer of plasma cells characterized by accumulation of aberrant plasma cells in bone marrow and production of an abnormal antibody called M protein (Hemminki et al., 2021, Sadaf et al., 2022). In most cases, MM produces IgG (52%) immunoglobulins, followed by IgA (21%), light-chain (16%) and in less than 5% of the cases produces IgD and IgM (Hemminki et al., 2021). Furthermore, some cases of oligo-secretion or non-secretion of M protein have also been reported (Kyle et al., 2003).

Multiple Myeloma is the latest stage of a progressive disease, preceded by two initial stages that are refereed as monoclonal gammopathy of unknown significance (MGUS) and

smoldering multiple myeloma (SMM) (Georgakopoulou et al., 2021). MGUS is characterized by the absence of symptoms and 10% of aberrant plasma cells inside bone marrow. The risk of progression from MGUS to MM is 1% per year and overall age of diagnosis is around 50 years (Kyle et a., 2018). SMM is defined by the absence of symptoms and the accumulation of 10-60% of plasma cells inside the bone marrow, with a risk of progression to MM of 10% per year (Schmidt et al., 2021, Sadaf et al., 2022). Finally, MM can be defined as accumulation of more than 10% of aberrant plasma cells inside bone marrow and presence of end organ damage (Hemminki et al., 2021).

Most frequently observed MM symptoms can be summarised by the acronym CRAB, represented by hypercalcemia, renal failure, anemia, and bone lesions (Nakaya et al., 2017). Altered balance of osteoblast and osteoclast activity mediated through secreted cytokines from MM cells causes severe bone lesions and osteoporosis (Reagan et al., 2015, Zagouri et al., 2017). Increased osteoclast activity has been shown to promote MM development through secretion of growth factors, which creates a growth loop between osteoclasts and MM cells (Reagan et al., 2015). Other than that, increased bone resorption resulted from osteoclast activity has shown to drive hypercalcemia, observed in 15% of newly diagnosed MM patients (Zagouri et al., 2017).

Renal failure is one of the most common symptoms observed in MM patients. It is present in almost 50% of new diagnoses (ACHIM et al., 2021). The underlying mechanism behind kidney injuries is complex and mostly chronic, but secretion of free light-chain by MM cells seems to play a major role in this process (Bridoux et al., 2021, Menè et al., 2022). Increased protein retention in nephrons cause accumulation of water and damage to epithelial cells (Liu et al., 2019). Physiological compensatory mechanism induces water reabsorption, often counteracted by high calcium concentration in blood (characteristic on MM patients), which leads to increase hydraulic pressure in nephrons, contributing to acute kidney injury

(Bridoux et al., 2021, Menè et al., 2022). Other mechanisms also take place due to massive accumulation of immunoglobulin free light-chains into glomerular tubules, contributing to chronic proteinuria (Bridoux et al., 2021).

Infiltration and proliferation of MM cells inside the bone marrow promotes impairment of erythropoiesis (production of red blood cells) and deregulation of iron metabolism, leading to MM associated anemia (Banaszkiewicz et al., 2019, Rassner et al., 2020). Release of cytokines by MM cells, decreased production of erythropoietin, and reduction in iron reabsorption, associated with kidney failure, seems to play a major role in this process (Maes et al., 2010, Banaszkiewicz et al., 2019, Rassner et al., 2020). Moreover, some chemotherapeutic agents have been shown to induce hemolysis, contributing to MM associated anemia (Rassner et al., 2020).

Beyond CRAB, MM patients present a variety of secondary symptoms mostly related to standard clinical manifestations of the disease. Most common involves neuropathy, amyloidosis, body pain, systemic infections, fatigue, and peripheral sensory loss, among others (Talamo et la., 2010, Lu et al., 2021, Dissanayaka et al., 2022, Khalyfa et al., 2022). This highlights a heterogeneous and complex disease phenotype that severely affect a patients' life quality.

1.3. Multiple Myeloma Genomic Landscape

MM has a complex genomic landscape characterized by the acquisition of several chromosomal abnormalities and somatic gene mutations. Most common genomic alterations involve chromosome aneuploidies (gain or loses of chromosomes or chromosome parts), chromosome translocations mostly comprising the immunoglobulin heavy-chain locus, placed on chromosome 14q32, and gene mutations that drive disease progression (Morgan et al., 2012, Corre et al., 2015, Manier et al., 2017). The etiology of MM genome instability is still

unknown, but several studies have been pointing to a role of clonal evolution that occurs from pre-malignant stages to MM and during MM (Landgren et al., 2009, Roschke et al., 2013, Manier et al., 2017). Chromothripsis (chromosome rearrangement often involving one or two chromosomes) and chromoplexy (complex structural rearrangement involving multiple chromosomes) events were thought to be drivers of genomic instability in MM cells (Kloosterman et al., 2014, Ashby et al., 2019). However, recent studies have shown the acquisition of consecutives chromosome abnormalities would lead to tumor adaptability and clonal heterogeneity that would carry the disease to final stages of development or could trigger patient remission after treatment (Roschke et al., 2013, Manier et al., 2017, Maura et al., 2019, Bustoros et al., 2020, Furukawa et al., 2020, Neuse et al., 2020).

1.4. Chromosomal Abnormalities and Somatic Gene Mutation

Structural chromosome abnormalities are thought to be early events in myelomagenesis, being present in pre-malignant stages of disease (Bolli et al., 2018). Chromosome translocations, mostly involving the immunoglobulin heavy-chain (IGH) locus, placed on chromosome 14, drives tumorigenesis by enhancing the expression of oncogenes (Maura et al., 2019) (Figure 2). The most frequent translocations associated with MM are t(4; 14), t(6; 14) t(11; 14), t(14; 16), and t(14; 20) (Bergsagel et al., 2001). The t(4; 14) triggers the expression of fibroblast growth factor receptor 3 (*FGFR3*) gene located on chromosome 4, present in 15% of MM patients, commonly associated with MM's poor prognosis and low response to chemotherapy (Keats et al., 2003, Brito et al., 2009, Chng et al., 2014, Barwick et al., 2019) (Figure 2). The t(6; 14) is rare, being present in 1% of MM patients and triggers the overexpression of the Cyclin D3 gene (*CCDN3*) (Barwick et al., 2019, Abdallah et al., 2020) (Figure 2). Patients carrying the t(6; 14) were classified as high-risk and less responsive to immunomodulatory drug-based treatment (Abdallah et al., 2020). The t(11; 14) is the most common, being present in almost 20% of MM patients and triggers the overexpression of the

Cyclin D1 gene (*CCDN1*) (Manier et al., 2017, Barwick et al., 2019). Investigations of patients carrying the t(11; 14) revealed better overall survival rate, compared to patients with other structural chromosomal alterations (Gertz et al., 2005, Stewart et al., 2007, An et al., 2013) (Figure 2). Translocation (14; 16) and t(14; 20) drive the overexpression of *c-MAF* and *MAFB* genes, respectively, being associated with poor patient outcome (Maura et al., 2019, Murase et al., 2019, Goldman-Mazur et al., 2020) (Figure 2). Furthermore, t(14; 16) was shown to induce MM resistance to proteasome inhibitor therapy (Qiang et al., 2016). Translocations involving the immunoglobulin light-chain locus (IGL), located on chromosome 21, are also present in MM, mostly rearranged with *MYC* gene (Walker et al., 2015, Barwick et al., 2019). *MYC* translocations have been observed in 14% of MM patients, commonly associated with a patient's poor prognosis (Walker et al., 2015, Barwick et al., 2019).

Besides structural chromosomal abnormalities, MM also display chromosome aneuploidies (gains or loses of whole chromosomes or chromosome parts) (Chretien et al., 2015). Whole chromosome trisomy often involving odd numbered chromosomes, such as 3, 5, 7, 9, 11, 15, 19, 21, have been reported in MM patients (Chng et al., 2006, Chretien et al., 2015, Aktas Samur et al., 2019) (Figure 2). Hyperploid MM is associated with good patient outcome when other chromosomal abnormalities are absent (Chng et al., 2006, Manier et al., 2017, Barwick et al., 2019). Additionally, deletion of 1p, del(12p), del(13p), del(13) whole chromosomes, del(16p), del(17p), and 1q gain have also been reported in MM patients harboring chromosome aneuploidies (Morgan et al., 2012, Maura et al., 2019) (Figure 2). Loss of tumor suppressor genes, through chromosome deletions is associated with MM progression and patient poor prognosis (Fonseca et al., 2001, Shaughnessy et al., 2005, Fonseca et al., 2009, Boyd et al., 2011, Manier et al., 2017).

In MM, somatic gene mutations often affect survival pathways, gene repair mechanisms, cell cycle pathways, and gene expression profile (Chapman et al., 2011, Lohr et

al., 2014, Bolli et al., 2018). Next generation sequencing (NGS) data of MM samples described several gene mutation across MM genome, even in pre-symptomatic stages (Bolli et al., 2018, Bolli et al., 2018, Samur et al., 2020, Furukawa et al., 2020, Yellapantula et al., 2020). However, somatic gene mutations were not described as drivers of MM progression from asymptomatic stages, occurring mostly in late stages of MM disease as a consequence of clonal evolution and tumor adaptability (Bolli et al., 2018, Samur et al., 2020, Furukawa et al., 2020, Maura et al., 2020).

1.5. Multiple Myeloma Clinical Treatment and Current Challenges

Discovery and introduction of new drugs changed MM treatment approach over time. Today, first line treatment options vary according to disease phenotype and secondary patient's characteristics, such as age and any presence of comorbidities (Palumbo et al., 2011, Moreau et al., 2015, Rajkumar et al., 2018, Kumar et al., 2019). Disease phenotype (presence of CRAB symptoms and M protein) is predominantly determining the choice of treatment, once presence of multiple end organ damage, and genomic abnormalities, can lead to adverse patient outcome and heterogeneous response to treatment (Chng et al., 2014, Lonial et al., 2015, Palumbo et al., 2015).

The treatment of MM often involves usage of different drugs with multiple targets and distinct mechanisms of action. The most common drug classes in use are proteasome inhibitors (PIs), corticosteroids, immune-modulatory drugs (IMIDs), monoclonal antibodies (mAbs), histone deacetylase inhibitors (iHDACs), nuclear export inhibitors and high-dose chemotherapy (HDC) associated with autologous stem cell transplantation (ASCT) (Cejalvo et al., 2017, Al Hamed et al., 2019, Rajkumar et al., 2019). The order and combination of drugs used before ASCT have been widely tested in clinical trials and the combination of PI (bortezomib), corticosteroid (dexamethasone), and IMID (thalidomide), has become the

standard procedure prior ASCT (Cavo et al., 2010, Moreau et al., 2011, Rosiñol et al., 2012) (Figure 3).

The use of PI in MM relies on inhibiting degradation of pro-apoptotic proteins, suppression of nuclear factor B (NFκB) pathway (decreasing degradation on IkBs) and increase expression of pro-apoptotic proteins of B-cell lymphoma 2 protein (Bcl-2) family (Richardson et al., 2003, Chen et al., 2011). Furthermore, use of Bortezomib has shown to stimulate osteoblast activity through alkaline phosphatase production and inhibit osteoclast-mediated bone degradation, thus preventing bone resorption (Zangari et al., 2006, Mohty et al., 2014). Moreover, PI have been used for treatment of newly diagnosed MM patients as well as in refractory/relapsed MM, when associated with other drugs (Kuhn et al., 2009, Campbell et al., 2015, Dimopoulos et al., 2016). However, acquisition of resistance mechanisms to PIs activity was reported in MM. Punctual gene mutations in proteasome subunits associated with overexpression of proteasome proteins and enhanced proteasome activity has been associated with resistance to PI in MM (Brünnert et al., 2019, Xie et al., 2020). Furthermore, epigenetic modulation through histone acetylation, MM clonal evolution as well as exosome-transfer mediated resistance by tumor microenvironment cells also plays a key role in MM resistance to PI (Xu et al., 2019, Xie et al., 2020) (Figure 3).

Immune-modulatory drugs such as Thalidomide, Lenalidomide, and Pomalidomide targets different pathways related to MM development. They inhibit the interaction of MM cells with stroma cells in bone marrow (BM), inhibit the secretion of several interleukin and growth factors, essential for MM cells growth, decreases of inflammatory responses, and increase in proliferation of T-cell lymphocytes as well as natural killers (Anderson et al., 2005, Kotla et al., 2009, Lagrue et al., 2015). Moreover, lenalidomide has shown anti-angiogenic activity, thus impairing formation of new vessels required for growth of primary and secondary tumors (Anderson et al., 2005, Kotla et al., 2009). Despite this, MM cells develop different

resistance mechanisms to IMIDs. Some studies have shown that MM cells acquire point mutations in the cereblon protein gene (main binding target of IMIDs), impairing IMIDs effects (Kortüm et al., 2016). Other studies have shown that overexpression of competitive binding proteins of cereblon have been associated with IMIDs resistance in MM (Zhu et al., 2014). Furthermore, the role of the tumor microenvironment driving MM clonal evolution has been also associated with IMIDs resistance (Suzuki et al., 2021) (Figure 3).

The use of monoclonal antibodies to treat MM has shown promising results in newly diagnosed MM patients, as monotherapy, and in relapsed/refractory MM, when combined with other drugs (Usmani et al., 2014, Lonial et al., 2015, Lonial et al., 2016, Orlowski et al., 2018). Monoclonal antibodies targeting CD38 or CS1 antigens on the surface of MM cells, such as Isatuximab, Daratumumab, and Elotuzumab, promote MM killing through immune-mediated complex mechanisms (Collins et al., 2013, Krejcik et al., 2016, van de Donk et al., 2016). Furthermore, the new explored B-cell maturation antigen (BCMA) associated with drug conjugates or chimeric antigen receptor modified T-cell therapy (CAR-T) showed remarkably anti-myeloma activity and minimal residual disease after treatment (Shah et al., 2020). However, heterogeneous expression of surface antigens has been associated to MM resistance to mAbs therapy (Nijhof et al., 2015, Nijhof et al., 2016). Furthermore, loss or decrease expression of the target antigens surfaces, and increase expression of CD55 and CD59 (self recognizing antigens for complement system) have been observed in refractory/relapsed MM (Nijhof et al., 2015, Nijhof et al., 2016, D'Agostino et al., 2020) (Figure 3).

Histone deacetylase inhibitors (iHDACs) have been recommended for the treatment of refractory/relapsed MM, usually associated with other drugs (Siegel et al., 2014, San-Miguel et al., 2014, Hansen et al., 2018). iHDACs promote expression of tumor-suppressor genes previously silenced by aberrant chromatin acetylation (Laubach et al., 2015). iHDACs also induce apoptosis through regulation of pro-apoptotic proteins and association with protein

recycling systems (Laubach et al., 2015, Yee et al., 2018). The mechanism of resistance to iHDACs in MM remains elusive, but up-regulation of survival pathways has been associated with resistant MM cell clones (Chüeh et al., 2017).

Even though introduction of new drugs and changes in therapeutical approaches have improved patient overall survival, MM remains an incurable disease. Challenges remain regarding discovery of new disease biomarkers, risk stratification algorithms, strategies to overcome disease resistance and improvements on disease diagnosis of pre-symptomatic forms of the disease.

1.6. High-order Genome Architecture in Human Cells

The human genome is hierarchically organized (Berezney et al., 2002, Chang et al., 2018, Soler-Vila et al., 2020). Such organization is necessary given the DNA length compared to nuclear size (Berezney et al., 2002, Zinchenko et al., 2018). First, nucleotides interact through hydrogen bounds to create the DNA helix structure (Yakovchuk et al., 2006). Such organization is a key element conferring DNA stability and folding (Yakovchuk et al., 2006, Privalov et al., 2018). The double strand DNA associated with histones and other proteins give rise to nucleosomes (Oudet et al., 1975). Small interactions between nucleosomes occur in order to build the 30nm chromatin fibers (Adkins et al., 2004). Chromosome scaffold proteins interacts with chromatin fibers to generate chromatin loops (Hansen et al., 2020). The loop-chromatin organization is essential for gene expression regulation as well as chromatin interaction (Schoenfelder et al., 2015, Sanborn et al., 2016, Yu et al., 2021). Chromatin segregation mediated by chromosome scaffold proteins give rise to chromatin domains (chromatin loops aggregates surrounded by interchromatin spaces) (Nozaki et al., 2017, Shaban et al., 2018). Organization of chromatin domains in specific areas of human nuclei represents

the highest level of genome organization, as entitle chromosome territories (CT) (Cremer et al., 2010, Kinney et al., 2018).

Chromosomes are non-randomly organized and occupy distinct areas in interphase nuclei (Tanabe et al., 2002, Bolzer et al., 2005, de Castro et al., 2022) (Figure 1). Some studies demonstrate that chromosomes would follow a size rule of distribution (big chromosomes would be located at nuclear periphery while small chromosomes would be located at nuclear center) (Sun et al., 2000, Tanabe et al., 2002, Bolzer et al., 2005) (Figure 1). Others have implied that gene density would determine chromosome position (gene-rich chromosomes would be located at nuclear center, while gene-poor chromosomes would be placed at nuclear periphery) (Mayer et al., 2005, Tanabe et al., 2005) (Figure 1). The chromosome position is a key element regulating gene expression (Mahy et al., 2002, Malyavantham et al., 2008, Han et al., 2020) (Figure 4). Highly transcribed genes are placed in nuclear center, where most of the transcriptional machinery is located, while late replicating genes are commonly found on nuclear borders, where transcriptional machinery is less concentrated (Mahy et al., 2002, Malyavantham et al., 2008). Furthermore, extraterritorial gene expression has been reported, where genes move outward their CT for transcription, returning to their CT position after replication (Williams et al., 2003, Wegel et al., 2005). Besides this, several studies have demonstrated that chromosome positions are cell type specific and may alter position according to differentiation cell status (Kuroda et al., 2004, Mayer et al., 2005, Wegel et al., 2005, Sehgal et al., 2016). Moreover, CT studies revealed a portion of chromosomes (Ch 13, 14, 15, 21, and 22) that associate with the nucleoli, to transcribe ribosomal proteins (van Sluis et al., 2020, Mangan et al., 2021) (Figure 1).

Figure 1 – Chromosome Territories organization rules.

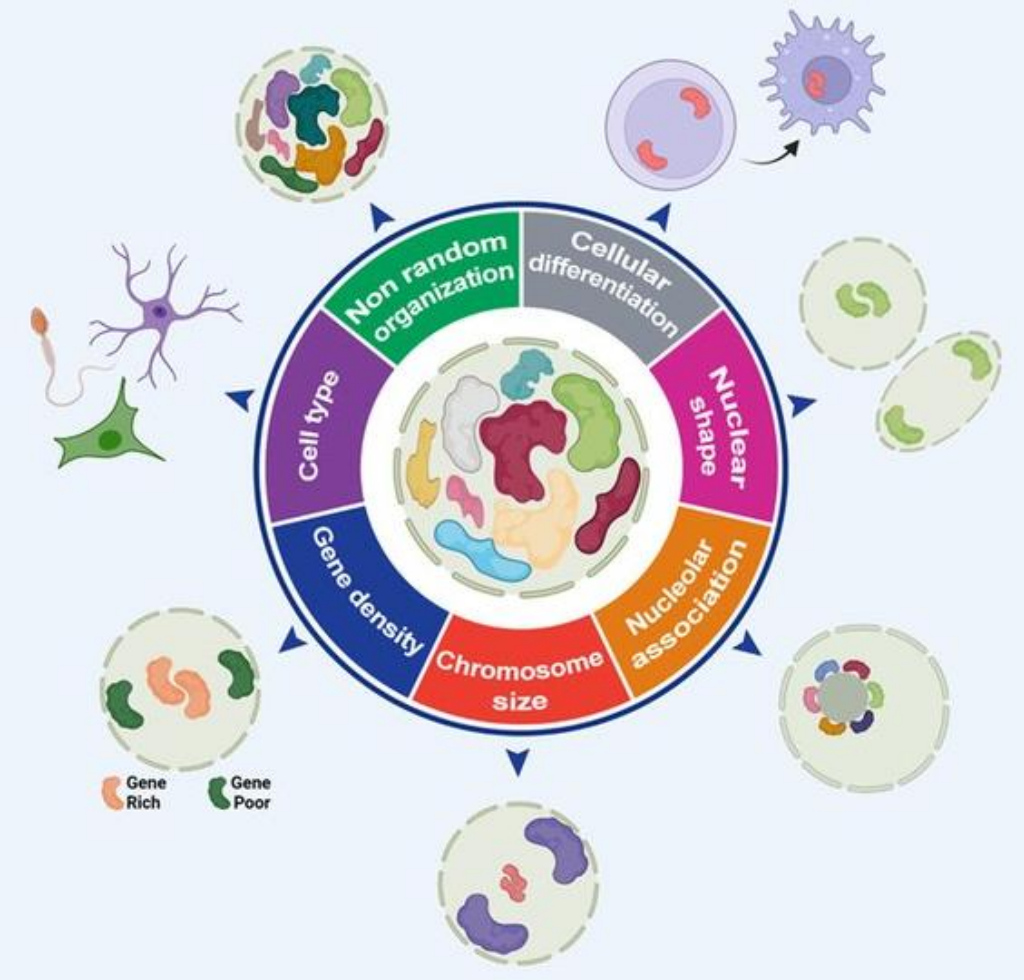

Figure 1. Chromosome territories etiology models and factors influencing chromosome organization. Image from Lima et al., 2022.

1.6.1. Chromosome Territories in Multiple Myeloma

In multiple myeloma chromosome territories are altered. Sathitruangsak et al. (2017) reported that position of chromosomes 4, 9, 11, 14, and 18 is more internal located compared to normal B-lymphocytes (Figure 2). The consequences of CT alteration in MM gene expression were not investigated, but studies using MM-derived patient samples revealed that several genes placed on those chromosomes were up regulated (Broyl et al., 2010, Chen et al., 2022). Furthermore, several studies have been associating chromosome position with the acquisition of MM translocations. Balajee et al. (2018) showed that frequency of chromosome

translocation in B-lymphocytes irradiated with X-ray and neutrons were dependent of chromosome proximity. Others have shown that chromosome proximity would facilitate intermingling of chromosome parts, thus facilitating translocation event to occur (Branco et al., 2006, Righolt et al., 2011). Moreover, chromatin analysis of MM samples using super-resolution microscopy revealed a less condensed open chromatin (Sathitruangsak et al., 2015) (Figure 2). Regulation of chromatin state in MM has been associated with changes on gene expression that may favor disease progression (Jin et al., 2018, Ordoñez et al., 2020). However, it is not clear if alteration of CTs drives myelomagenesis or if it is a consequence of tumorigenesis process. Furthermore, altered expression of nuclear proteins has been associated with aberrant chromatin organization, commonly correlated to cancer development (Prokocimer et al., 2006, Sunkara et al., 2018).

Figure 2 – Chromatin architecture in Multiple Myeloma.

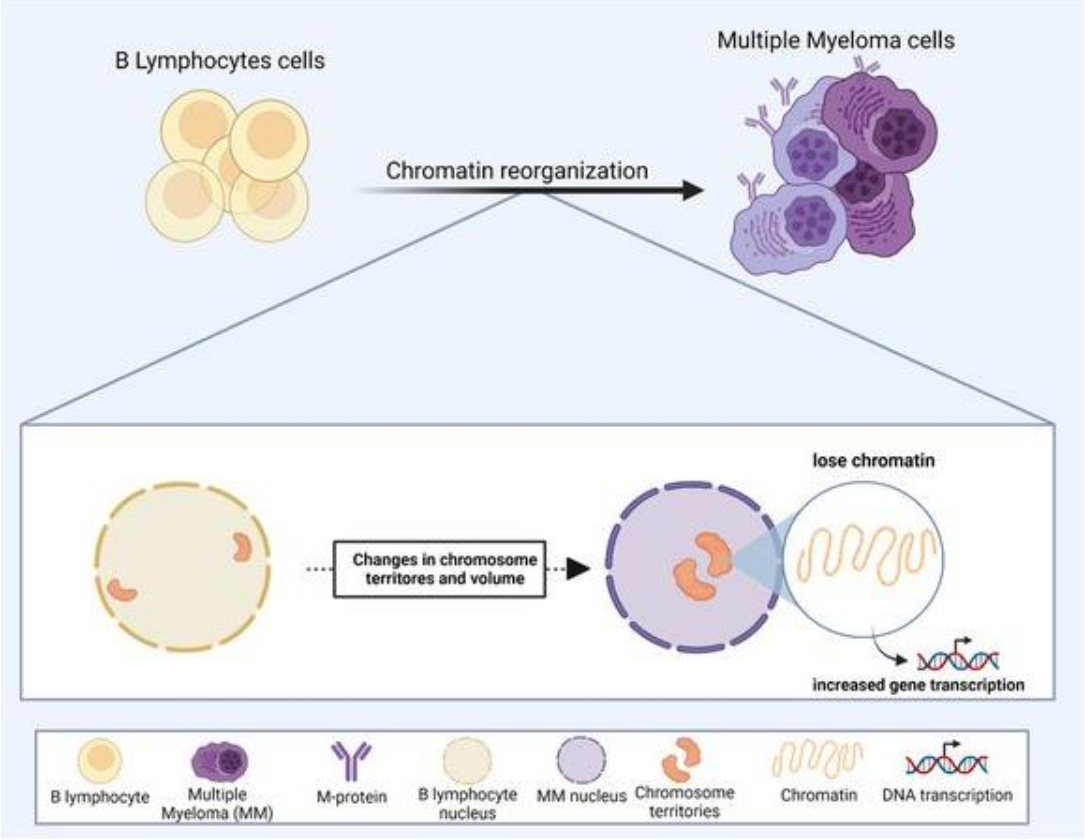

Figure 2. Altered chromatin organization in Multiple Myeloma. Changes of chromosome position and chromatin state seems to play a role in Multiple Myeloma development. Image from Lima et al., 2022.

1.7. Lamin A/C

1.7.1. Lamin A/C Role on Genome Organization, Gene Expression and Cancer

Lamin A/C is an intermediate filament protein type V (Dittmer et al., 2011). It is a product of human *LMNA* gene, which encodes for both Lamin A and Lamin C proteins (Dittmer et al., 2011). Alternative message RNA splicing at exon 10 leads to the expression of Lamin C (Dittmer et al., 2011, Al-Saaidi et al., 2015). Lamin A/C is commonly located at the inner nuclear lamina, and it also forms a nucleoplasm network, in association with other proteins (Dittmer et al., 2011, Naetar et al., 2017). Furthermore, lamin A/C has been involved in the regulation of different cellular processes, such as nuclear structural stability, cell motility, cell differentiation, mechanosensory responses, gene expression regulation, DNA damage repair mechanism, telomere protection and chromatin organization (Mewborn et al., 2010, Dittmer et al., 2011, Singh et al., 2013, Wood et al., 2014, Piekarowicz et al., 2017, Ranade et al., 2019, Srivastava et al., 2021). In addition, lamin A/C has emerged as a key protein regulating chromosome position, as its depletion leads to changes in chromosome territories (Ranade et al., 2019).

Lamin A/C provides attachment regions for the genome through direct interaction with chromatin or by association with other proteins (Wood et al., 2014, Naetar et al., 2017). Some studies demonstrate that lamin A/C is required for heterochromatin position at nuclear periphery, and in its absence, heterochromatin moved to nuclear center (Solovei et al., 2013). Furthermore, lamin A/C also interacts with nucleoplasm chromatin in genomic regions called lamina associated domains (LADs), mostly mediating gene expression regulation (Naetar et

al., 2017). In fact, nuclear investigations showed that around 60% of lamin A/C is found into the nucleoplasm, representing a high mobile and dynamic structure (Broers et al., 1999, Bronshtein et al., 2015). Mutations in both Lamin A and Lamin C gene causes inner nuclear lamina instability and disassemble of Lamin nucleoplasm (Broers et al., 2005). Additionally, it was demonstrated that lamin A/C binds to telomeric ends and telomeric interstitial sequences through association with telomere repeating binding factor 2 (TRF2), providing telomere protection and chromosome organization (Wood et al., 2014). Loss of functional lamin A/C has been associated to increased telomere mobility and altered chromatin dynamics (Bronshtein et al., 2009, De Vos et al., 2010, Bronshtein et al., 2015).

Lamin A/C is key for the maintenance of chromosome territories. Several studies have shown that absence of lamin A/C or point mutations in the *LMNA* gene causes chromosomes to intermingle. Bronshtein et al. (2015) showed, using live cell imaging-based methods, that depletion of lamin A/C increases chromatin mobility. Furthermore, mutations in the LMNA gene were associated with mispositioning of chromosome 13 and altered gene expression in heart-derived cells (Mewborn et al., 2010, Puckelwartz et al., 2011). In lamin A/C deficient cells, condensation of CT and repositioning of centromeric heterochromatin were observed (Galiová et al., 2008). Moreover, recent studies demonstrate that downregulation of lamin A/C and other nuclear proteins causes CT changes as well as gene repositioning in the nucleoplasm (Ranade et al., 2019).

Changes of chromatin position have been associated with altered gene expression. Chromatin replication events and transcriptional machinery are more concentrated at the nuclear center compared to nuclear periphery (Tanabe et al., 2002, Malyavantham et al., 2008, Malyavantham et al., 2008). In fact, attachment of genes to the nuclear lamina leads to gene transcription suppression while movements towards nuclear center showed to increase gene expression (Reddy et al., 2008, Peric-Hupkes et al., 2010, Shevelyov et al., 2018, Shevelyov et

al., 2019). Besides high-order chromatin regulation of gene expression, lamin A/C also interacts with gene promoter regions and transcription factors regulating both gene expression and gene repression (Lund et al., 2013, Ikegami et al., 2020). Furthermore, lamin A/C also associates with histone proteins, thus promoting indirect gene expression regulation (Lund et al., 2013, Dittmer et al., 2011, Osmanagic-Myers et al., 2015). Moreover, loss of lamin A/C has shown to affect gene expression even outside of LADs (Lund et al., 2013).

1.7.2. *Lamin A/C in Cancer*

Reports of lamin A/C in cancer are controversial and have described both its enhanced and decreased expression (Foster et al., 2010, Wang et al., 2015, Sakthivel et al., 2016). Studies in hematological malignancies such as leukemia and lymphomas have shown downregulation of lamin A/C through hypermethylation of *LNMA* promoter (Foster et al., 2011, Redwood et al., 2011). Furthermore, demethylation agents have shown to revert lamin A/C downregulation in neuroblastoma cells (Rauschert et al., 2017). On the other hand, overexpression of lamin A/C in breast cancer cell lines were associated with increased circulating tumor cells (CTCs) in the bloodstream through a mechanism of sheer-stress resistance (Mitchell et al., 2015). Lamin A/C downregulation has been implicated in decreased CTCs number in bloodstream (Mitchell et al., 2015). Furthermore, an increase in lamin A/C expression was associated with the attachment of CTCs to epithelial cells, facilitating the metastatic process and the formation of new tumor sites (Zhang et al., 2017). In prostate cancer, lamin A/C overexpression was associated to enhanced cell growth, migration, and cancer invasiveness, thus promoting an aggressive phenotype in prostate cancer cells (Kong et al., 2012).

Overall, there is no expression pattern of lamin A/C when it comes to cancer cells as many studies reported. However, heterogeneous expression of lamin A/C has been correlated to cancer aggressiveness, mostly varying according to cancer type (Dubik and Mai, 2020).

Therefore, some authors have proposed lamin A/C as a cancer biomarker or prognostic factor as its modulation is related to the tumorigenesis process and to cancer progression (Dubik and Mai, 2020).

2. RATIONALE

Lamin A/C expression varies depending on the cancer types. It is thought to promote cancer aggressiveness and contribute to cancer progression. In our preliminary data, we observed that lamin A/C was overexpressed in a multiple myeloma cell line and in myeloma cells of 10 primary treatment-naïve myeloma patients, compared to normal B-lymphocytes. Therefore, I examined if the disruption of lamin A/C in the MM cell line RPMI 8226 by siRNA, shRNA, or CRISPR/Cas 9 will lead to disruption of chromosome territories, and, as a result, impair cell division in myeloma cells. This work represents a new approach in the field of genomic instability, nuclear genome architecture and in translational research into multiple myeloma.

3. HYPOTHESIS

Lamin A/C is required for the maintenance of the chromosome territories in multiple myeloma. In its absence, chromosomes will intermingle and recombine as they are no longer able to maintain their regular positions in their territories and this will prevent proper cell division.

4. OBJECTIVES

Aim 1. Disruption of lamin A/C to identify the role of lamin A/C on genome organization and chromosome territories in myeloma cells

Aim 2. Analysis if lamin A/C downregulation will affect cell viability and gene expression in MM cells.

5. MATERIAL AND METHODS

5.1. Cell lines

MM cell lines, RPMI 8226 (CRM-CCL-155™) and MM.1R (CRL-2975™), were obtained from ATCC®. The cell lines were maintained using Gibco™ RPMI 1640 medium (ATCC modified – 2 mM L-glutamine, 10 mM HEPES, 1 mM sodium pyruvate, 4500 mg/L glucose, and 1500 mg/L sodium bicarbonate,) supplemented with 10% Fetal Bovine Serum (FBS) and 1% Penicillin-Streptomycin (reagents from Gibco, Burlington, ON, Canada). The cells were cultured in Nunc™ EasYFlask™ 75cm^2 (Thermo Scientific, Roskilde, Denmark), kept at standard conditions of CO2 (5%) and temperature (37°C) and sub-cultured every 48-72 hours, according to their specific doubling time.

5.2. Protein Extraction and Quantification – Lamin A/C expression in MM cell lines

RPMI 8226 and MM.1R were cultivated in 75cm^2 flasks util 80% confluency could be observed using inverted light microscopy. MM.1R was harvested using cell scrapers (Thermo Scientific™, NY, USA) followed by centrifugation at 1200 rpm for 5 minutes. RPMI 8226 were harvested using 10 ml serological pipets (Thermo Scientific™, NY, USA) followed by centrifugation at 1200 rpm for 5 minutes. After centrifugation, the supernatant was removed, using serological 10 ml pipets, and the cells were washed once using cold 1X Phosphate Buffered Saline (PBS), pH 7.4, followed by centrifugation at 1200 rpm for 5 minutes. Then, the supernatant was removed, using serological 10 ml pipets, followed by addition of 50-200 µl of cold RIPA buffer (with addition of Pierce Protease Inhibitor Tablets and Phosphatase Inhibitor Cocktail) (Thermo Scientific™, NY, USA). RIPA volume was determined according to the cell pellet size. The cells were incubated in ice for 15 minutes followed by sonication for 10 seconds. The cells were then centrifugated at 13.000 rpms for 6 minutes at 4°C. The

supernatant was collected and transferred to a new tube. The proteins were storage at -20°C until further analysis.

In this study, all proteins were quantified using the Pierce™ BCA Protein Assay Kit (Pierce Biotechnology, Rockford, IL, USA) according to manufacturer's instructions.

5.3. Western Blot Analysis

The proteins were mixed with 2X Laemmli Sample Buffer (65.8 mM Tris-HCl, pH 6.8, 2.1% SDS, 26.3% (w/v) glycerol, 0.01% bromophenol blue and 0.05% (v/v) of β-mercaptoethanol) in a 1:1 ratio (v/v), followed by heating at 80°C for 5 minutes. Proteins were loaded (30µg) in polyacrylamide gels (5% acrylamide/bis-acrylamide for stacking gel and 10% acrylamide/bis-acrylamide for resolving gel) and allowed to run for 30 minutes at 55V followed by 60 minutes at 110V. The proteins were transferred to nitrocellulose membranes (0.45µm) (Bio-Rad Laboratories, Mississauga, ON, Canada) using Pierce™ 1-Step Transfer Buffer and the Pierce Power Blot Cassette (Thermo Scientific, NY, USA) for 7 minutes at 25V. After transfer step, the membranes were blocked in 5% Blotting Grade Blocker Non-Fat Dry Milk (Bio-Rad Laboratories, Mississauga, ON, Canada) in Tris-buffered saline with 0.1% Tween-20 (TBS-T) for 1 hr. All antibodies were diluted in block solution (5% milk in TBS-T). The membranes were incubated with rabbit anti-human Lamin A antibody (1:1000, Abcam® Plc, MA, USA) and mouse anti-human α-tubulin (1:5000, Abcam® Plc, MA, USA) on a shaker, overnight at 4°C. After incubation with primary antibody, the membranes were washed three times in 1X TBS-T for 10 minutes, room temperature (RT), shaking. After washing, the membranes were incubated with secondary antibodies goat anti-rabbit (1:5000, Abcam® Plc, MA, USA) and goat anti-mouse (1:5000, Abcam® Plc, MA, USA) for 1 hour, at RT, shaking. The membranes were washed three times in 1X TBS-T for 10 minutes, followed by incubation with enhanced chemiluminescence (ECL) solution (Immobilon, Millipore, MA, USA),

according to manufacturer's instructions. Protein signals was acquired using the C-digit blot scanner (Licor, NE, USA). The western analyses were performed using the pixel densitometry obtained using software ImageJ (NIH, ImageJ 1.49v, Madison, WI, USA) of target bands (lamin A/C) and its respective constitutive bands (α-tubulin). The protein of interest was normalized to its the respective constitutive protein (α-tubulin). All WB assays were done in triplicate.

5.4. Lamin A/C downregulation using siRNA

Transient downregulation of lamin A/C was performed using siRNA lamin A/C (Target Sequence: GGUGGUGACGAUCUGGGCU), while scrambled RNA (scrRNA) (Target Sequence: UAGCGACUAAACACAUCAA) was used as a negative control for the silencing. The cell (RPMI 8226 – $1x10^6$) underwent electroporation with 2µM of siRNA lamin A/C as well as 2µM of scrRNA, using Nucleofector® 2b Device (Lonza Canada Inc, QC, Canada), according to the manufacture's instructions. After electroporation, the cells were transferred to 6-well plates (Nunc™ Cell-Culture Treated Multidishes, Thermo Scientific, NY, USA), cultured for 0 to 96 hours, under standard conditions of CO2 (5%) and temperature (37°C). In order to analyse lamin A/C downregulation kinetics, cells were harvested every 24 hours until 96 hours, for protein extraction, quantification and western blot analysis as previously described. These experiments were performed in triplicate.

5.5. Trypan Blue exclusion Assay

Trypan blue exclusion assay was performed in RPMI 8226 to analyse the impact of lamin A/C downregulation to cell viability. The cells ($1x10^6$) underwent electroporation with 2µM of siRNA lamin A/C and 2µM of scrRNA, as previously described here. After electroporation, cells were transferred to 6-well plates (Nunc™ Cell-Culture Treated Multidishes, Thermo Scientific, NY, USA) and maintained under standard conditions of CO2

(5%) and temperature (37°C). After 24 hours the cells were homogenized, 10µl was collected and mixed with trypan blue solution 0.4% (Thermo Scientific, NY, USA) in a 1:1 ration, followed by cell counting using hemocytometer.

5.6. MTT assay

MTT assay was used to analyse the impacts of lamin A/C downregulation on cell proliferation, in RPMI 8226. The cells ($1x10^6$) underwent electroporation with 2µM of siRNA lamin A/C and 2µM of scrRNA, as previously described above. After electroporation, the cells were seeded in 96-well plates (Thermo Scientific, NY, USA) at $5x10^4$ cells per well and cell proliferation was analysed through metabolism of 3-(4,5-dimethylthiazol-2-yl)-2,5-diphenyltetrazolium bromide (MTT) to its insoluble form of formazan crystals. Every 24 hours MTT solution (5mg/ml of MTT in ddH_2O) was added to the wells to a final concentration of 0.5mg/ml, followed by incubation at 37°C, for 4 hours. After incubation, the cells were centrifuged at 1600 rpm for 5 minutes, followed by media removal, using multichannel pipets (Eppendorf, Mississauga, ON, Canada). Formazan crystals were solubilized using 200µl of Dimethyl sulfoxide (DMSO) (Millipore Sigma, Merck, MA USA) per well, and absorbance were acquired using Spectra max 190 (Molecular devices, CA, USA) at 570nm wavelength. All MTT assays were done in triplicate. 96-well plate background absorbance were subtracted by specific sample optical densitometry.

5.7. Immunostaining of Lamin A/C

RPMI 8226 ($1x10^6$ cells) underwent electroporation with 2µM of siRNA lamin A/C as well as 2µM of scrRNA, as previously described here. After electroporation the cells were seeded in 6-well plates (Nunc™ Cell-Culture Treated Multidishes, Thermo Scientific, NY, USA) and incubated at standard conditions of CO2 (5%) and temperature (37°C). After 96 hours the cells were harvested and centrifuged at 800 rpm for 10 minutes. The supernatant was

removed, and cells were washed once with 1X PBS (37°C), followed by centrifugation at 800 rpm for 10 minutes. The supernatant was removed, followed by addition of 200 µl of 1X PBS (37°C) to concentrate the cells. The cells were seeded in pre-coated (10% of poly-L-lysin - Millipore Sigma, Merck, MA USA) glass slides (Orsatec, BY, Germany) and fixed in 3.7%formaldehyde / 1xPBS for 10 minutes (RT). The slides were washed three times in 1X PBS (RT) for 5 minutes, shaking, followed by incubation with 0.1% Triton X-100, for 12 minutes (Millipore Sigma, Merck, MA USA). The slides were washed three times in 1X PBS (RT) for 5 minutes, shaking, followed by incubation with blocking solution (4% bovine serum albumin (BSA) (Millipore Sigma, Merck, MA USA) in 4X saline-sodium citrate (SSC) buffer) for 1 hour at 37°C in humidified atmosphere. After 1 hour, the slides were incubated with primary antibody (rabbit anti-human Lamin A 1:100, Abcam® Plc, MA, USA) diluted in block solution, overnight at 37°C in humidified atmosphere. After primary antibody incubation, the slides were washed three times with 1X PBS (RT) for 5 minutes, shaking, followed by incubation with secondary antibody (1:500 goat anti-rabbit conjugated with Cy5 fluorophore, Thermo Scientific, NY, USA) diluted in blocking solution, for 1 hour at 37°C, in humidified atmosphere. After secondary antibody incubation, the slides were washed three times with 1X PBS (RT) for 5 minutes, shaking, followed by incubation with 0.1µg/ml of 4′,6-diamidino-2-phenylindole – DAPI, for 5 minutes at RT. The DAPI excess was removed by washing slides once with 1X PBS (RT) for 1 minute, shaking. The slides were mounted using Glycerol-based mounting medium Vectashield (Vector Laboratories Inc, Burlingame, CA, USA) to prevent photobleaching of the fluorophore.

5.8. λ light-chain quantification

RPMI 8226 underwent electroporation with siRNA and scrRNA as previously described here. The cells were maintained in 6-well plates until 96 hours at regular conditions of CO2 (5%) and temperature (37°C). Every 24 hours the media was collected and storage at -

20°C. After collection of all time points, proteins were quantified as previously described here and media underwent western blot analysis (100 µg of protein) using goat anti-human (IgG, IgM, IgA) polyclonal antibody (1:2000, Abcam® Plc, MA, USA) followed by rabbit anti-goat (1:5000, Thermo Scientific, NY, USA). λ light-chain protein was normalized by total protein signals obtained using Ponceau S (0.01% in 1% acetic acid) staining (Millipore Sigma, Merck, MA USA). These experiments were performed in triplicate.

5.9. Gene expression – qPCR

5.9.1. RNA extraction and quantification

RPMI 8226 underwent electroporation with siRNA lamin A/C and scrRNA, as previously described here. The cells were maintained in 6-well plates at regular conditions of CO2 (5%) and temperature (37°C). After 72 hours, the cells were harvested for RNA extraction using RNeasy Kit (Qiagen, ON, CA) according to manufacturer's instructions. After extraction, RNA integrity was analysed by electrophoreses in 1% agarose gel, in 1X TAE (Tris-base, acetic acid, Ethylenediaminetetraacetic acid – EDTA). RNA was quantified using spectrophotometer NanoDrop™ 1000 (Thermo Scientific, NY, USA).

5.9.2. cDNA synthesis and qPCR

Complementary DNA (cDNA) was produced by reverse transcriptase reaction, using AMV LongAmp® Taq RT-PCR Kit (New England Biolabs Inc., MA, USA), according to manufacture's instructions. Quantitative polymerase-chain reaction (qPCR) was performed using the LunaScript® Multiplex One-Step RT-PCR Kit (New England Biolabs Inc., MA, USA), according to manufacture's instructions. qPCR data was expressed as fold change product ($2^{-\Delta\Delta CT}$). Human Hemoglobin subunit beta (*HBB*) gene was used for Ct normalization. Primers used for qPCR are listed bellow (Table 1).

Table 1. Primer List

Gene Name	*Sequence (5'->3')*
FGFR3 (F)	CAGGCATCCTCAGCTACGGG
FGFR3 (R)	GCGTTGGACTCCAGGGACA
RHOH (F)	CTGAAGCCGTGGAGAACGCT
RHOH (R)	TTCTCCCTGCCCATCCAAGC
PAX5 (F)	CACTCCCGGATGTAGTCCGC
PAX5 (R)	ACCCCAGGCTTGATGCTTCC
CCND1 (F)	TGCCAACCTCCTCAACGACC
CCND1 (R)	GTAGTTCATGGCCAGCGGGA
MAF (F)	GCTTCCGAGAAAACGGCTCG
MAF (R)	AGCTGGAATCGCGTGTCAGA
BCMA (F)	TGTAATGCAAGATCAGGTCTCCTGG
BCMA (R)	ACTCGAGGCCTCTCGGAAGA
MALT1 (F)	GGAAGAACAGATGAGGCAGTGGA
MALT1 (R)	CGCCAAAGGCTGGTCAGTTG
BCL2 (F)	GAGTTCGGTGGGGTCATGTGT
BCL2 (R)	AGCCCAGACTCACATCACCAAG
BCL3 (F)	AGCAGCCTCAAGAACTGCCA
BCL3 (R)	GGATGTCGATGACCCTGCGG
HBB (F)	CGGCGGCGGGCGGCGCGGGCTGGGCGGCTTCATCCACGTTCACCTTG
HBB (R)	GCCCGGCCCGCCGCGCCCGTCCCGCCGGAGGAGAAGTCTGCCGTT

5.10. Fluorescence in situ hybridization - FISH in Metaphase chromosomes (Validation)

In order to attest the specificity of the whole chromosome painting probe, fluorescence in situ hybridization was used in chromosome metaphase spreads of MM.1R.

5.10.1. Metaphase preparation

MM.1R cell line was cultivated in 75cm^2 flasks, at standard conditions of CO2 (5%) and temperature (37°C) until 70% confluence could be observed, using inverted light microscopy. The cells were incubated with nocodazole 1µg/ml (Millipore Sigma, Merck, MA USA) for 4 hours, at 37°C, to induce cell cycle arrest. The cells were harvested using 0.25% Trypsin/ 0.02% EDTA (Ethylenediaminetetraacetic acid) (Thermo Scientific, NY, USA) followed by centrifugation at 800 rpm for 10 minutes. After centrifugation, supernatant was discarded, and cells were washed once using 1X PBS (37°C) followed by centrifugation at 800

rpm for 10 minutes. After washing, supernatant was discarded and 0.75M of fresh prepared potassium chloride - KCL (37°C) was added. The cells were incubated in water bath (37°C) for 40 minutes, with cell mixing every 5 minutes using Pasteur pipes (Millipore Sigma, Merck, MA USA). After KCL incubation, cells were fixed using 3:1 methanol/ acetic acid solution (Millipore Sigma, Merck, MA USA) followed by centrifugation at 800 rpm for 10 minutes. Supernatant was discarded and cells were washed using in 3:1 methanol/ acetic acid solution, followed by centrifugation at 800 rpm for 10 minutes. This process was repeated three times. After washing, metaphases were stored in 3:1 methanol/ acetic acid solution at -20°C until further experiments. All metaphases preparation were done in triplicate.

5.10.2. Fluorescence in situ hybridization – FISH in Metaphase chromosomes

Fluorescence *in situ* hybridization of metaphase chromosomes was used to validate the specificity of whole chromosome painting probes (ASI, CA, USA). MM.1R metaphases were prepared as previously described here. Metaphase chromosomes were placed onto glass slides by air dropping (Orsatec, BY, Germany) followed by washing in 2X SSC, for 10 minutes, at RT, shaking. After washing slides were incubated with RNAase A (100µg/ml in 2X SSC) (Millipore Sigma, Merck, MA USA) for 1 hour, at 37°C followed by washing three times in 2X SSC, for 5 minutes, at RT, shaking. Then, slides were incubated with pepsin (50µg/ml in freshly prepared 0.01M hydrogen chloride – HCL) for 1 hour, at 37°C, followed by washing two times in 1X PBS and once with 1xPBS/50mM magnesium chloride ($MgCl_2$), for 5 minutes, at RT, shaking. Next, cells were fixed using 1% formaldehyde (Millipore Sigma, Merck, MA USA) in 1xPBS+50mM $MgCl_2$, for 10 minutes at RT, followed by washing once in 1X PBS, at RT, shaking. Then, slides underwent dehydration using ethanol 70%, 90% and 100%, consecutively, for 3 minutes each, at RT. The slides were prewarmed at 70°C for 5 minutes, followed by denaturation in 70% formamide/2X SSC, pH 7.0 (Millipore Sigma, Merck, MA USA) for 2 minutes at 70°C. Immediately after, slides underwent dehydration using ice cold

ethanol (-20°C) 70%, 90% and 100%, consecutively, for 3 minutes each. Human whole chromosome painting probes (chromosomes 4, 9, 11, 14, 16, 18, 19, 22) underwent denaturation for 7 minutes, at 80°C, followed by incubation in water bath at 37°C for 30 minutes. After denaturation, the probes were placed over dehydrated slides and incubated at 37°C, overnight. Next day, the slides were washed three times in 50% formamide in 2X SSC at 45°C, for 5 minutes, shaking, followed by washing two times in 4X SSC/0.1% Tween 20 (Millipore Sigma, Merck, MA USA) at 45°C, shaking and once in 2X SSC at 45°C, for 5 minutes. The DNA was counterstained with DAPI 0.1µg/mL, for 5 minutes followed by slide mounting using Vectashield (Vector Laboratories Inc, Burlingame, CA, USA). Whole chromosome painting probes validation is shown in supplementary figure1.

5.10.3. 3D Fluorescence in situ hybridization – 3D-FISH in interphase cells

Chromosome territories of health patient derived lymphocytes, MM.1R, and RPMI 8226 with lamin A/C downregulation using siRNA were investigated using fluorescence *in situ* hybridization in interphase cells. RPMI 8226 underwent electroporation with siRNA and scrRNA as previously described here. The cells were maintained in 6-well plates for 96 hours until harvesting. MM.1R were maintained in 75cm^2 flasks, at standard conditions of CO2 (5%) and temperature (37°C) until harvesting using trypsin 0.25%. After harvesting the cell lines (MM.1R, RPMI 8226 siRNA and scrRNA) were washed in 1X PBS (37°C) and seeded at pre-coated (10% poly-L-lysin) glass slides.

Lymphocytes from healthy donors were obtained from blood and diluted with PBS (3.5:1) and layered on top of Ficoll (GE Healthcare Life Sciences, Baie d'Urfe, Quebec) with a ratio of 1.5:1. The obtained buffy coat was collected and washed twice in a PBS solution. The cells were then placed onto Poly-L-lysine coated slides before being fixed in a 3.7% formaldehyde solution for 10 minutes. The slides were then dehydrated with increasing ethanol

(EtOH) concentrations of 70%, 90% and 100%. Dehydrated slides were then stored at -20 ◦C. Rehydration of the slides in decreasing EtOH concentrations was performed before starting with the protocol to maintain the cell 3D structure. This study was approved by the Research Ethics Review Board on Human Studies of the University of Manitoba (Ethics Reference No. H2010:170).

The slides were fixed in 3.7% formaldehyde/1X PBS for 10 minutes, at RT, followed by washing three times in 1X PBS for 5 minutes, at RT, shaking. The cells were permeabilized using 0.5% Triton X-100 (Millipore Sigma, Merck, MA USA) in 1X PBS, for 12 minutes, at RT, followed by washing three times in 1X PBS, at RT, shaking. 20% glycerol (Millipore Sigma, Merck, MA USA) in 1X PBS was used, at RT, for 40 minutes, to maintain the 3D cell architecture. After incubation, the slides were freeze using liquid nitrogen, thaw at RT and dived in 20% glycerol in 1X PBS, this process were repeated four times. After freeze and thaw cycles, the slides were washed three times in 1X PBS at RT, for 5 minutes each, shaking, followed by incubation with 0.1M of hydrogen chloride – HCL (Millipore Sigma, Merck, MA USA) for 5 minutes, at RT. The slides were washed twice in 1X PBS at RT, for 5 minutes, shaking, followed by incubation with 70% formamide/2X SSC (pH 7.0) for 1 hour, at RT. Whole chromosome painting probes were prepared in pares (Chromosomes 4, 9, 11, 14, 16, 18, 19, 22) and applied to the slides after formamide incubation. The slides were heated at 80°C for 5 minutes followed by incubation in 37°C, overnight, in humidified atmosphere. On the day after, slides were washed three times in 50% formamide in 2X SSC at 45°C, for 5 minutes, shaking, followed by washing two times in 4X SSC/0.1% Tween 20 (Millipore Sigma, Merck, MA USA) at 45°C, shaking and once in 2X SSC at 45°C, for 5 minutes. The DNA was counterstained with DAPI 0.1µg/mL, for 5 minutes followed by slide mounting using Vectashield (Vector Laboratories Inc, Burlingame, CA, USA).

5.11. Chromatin Analysis using 3D structural Illumination microscopy – SIM

RPMI 8226 underwent electroporation with siRNA and scrRNA for lamin A/C as previously described here. The cells were maintained from 24 to 96 hours in 6-well plates at regular conditions of CO2 (5%) and temperature (37°C). Cells were harvested every 24 hours, washed once with 1X PBS (37°C), placed in glass slides and fixed in 3.7% formaldehyde/1X PBS, for 10 minutes, followed by three washes of 5 minutes in 1X PBS, at RT, shaking. Chromatin were counterstained with DAPI (10µg/ml) overnight, at 37°C in a humidified atmosphere. The slides were mounted using Vectashield. Three independent experiments were performed and total of 60 individual cells were analysed per time point.

5.12. 2D and 3D Image Acquisition

5.12.1. 2D Image Acquisition

Manual 2D imaging was performed in MM.1R chromosome metaphases, RPMI 8226 under lamin A/C downregulation using siRNA (96 hours), and RPMI 8226 scrRNA (96 hours). The chromosome metaphases images were taken using ZEISS Axio Imager.Z2 (Carl Zeiss, Toronto, ON, Canada) with a cooled AxioCam HR B&W, FITC, Cy3 and DAPI filters in combination with a Planapo 63x/1.4 oil objective lens (Carl Zeiss, Toronto, ON, Canada). Images were obtained using AxioVision 4.8 (Carl Zeiss, Toronto, ON, Canada). 20 images of MM.1R chromosome metaphases were acquired for each chromosome combination, in each experiment, totalizing 3 independent experiments. Images of RPMI 8226 (lamin A/C (Cy5) siRNA, 96 hours) were taken using ZEISS Axio Imager.Z1 (Carl Zeiss, Toronto, ON, Canada) with a cooled AxioCam HRm camera in combination with a Planapo 63x/1.4 oil objective lens (Carl Zeiss, Toronto, ON, Canada). Images were obtained using ZEN 2.3 blue version software (Carl Zeiss, Toronto, ON, Canada). Cells displaying week lamin A/C signals were selected

(using crop region of interest tool, on ZEN blue version software) for chromosome territories analysis.

5.12.2. 3D Image acquisition

Manual 3D imaging was performed in human derived lymphocytes, MM.1R, RPMI 8226 with lamin A/C downregulation using siRNA (96 hours), and in RPMI 8226 scrRNA. The images were taken using ZEISS Axio Imager.Z2 with a cooled AxioCam HR B&W, FITC, Cy3 and DAPI filters in combination with a Planapo 63x/1.4 oil objective lens. 60 z-stacks at 200nm step-size were imaged for every fluorophore of every cell. Images were obtained using AxioVision 4.8, deconvolved using the constrained iterative restoration algorithm (Schaefer, and Herz, 2001) with Theoretical PSF and Clip Normalization.

3D structured illumination microscopy (SIM) imaging was performed with RPMI 8226 with lamin A/C downregulation, using siRNA (from 24 to 96 hours), and with RPMI 8226 scrRNA (from 24 to 96 hours) using Zeiss PS.1 ELYRA microscopy system equipped with 63x 1.4 NA objective lens and IXon 885 EMCCD Camera (Andor, Oxford, UK). Images were acquired using 1.518 refractive index (RI) immersion oil and DAPI were exited using a 405 nm laser. The number of image z-stacks was adjusted based on the size of every cell. After acquisition, image reconstruction was performed using ZEN 2012 black edition software (Carl Zeiss, Jena, Germany) with Noise filter set to −3.0 and deactivation of the Baseline Cut option.

5.13. Chromosome territories analysis

Single-cell analysis were performed in patient derived lymphocytes, MM.1R, RPMI 8226 siRNA lamin A/C and scrRNA using the software Chromoview® (Harizanova, Jana, Taylor-Kashton, and Mai, 2008, Martin et al., 2013) in DIPimage toolbox of Matlab (version R2012a, MathWorks, Natick, MA, USA). The relative radial position of chromosome territories was determined by measuring the distance between the mass center of each

chromosome to the center of the nucleus divided by the radius of the nucleus (Chromoview® - Harizanova, Jana, Taylor-Kashton, and Mai, 2008, Martin et al., 2013). The intrachromosomal distance was measured by tracing the distance between the chromosome territories pair analysed.

5.14. Statistical Analysis

Protein statistics were made using one-way ANOVA followed by Tukey multi-comparison test, while $p<0.05$ was considered statistically significant. Graphs represented using GraphPad Prism 8.0 software. Chromosome territory analysis (relative radial position and intrachromosomal distance) were made using frequency distribution represented by a Gaussian curve. Chromosome territories statistics were determined by a non-parametric test (Man-Whitney) comparing MM cell lines with lymphocytes and comparing RPMI 8226 siRNA lamin A/C with scrRNA. $P<0.05$ was considered statistically significant. Graphs were prepeared using GraphPad Prism 8.0 software. Cell viability assays (Trypan Blue exclusion and MTT) was illustrated by a two-dimensional graph and statistics were determined by T-test, considering $p<0.05$ as statistically significant. Graphs represented using GraphPad Prism 8.0 software. Chromatin analysis using SIM of super-resolved DNA structure, DNA-free space and all computations were performed using the DIPimage toolbox of Matlab (version R2012a, MathWorks, Natick, MA, USA). Chromatin analysis statistic was performed using non-parametric Kolmogorov–Smirnov test considering $p<0.05$ as statistically significant.

5.15. CRISPR/Cas 9

5.15.1. Lentivirus Production

Lentiviral particles were generated by transfecting HEK-293T (CRL-11268, ATCC®) cells with psPAX2, pMD2.G, and with the lentiviral vector encoding the genes of interest (Cas9 conjugated with green fluorescent protein (GFP) or lamin A/C guides, conjugated with blue

fluorescent protein (BFP)). Transfection took place in 10 mL of culture medium (RPMI 1640 ATCC modified) with 540 μL Opti-Mem (Gibco, Burlington, ON, Canada) and 36 μL X-treamGENE DNA Transfection Reagent (Roche, Mississauga, ON, Canada). Medium was changed after 18 hr and replaced with Dulbecco's Modified Eagle Medium (DMEM) containing 20% v/v bovine serum albumin (reagents from Gibco, Burlington, ON, Canada) and viral particles were collected after 24 and 48 hours. Viral harvests were pooled and centrifuged at 1000 rpm for 3 minutes and stored at -80°C for subsequent use.

5.15.2. Generation of Cas9 Stable Cell Lines

Stable Cas9 RPMI 8226 cell were generated by transducing the cell line with the lentiviral cas9 particles with polybrene (Millipore Sigma, Merck, MA USA) (8ug/mL) for 24 hours. Cas9-GFP and BFP positive cells underwent fluorescence-activated cell sorting (FACS Aria II, BD Biosciences, ON, CA) and selection with puromycin (2μg/mL) for BFP positive cells (Ling et al., 2012). Media with puromycin was changed every 2 to 3 days until the uninfected cells showed complete cell death. Cas 9 and lamin A/C expression was analysed through western blot as previously described here.

5.16. Lamin A/C downregulation using small hairpin RNA (shRNA)

5.16.1. Lentivirus Production

Lentiviral particles were generated by transfecting HEK-293T (CRL-11268, ATCC®) cells with pHR'8.2ΔR, pCMV-VSV-G, and with the lentiviral vector encoding the genes of interest (shRNA of human mRNA of lamin A/C). Transfection took place in 0.094 mL of culture medium Dulbecco's Modified Eagle Medium (DMEM) without FBS, with 6 μL of FUGENE DNA Transfection Reagent (Promega Corporation, WI, USA). Medium was changed after 24 hours and replaced with DMEM containing 20% v/v bovine serum albumin (reagents from Gibco, Burlington, ON, Canada) and viral particles were collected after 24 and

48 hours. Viral harvests were pooled and centrifuged at 1000 rpm for 3 minutes and stored at -80°C for subsequent use.

5.16.2. Generation of shRNA Stable Cell Lines

Stable downregulation of lamin A/C in RPMI 8226 was generated by transfecting RPMI 8226 with the lentiviral shRNA lamin A/C particles with polybrene (Millipore Sigma, Merck, MA USA) (8uG/mL) for 24 hours. Transduced cells underwent selection with puromycin (2μg/mL) (Ling et al., 2012). Media with puromycin was changed every 2 to 3 days until the uninfected cells showed complete cell death. lamin A/C expression was analysed through western blot as previously described here.

6. RESULTS

6.1. Lamin A/C expression in Multiple Myeloma Cell lines

Preliminary data showed overexpression of lamin A/C in treatment naïve MM patient samples. Therefore, I investigated lamin A/C protein levels in two MM cell lines (MM.1R and RPMI 8226) using immunofluorescence and western blot, in order to determine which cell line to use for further experiments. Figure 3A shows lamin A/C expression by immunofluorescence. The MM cell line RPMI 8226 have an expected nuclear ring of lamin A/C but also shows internal lamin A/C structures (white arrows). On the other hand, the MM cell line MM.1R, do not express lamin A/C in the same degree. MM.1R display a weak expression of lamin A/C by immunofluorescence (Figure 3A). Next, I compared the lamin A/C protein expression between these cell lines using western blot. Figure 3B shows lamin A/C protein expression where lamin A/C protein was normalized by the housekeeping protein α-tubulin. In figure 3C, we show a graphical representation of the densitometric analysis as a more objective parameter in interpreting your results/bands. RPMI 8226 express more lamin A/C compared to MM.1R ($p<0.05$). These results highlight heterogeneous expression of lamin A/C in MM cell lines.

Further experiments will focus on use of RPMI 8226, due to higher lamin A/C expression in comparison with MM.1R.

Figure 3 – Analysis of Lamin A/C expression in MM cell lines.

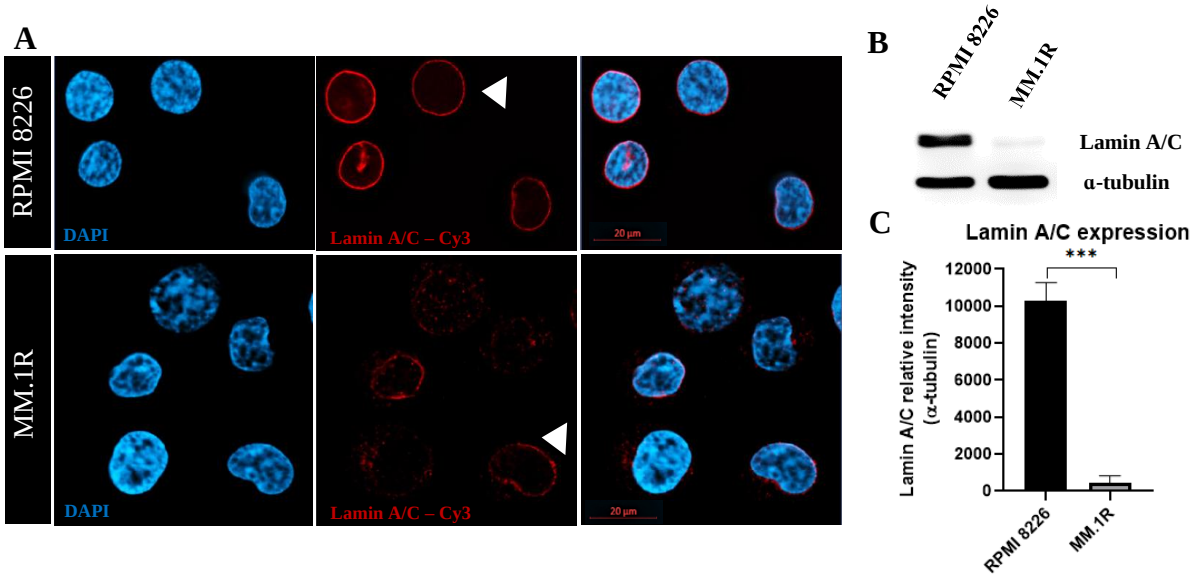

Figure 3. **A** - Immunofluorescence of lamin A/C in MM cell lines RPMI 8226 and MM.1R, showing peripheral (white arrows) and internal lamin A/C structures. **B** – Western Blot analysis of lamin A/C in RPMI 8226 and MM.1R, targeted protein was normalized by α-tubulin. **C** – RPMI 8226 shows more lamin A/C protein expression compared to MM.1R. Data expressed as mean ± SD. * $p < 0.05$ and *** $p < 0.001$. Blue - DAPI, Red - lamin A/C (Cy3 – Exposure time 120 milliseconds).

6.2. Lamin A/C downregulation in RPMI 8226 using siRNA

To evaluate the effects of lamin A/C downregulation on chromosome territory positions and cell viability, I performed a transient downregulation of lamin A/C using two different siRNAs and scrambled RNA (scrRNA – control). Figure 4A shows immunofluorescence of lamin A/C after 96 hours of siRNA transfection. The downregulation was followed for 96 hours by WB. Interesting, the degree of downregulation was different within cells, and this is only observed by single cell analysis (Figure 4A) (white arrows). Figure 4B shows siRNA downregulation kinetics (0 to 96 hours), with gradual decrease of lamin A/C protein over time.

I compared the effectiveness of lamin A/C downregulation of two different siRNAs. They were used individually or in combination (Figure 4C). However, I have not observed additive effects in the combination experiment. Significant downregulation was observed after 24 hours of siRNA transfection (50% of protein expression was reduced) in both individual and combination approach (Figure 4C). Maximum downregulation of lamin A/C was achieved in 48-72 hours after transfection, which showed lamin A/C protein downregulation up to 70% (Figure 4C). For convenience, further experiments were performed using siRNA1.

Figure 4 – Transient downregulation of Lamin A/C using siRNA.

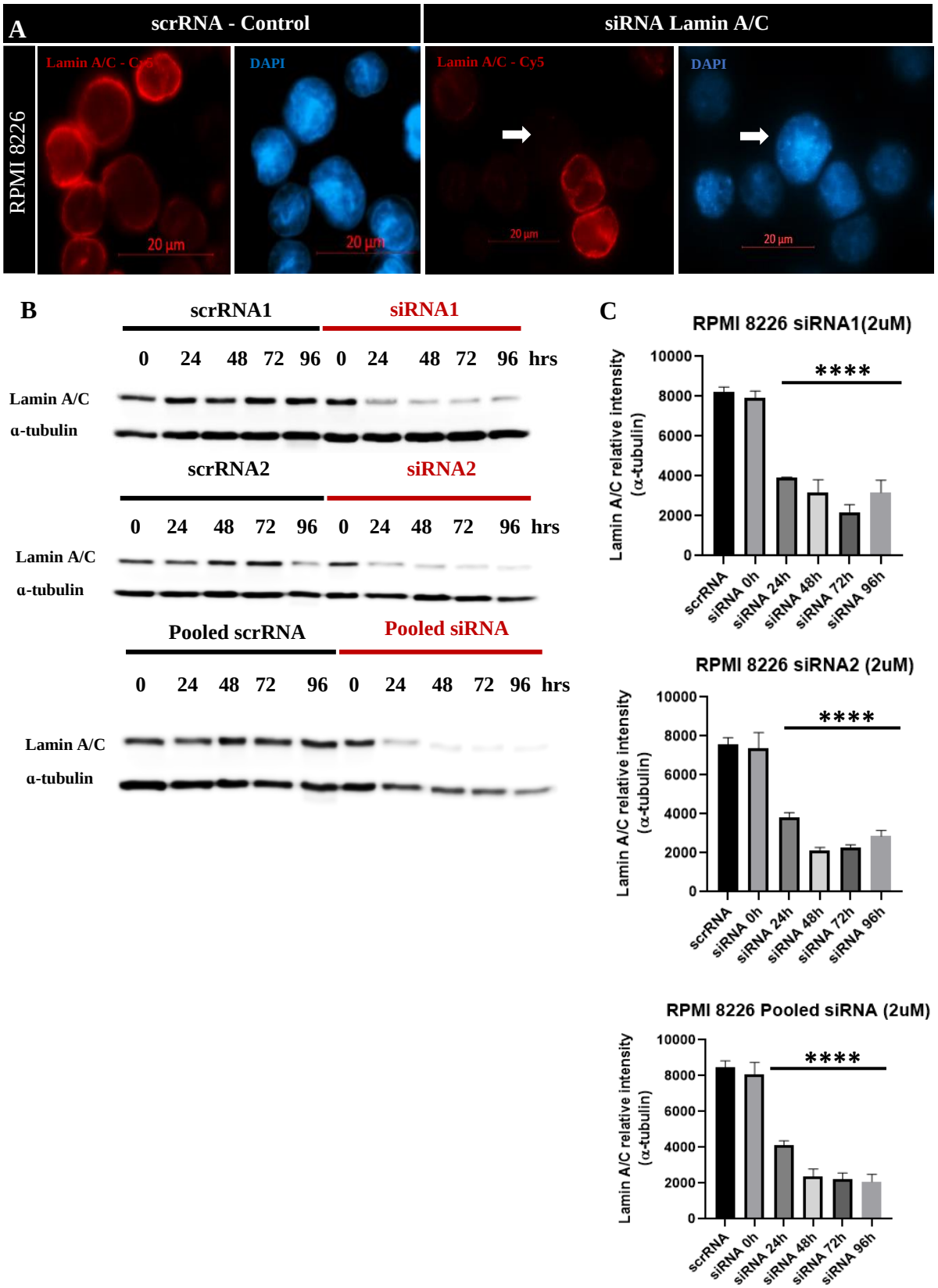

Figure 4. **A** - Immunofluorescence of lamin A/C downregulation (96 hours) in RPMI 8226. White arrowheads illustrate loss of lamin A/C structures under siRNA treatment. **B** – Western Blot (30µg of protein) of siRNA (2µM) and scrRNA (2µM) kinetics from 0 to 96 hours in RPMI 8226. Two different siRNA (2µM) were used separately or in combination. α-tubulin expression was used as control. **C** – Downregulation of lamin A/C using siRNA (2µM) compared to scrRNA (2µM). Significant protein downregulation was observed after 24 hours. Protein downregulation increased over time, with maximum inhibition at 48 to 72 hours. Data expressed as mean ± SD. * $p < 0.05$ and *** $p < 0.001$. Blue - DAPI, Red - lamin A/C (Cy5 – 5 seconds of exposure time).

6.3. Cell Viability Analysis of RPMI 8226 under Lamin A/C downregulation using siRNA

To evaluate whether lamin A/C downregulation would impact RPMI 8226 cell proliferation, I used the trypan blue exclusion method and 2,5-diphenyl-2H-tetrazolium bromide (MTT) assay. Figure 5A and 5B show no significant difference in cell growth between RPMI 8226 siRNA and control cells (scrRNA) from 0 to 96 hours (Cell counting Fig 5A and MTT Fig 5B) with trypan blue or MTT assay. Data expressed as mean ± SD.

Figure 5 – Analysis of cell viability in RPMI 8226 with downregulation of Lamin A/C using siRNA.

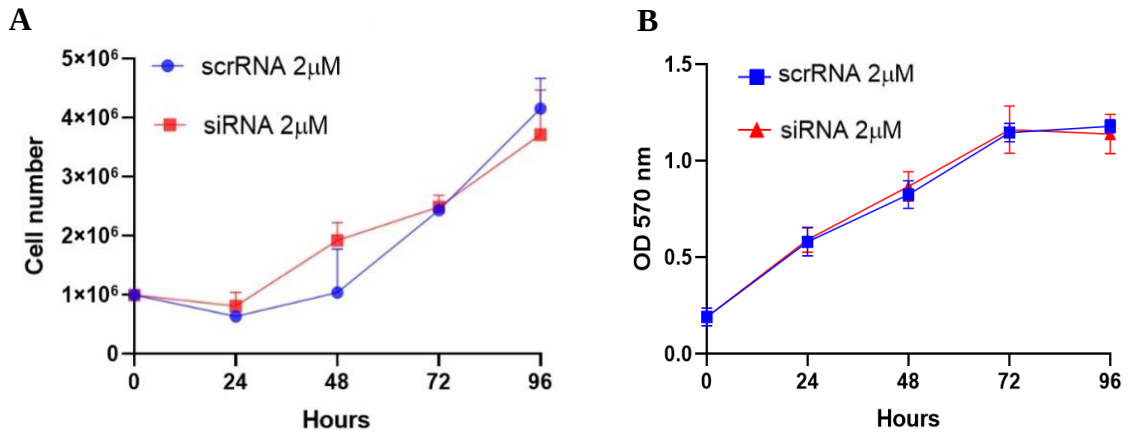

Figure 5. **A**- Cell counting analysis of RPMI 8226 with downregulation of lamin A/C using siRNA (2µM) from 0 to 96 hours. **B** – Indirect cell viability analysis of RPMI 8226 with downregulation of lamin A/C using siRNA (2µM) from 0 to 96 hours. Both approaches show no statistical difference between siRNA and scrRNA groups. Data expressed as mean ± SD.

6.4. Chromosome Territory analysis of B-lymphocytes, MM.1R, and RPMI 8226 with downregulation of Lamin A/C using siRNA

To evaluate chromosome territory positions in normal B-lymphocytes, MM.1R, and RPMI 8226 after siRNA treatment (96 hours), I performed a 3D fluorescence *in situ* hybridization (FISH). This technique uses whole chromosome painting probes, 3D epifluorescence microscopy and 3D image deconvolution. Since lamin A/C downregulation after siRNA treatment varies within the cell population (Figure 4A), a pre-staining of lamin A/C was necessary to correctly select the cell population for chromosome territories analysis. Chromosomes 18 and 19 were selected based on previous studies using B-Lymphocytes, which reported peripheral location of CT 18 and internal location of CT 19 (Tanabe et al., 2002). Chromosomes 9 and 22, were previously reported as assuming a neighborhood position in B-lymphocytes (Kozubek et al., 1999, Cremer et al., 2001). Chromosomes 4, 11, 14, and 16 are involved in common MM translocation (Pinto et al., 2020).

Figure 6A shows the chromosomes territories 18 and 19 in B-lymphocytes, MM.1R and RPMI 8226. Figures 6B and 6C shows the relative radial position of chromosome territories related to the center of the nucleus. In the graph, 0 represents the nuclear center and 100 represent the nuclear periphery (X- axis of graph). In the Y- axis, we can observe the frequency distribution of chromosome position, that displays the number of observations (chromosome position) in more than 100 cells. MM.1R displays a more internal position of CT 18, while RPMI 8226 display a periphery related position of CT 18, all compared to B-lymphocytes ($p<0.05$) (Figure 6B). Furthermore, down regulation of lamin A/C for 96 hours using siRNA

altered CT 18, in RPMI 8226, by moving it towards nuclear center, compared to scrRNA (*p<0.05)* (Figure 6B).

Figure 6 – Chromosome Territory analysis of CT 18 and CT 19 in B-lymphocytes, MM.1R, and RPMI 8226 with downregulation of Lamin A/C using siRNA

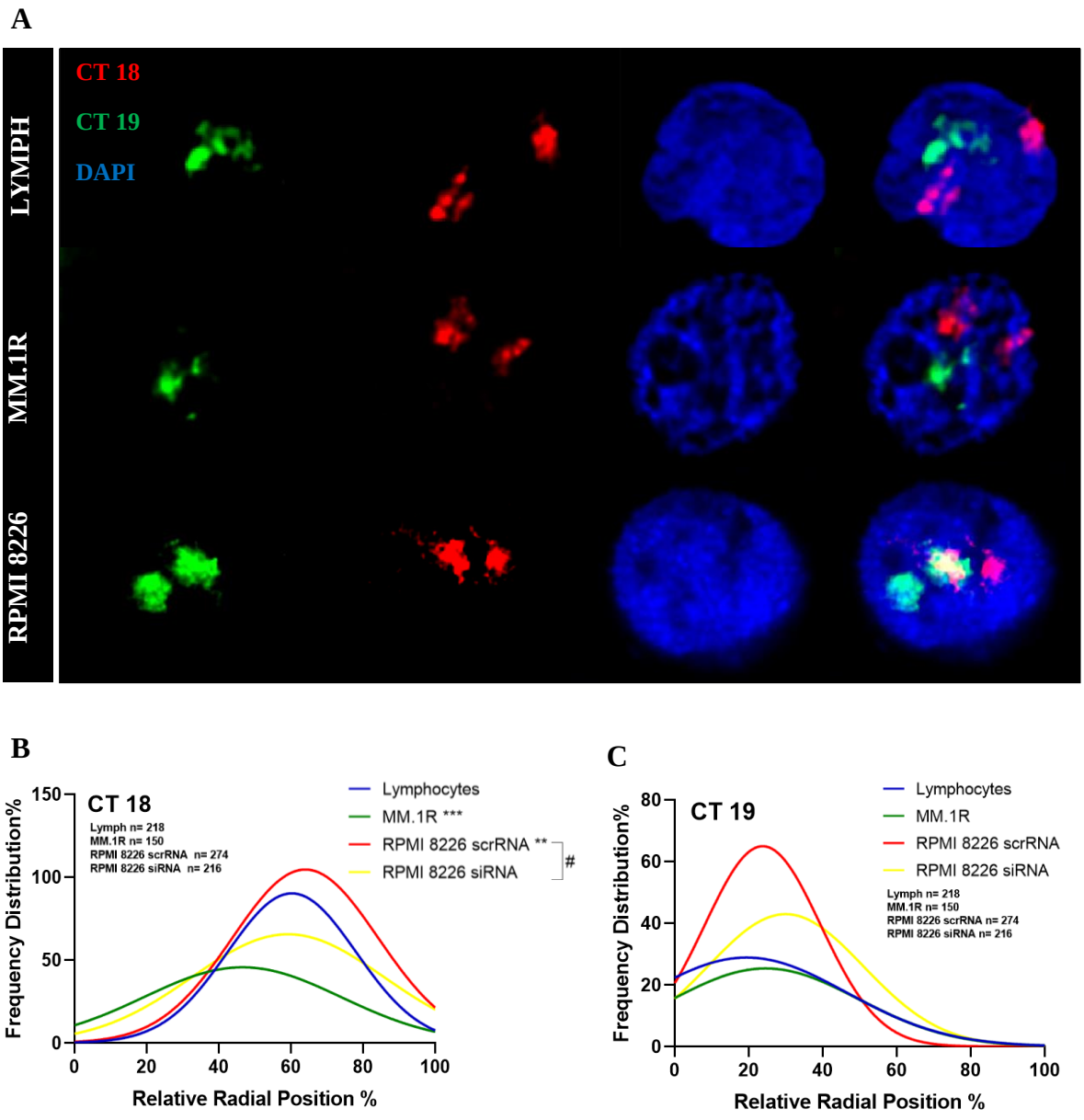

Figure 6. **A** – Chromosome territories 18 (red) and 19 (green), in B-lymphocytes, MM.1R and RPMI 8226. **B** – Quantitative analysis of CT 18 in B-lymphocytes, MM.1R and RPMI 8226 siRNA (2µM) lamin A/C (96 hours) and RPMI 8226 scrRNA (2µM) (96 hours). Analysis performed using Chromoview® software (Harizanova, Jana, Taylor-Kashton, and Mai, 2008, Righolt, et al., 2011, Martin et al., 2013). MM cell lines display altered CT 18 compared to B-

lymphocytes. Downregulation of lamin A/C in RPMI 8226 induces CT 18 movement towards nuclear interior, compared to scrRNA. **C** - Quantitative analysis of CT 19 in B-lymphocytes, MM.1R and RPMI 8226 siRNA (2µM) lamin A/C (96 hours) and RPMI 8226 scrRNA (2µM) (96 hours). No statistical differences were observed between MM cells lines and lymphocytes as well as between siRNA lamin A/C and scrRNA. Data expressed as non-linear regression. *, # $p < 0.05$ and *** $p < 0.001$. LYMPH – B-lymphocytes.

In Figure 6C we can observe the relative radial position of chromosome territories 19 in B-lymphocytes, MM1.R, RPMI 8226 with downregulation of lamin A/C using siRNA (96 hours) and RPMI 8226 scrRNA (96 hours). No statistical differences were observed between MM cell lines and B-lymphocytes. Lamin A/C downregulation did not alter CT 19 in RPMI 8226, compared to scrRNA.

Figure 7A shows the chromosomes territories 9 and 22 in B-lymphocytes, MM.1R and RPMI 8226. In Figure 7B we can observe the quantitative analysis of relative radial position of CT 9. First, we can observe that MM cell lines display an altered CT 9 position, compared to B-lymphocytes (Figure 7B). MM.1R displays a more internal position of CT 9, while RPMI 8226 displays a periphery related position of CT 9, all compared to B-lymphocytes ($p<0.05$) (Figure 10B). Furthermore, down regulation of lamin A/C for 96 hours using siRNA altered CT 9, in RPMI 8226, by moving it towards nuclear center, compared to scrRNA ($p<0.05$) (Figure 7B). In Figure 7C we can observe the relative radial position of chromosome territories 22 in B-lymphocytes, MM1.R, RPMI 8226 with downregulation of lamin A/C using siRNA (96 hours) and RPMI 8226 scrRNA (96 hours). MM cell lines display an altered CT 22 position, compared to B-lymphocytes (Figure 7C). MM.1R displays a more internal position of CT 22, while RPMI 8226 displays a periphery related position of CT 22, all compared to B-lymphocytes ($p<0.05$) (Figure 7C). Moreover, down regulation of lamin A/C for 96 hours

using siRNA altered CT 22, in RPMI 8226, by moving it towards nuclear center, compared to scrRNA (*p<0.05)* (Figure 7B).

Figure 7 – Chromosome Territory analysis of CT 9 and CT 22 in B-lymphocytes, MM.1R, and RPMI 8226 with downregulation of Lamin A/C using siRNA

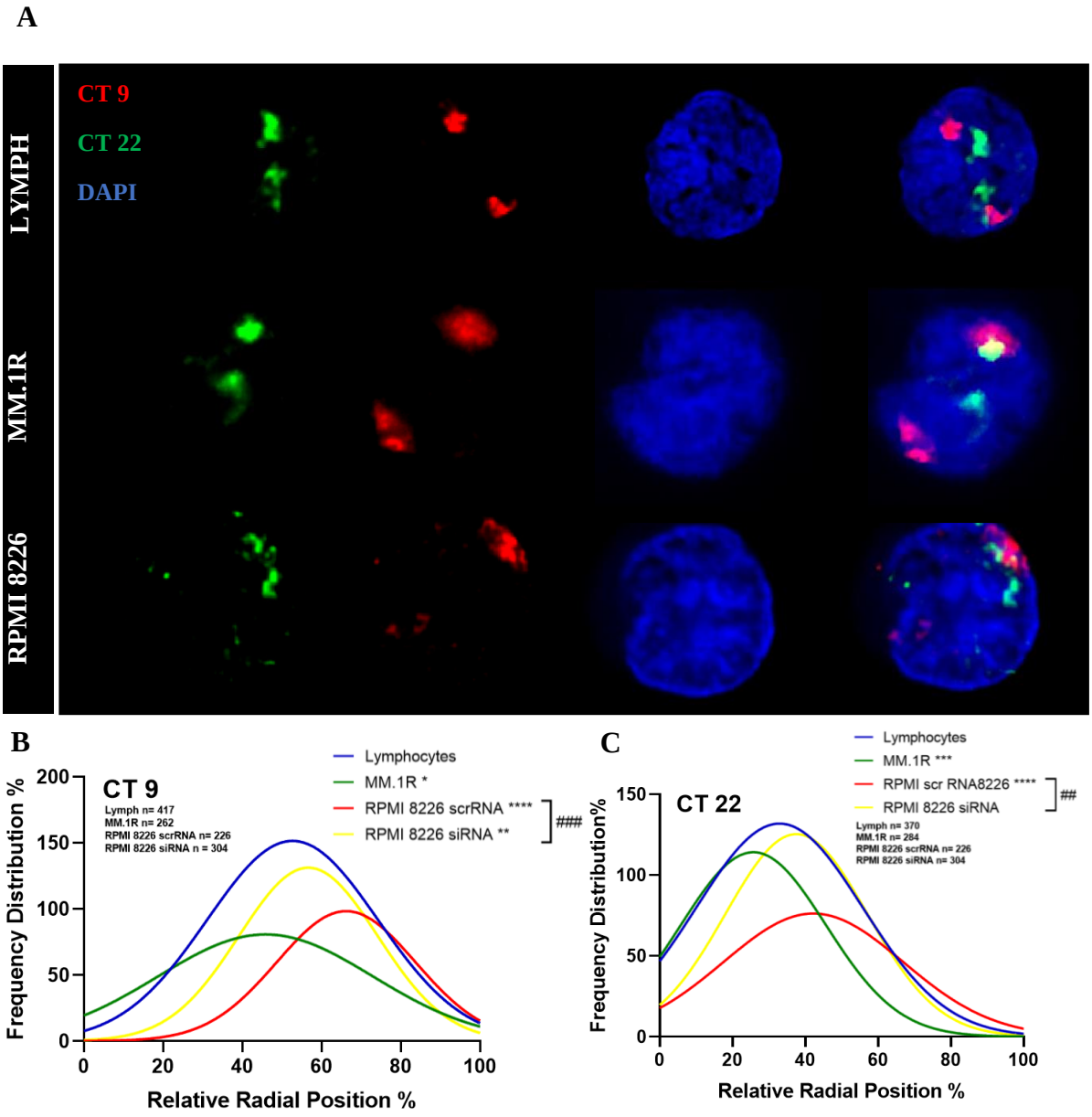

Figure 7. **A** – Chromosome territories 9 (red) and 22 (green), in B-lymphocytes, MM.1R and RPMI 8226. **B** – Quantitative analysis of CT 9 in B-lymphocytes, MM.1R and RPMI 8226 siRNA (2µM) lamin A/C (96 hours) and RPMI 8226 scrRNA (2µM) (96 hours). Analysis performed using Chromoview® software (Harizanova, Jana, Taylor-Kashton, and Mai, 2008, Righolt, et al., 2011, Martin et al., 2013). MM cell lines display altered CT 9 compared to B-

lymphocytes. Downregulation of lamin A/C in RPMI 8226 induces CT 9 movement towards nuclear interior, compared to scrRNA. **C** - Quantitative analysis of CT 22 in B-lymphocytes, MM.1R and RPMI 8226 siRNA lamin A/C (96 hours) and RPMI 8226 scrRNA (96 hours). Downregulation of lamin A/C in RPMI 8226 induces CT 22 movement towards nuclear interior, compared to scrRNA. Data expressed as non-linear regression. *, # $p < 0.05$ and ***, ### $p < 0.001$. LYMPH – B-lymphocytes.

Figure 8A shows the chromosomes territories 4 and 14 in B-lymphocytes, MM.1R and RPMI 8226. In Figure 8B we can observe the quantitative analysis of relative radial position of CT 4. First, we observe that only RPMI 8226 displays an altered CT 4 position, compared to B-lymphocytes, towards nuclear periphery (Figure 8B). Down regulation of lamin A/C for 96 hours using siRNA altered CT 4, in RPMI 8226, by moving it towards nuclear center, compared to scrRNA (*$p<0.05$)* (Figure 8B). Figure 8C shows the relative radial position of chromosome territories 14 in B-lymphocytes, MM1.R, RPMI 8226 with downregulation of lamin A/C using siRNA (96 hours) and RPMI 8226 scrRNA (96 hours). Only RPMI 8226 displays an altered CT 14 position, compared to B-lymphocytes, towards nuclear periphery (Figure 8C). Down regulation of lamin A/C for 96 hours using siRNA altered CT 14, in RPMI 8226, by moving it towards nuclear center, compared to scrRNA (*$p<0.05$)* (Figure 8C).

Figure 8 – Chromosome Territory analysis of CT 4 and CT 14 in B-lymphocytes, MM.1R, and RPMI 8226 with downregulation of Lamin A/C using siRNA

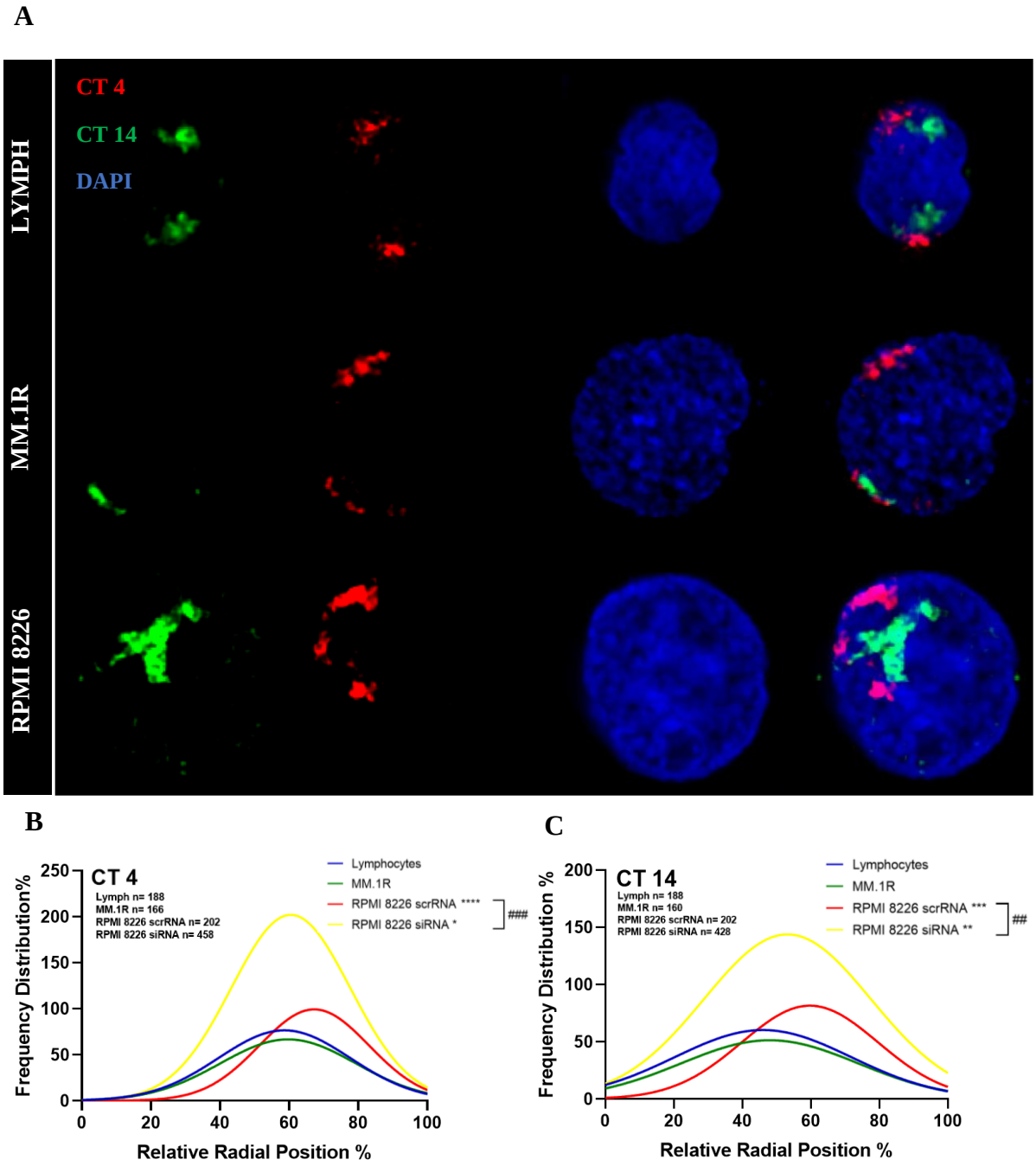

Figure 8. **A** – Chromosome territories 4 (red) and 14 (green), in B-lymphocytes, MM.1R and RPMI 8226. **B** – Quantitative analysis of CT 4 in B-lymphocytes, MM.1R and RPMI 8226 siRNA (2µM) lamin A/C (96 hours) and RPMI 8226 scrRNA (2µM) (96 hours). Analysis performed using Chromoview® software (Harizanova, Jana, Taylor-Kashton, and Mai, 2008, Righolt, et al., 2011, Martin et al., 2013). RPMI 8226 display altered CT 4 compared to B-

lymphocytes. Downregulation of lamin A/C in RPMI 8226 induces CT 4 movement towards nuclear interior, compared to scrRNA. **C** - Quantitative analysis of CT 14 in B-lymphocytes, MM.1R and RPMI 8226 siRNA lamin A/C (96 hours) and RPMI 8226 scrRNA (96 hours). RPMI 8226 display altered CT 14 compared to B-lymphocytes. Downregulation of lamin A/C in RPMI 8226 induces CT 14 movement towards nuclear interior, compared to scrRNA. Data expressed as non-linear regression. *, # $p < 0.05$ and ***, ### $p < 0.001$. LYMPH – B-lymphocytes.

Figure 9A shows the chromosomes territories 11 and 14 in B-lymphocytes, MM.1R and RPMI 8226. In Figure 9B we can observe the quantitative analysis of relative radial position of CT 11. First, we observe that only RPMI 8226 displays an altered CT 11 position, compared to B-lymphocytes, towards nuclear periphery (Figure 9B). Down regulation of lamin A/C for 96 hours using siRNA altered CT 11, in RPMI 8226, by moving it towards nuclear center, compared to scrRNA (*$p<0.05$)* (Figure 9B). Figure 9C shows the relative radial position of chromosome territories 14 in B-lymphocytes, MM1.R, RPMI 8226 with downregulation of lamin A/C using siRNA (96 hours) and RPMI 8226 scrRNA (96 hours). Only RPMI 8226 displays an altered CT 14 position, compared to B-lymphocytes, towards nuclear periphery (Figure 9C). Down regulation of lamin A/C for 96 hours using siRNA altered CT 14, in RPMI 8226, by moving it towards nuclear center, compared to scrRNA (*$p<0.05$)* (Figure 9C).

Figure 9 – Chromosome Territory analysis of CT 11 and CT 14 in B-lymphocytes, MM.1R, and RPMI 8226 with downregulation of Lamin A/C using siRNA

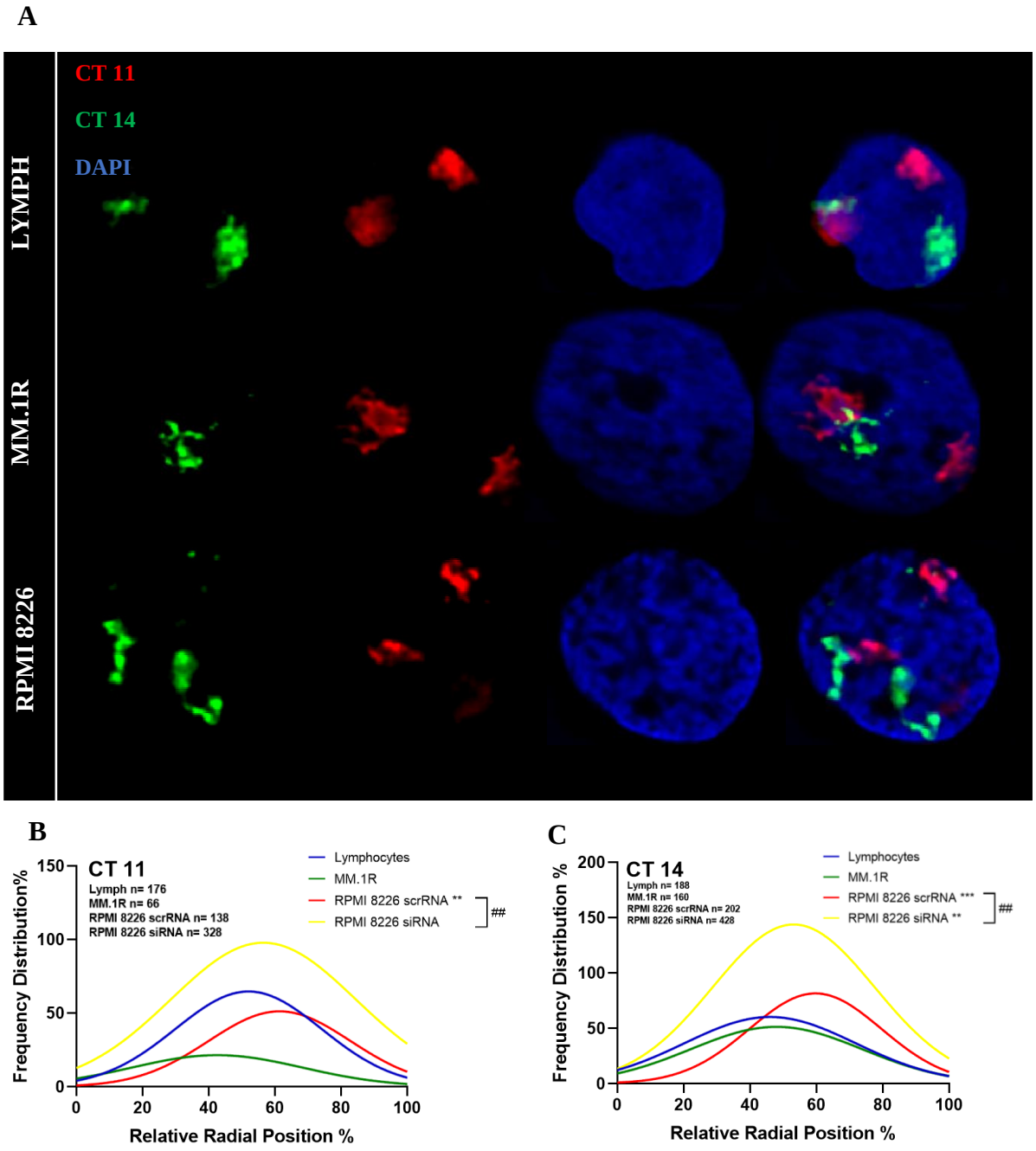

Figure 9. **A** – Chromosome territories 11 (red) and 14 (green), in B-lymphocytes, MM.1R and RPMI 8226. **B** – Quantitative analysis of CT 11 in B-lymphocytes, MM.1R and RPMI 8226 siRNA (2µM) lamin A/C (96 hours) and RPMI 8226 scrRNA (2µM) (96 hours). Analysis performed using Chromoview® software (Harizanova, Jana, Taylor-Kashton, and Mai, 2008, Righolt, et al., 2011, Martin et al., 2013). RPMI 8226 display altered CT 11

compared to B-lymphocytes. Downregulation of lamin A/C in RPMI 8226 induces CT 11 movement towards nuclear interior, compared to scrRNA. **C** - Quantitative analysis of CT 14 in B-lymphocytes, MM.1R and RPMI 8226 siRNA lamin A/C (96 hours) and RPMI 8226 scrRNA (96 hours). RPMI 8226 display altered CT 14 compared to B-lymphocytes. Downregulation of lamin A/C in RPMI 8226 induces CT 14 movement towards nuclear interior, compared to scrRNA. Data expressed as non-linear regression. *, # $p < 0.05$ and ***, ### $p < 0.001$. LYMPH – B-lymphocytes.

Figure 10A shows the chromosomes territories 16 and 14 in B-lymphocytes, MM.1R and RPMI 8226. In Figure 10B we can observe the quantitative analysis of relative radial position of CT 16. First, we observe that only MM.1R displays an altered CT 16 position, compared to B-lymphocytes, towards nuclear interior (Figure 10B). Down regulation of lamin A/C for 96 hours using siRNA altered CT 16, in RPMI 8226, by moving it towards nuclear center, compared to scrRNA (*p<0.05)* (Figure 10B). Figure 10C shows the relative radial position of chromosome territories 14 in B-lymphocytes, MM1.R, RPMI 8226 with downregulation of lamin A/C using siRNA (96 hours) and RPMI 8226 scrRNA (96 hours). Only RPMI 8226 displays an altered CT 14 position, compared to B-lymphocytes, towards nuclear periphery (Figure 10C). Down regulation of lamin A/C for 96 hours using siRNA altered CT 14, in RPMI 8226, by moving it towards nuclear center, compared to scrRNA (*p<0.05)* (Figure 10C).

Figure 10 – Chromosome Territory analysis of CT 16 and CT 14 in B-lymphocytes, MM cells lines and RPMI 8226 with downregulation of Lamin A/C using siRNA

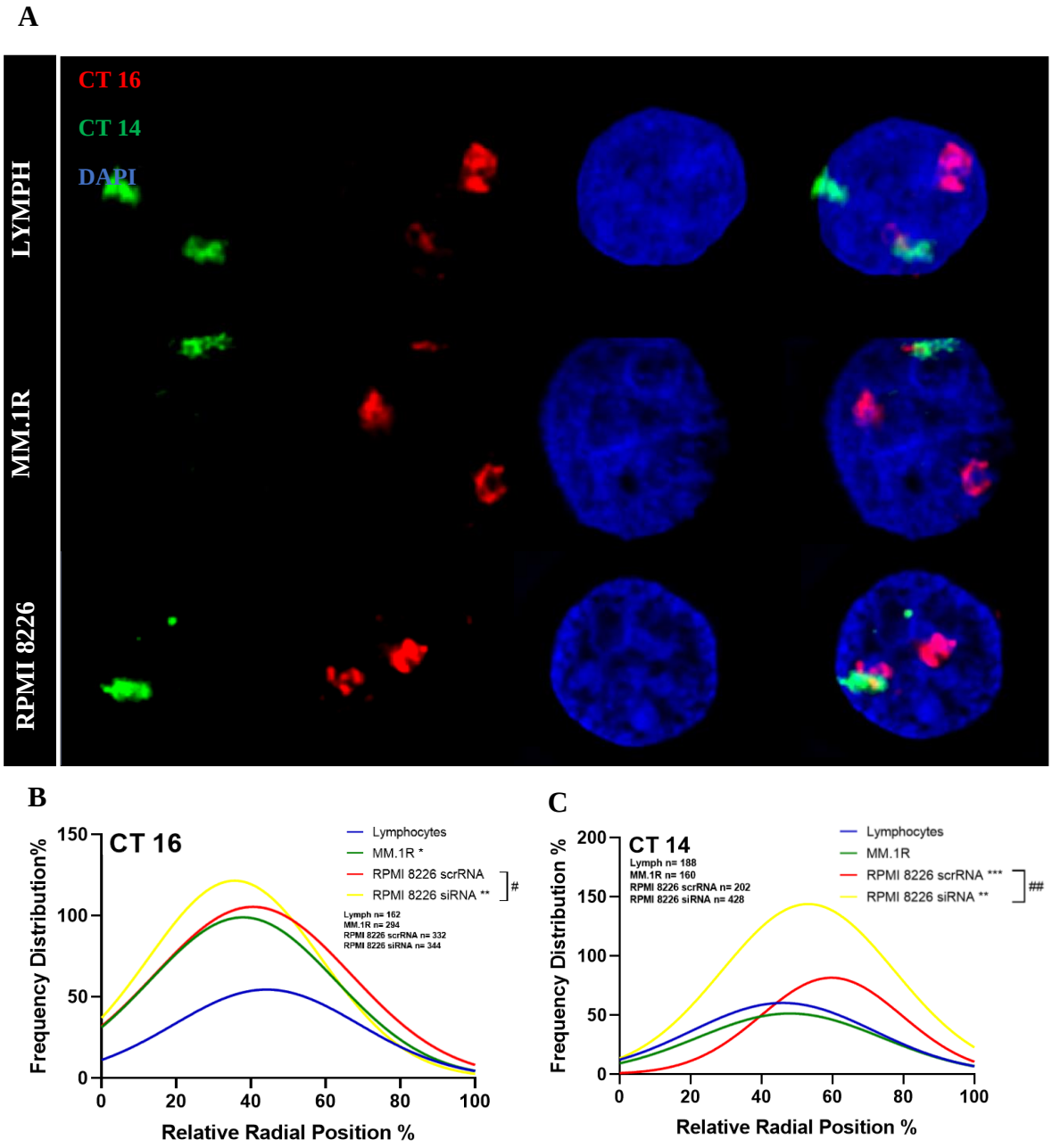

Figure 10. **A** – Chromosome territories 16 (red) and 14 (green), in B-lymphocytes, MM.1R and RPMI 8226. **B** – Quantitative analysis of CT 16 in B-lymphocytes, MM.1R and RPMI 8226 siRNA (2µM) lamin A/C (96 hours) and RPMI 8226 scrRNA (2µM) (96 hours). Analysis performed using Chromoview® software (Harizanova, Jana, Taylor-Kashton, and Mai, 2008, Righolt, et al., 2011, Martin et al., 2013). MM.1R display altered CT 16 compared to B-lymphocytes. Downregulation of lamin A/C in RPMI 8226 induces CT 16 movement towards

nuclear interior, compared to scrRNA. **C** - Quantitative analysis of CT 14 in B-lymphocytes, MM.1R and RPMI 8226 siRNA lamin A/C (96 hours) and RPMI 8226 scrRNA (96 hours). RPMI 8226 display altered CT 14 compared to B-lymphocytes. Downregulation of lamin A/C in RPMI 8226 induces CT 14 movement towards nuclear interior, compared to scrRNA. Data expressed as non-linear regression. *, # $p < 0.05$ and ***, ### $p < 0.001$. LYMPH – B-lymphocytes.

6.5. Intrachromosomal distance analysis of B-lymphocytes, MM.1R and RPMI 8226 with downregulation of Lamin A/C using siRNA

To analyse the intrachromosomal distance of CT in normal B-lymphocytes, MM.1R, RPMI 8226 with downregulation of lamin A/C using siRNA (2µM), and RPMI 8226 scrRNA (2µM), I performed a 3D fluorescence *in situ* hybridization (FISH) using whole chromosome painting probes, 3D epifluorescence microscopy and 3D image deconvolution. Analysis of intrachromosomal distance of CT in RPMI 8226 with downregulation of lamin A/C by siRNA was performed using co-immuno stanning and 3D FISH of lamin A/C and whole chromosomes. Single cell analysis of CT in RPMI 8226 siRNA lamin A/C cells was performed to analyse only cell population that was not showing lamin A/C stanning after 96 hours of siRNA treatment. Figures 11A-E shows the relative intrachromosomal distance between chromosome territories. The intrachromosomal distance was normalized by the size of the nucleus. In the graph, 0 represents the close CTs proximity and 100 represents the maximum intrachromosomal distance between CTs. In the Y- axis, we can observe the frequency distribution of chromosome position, that displays the number of observations (chromosome position) in more than 100 cells.

Figure 11A shows intrachromosomal distance of CT 18 and CT 19 in B-lymphocytes, MM.1R, RPMI 8226 with downregulation of lamin A/C using siRNA (96 hours) and RPMI

8226 scrRNA (96 hours). No statistical differences were observed between MM.1R, RPMI 8226, and lymphocytes as well as between siRNA and scrRNA RPMI 8226. In figure 11B we can observe the intrachromosomal distance of CT 9 and CT 22 in B-lymphocytes, MM.1R, RPMI 8226 with downregulation of lamin A/C using siRNA (2μM) (96 hours) and RPMI 8226 scrRNA (2μM) (96 hours). Only RPMI 8226 shows statistical difference in intrachromosomal distance of CT 9 and CT 22, which display increased CT distance, compared to B-lymphocytes (Figure 11B). Lamin A/C downregulation did not alter the intrachromosomal distance of the CT analysed (Figure 11B).

Figure 11C shows intrachromosomal distance of CT 11 and CT 14 in B-lymphocytes, MM.1R, RPMI 8226 with downregulation of lamin A/C using siRNA (96 hours) and RPMI 8226 scrRNA (96 hours). MM cell lines display increased intrachromosomal distance compared to B-lymphocytes for CT 11 and CT 14 (Figure 11C). Lamin A/C downregulation did not alter the intrachromosomal distance of the CT analysed comparing siRNA RPMI 8226 to scrRNA (Figure 11C). In figure 11D we can observe the intrachromosomal distance of CT 4 and CT 14 in B-lymphocytes, MM.1R, RPMI 8226 with downregulation of lamin A/C using siRNA (96 hours) and RPMI 8226 scrRNA (96 hours). MM cell lines display increased intrachromosomal distance compared to B-lymphocytes for CT 4 and CT 14 (Figure 11D). Lamin A/C downregulation did not alter the intrachromosomal distance of the CT analysed (Figure 11D).

Figure 11E shows intrachromosomal distance of CT 16 and CT 14 in B-lymphocytes, MM.1R, RPMI 8226 with downregulation of lamin A/C using siRNA (96 hours) and RPMI 8226 scrRNA (96 hours). MM cell lines display increased intrachromosomal distance compared to B-lymphocytes for CT 16 and CT 14 (Figure 11E). Lamin A/C downregulation did not alter the intrachromosomal distance of the CT analysed comparing siRNA RPMI 8226 to scrRNA (Figure 11E).

Figure 11 – Intrachromosomal distance analysis of CT 4, 9, 11, 14, 16, 18, 19 and 22 in B-lymphocytes, MM.1R and RPMI 8226 with downregulation of Lamin A/C using siRNA

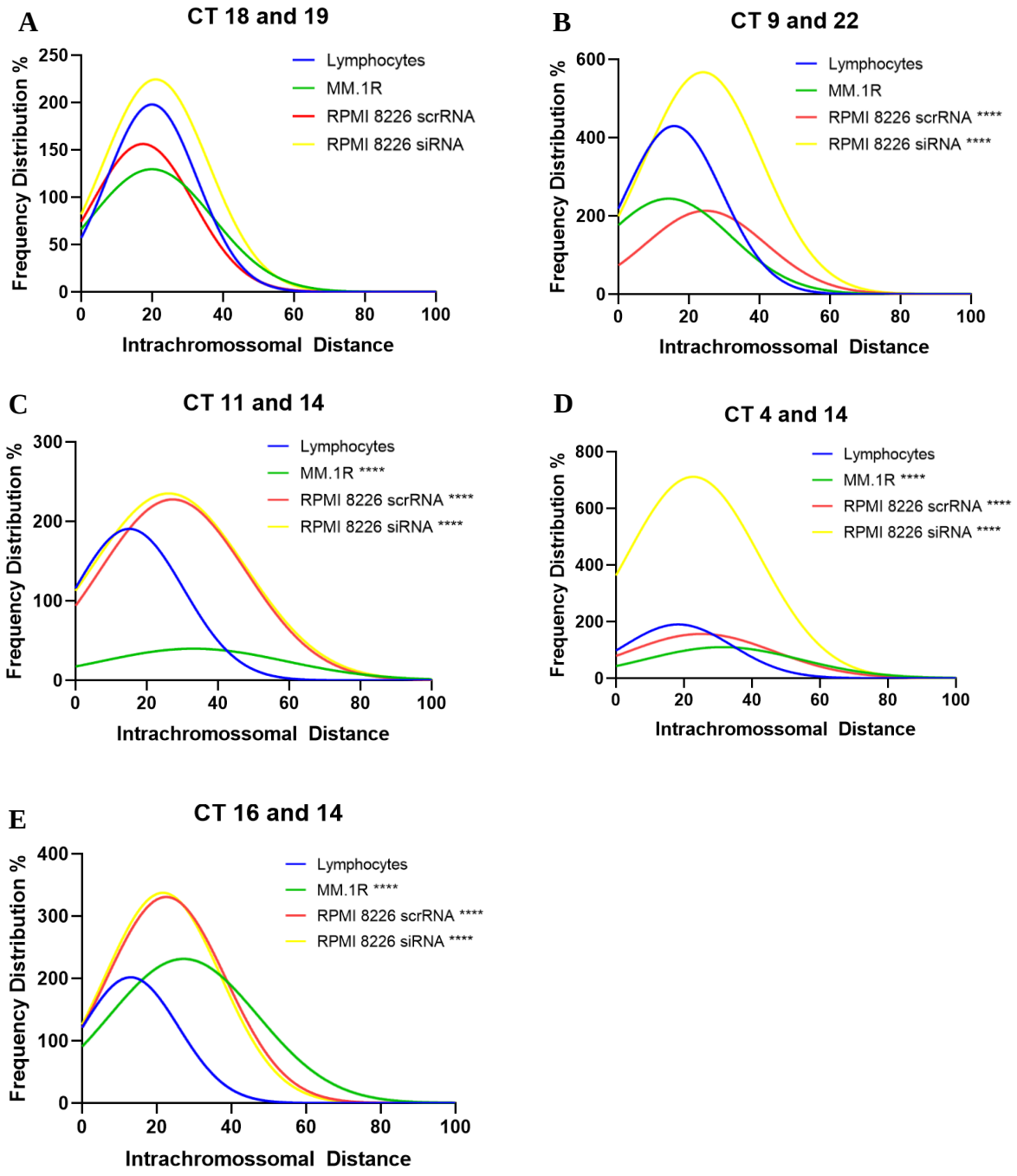

Figure 11. Intrachromosomal distance analysis of CT 18 and CT 19 (A), CT 9 and CT 22 (B), CT 11 and CT 14 (C), CT 4 and CT 14 (D), CT 16 and CT 14 (E), in B-lymphocytes, MM.1R, RPMI 8226 siRNA lamin A/C (96 hours) and RPMI scrRNA (96 hours). Analysis performed using Chromoview® software (Harizanova, Jana, Taylor-Kashton, and Mai, 2008, Righolt, et al., 2011, Martin et al., 2013). **A** – No statistical differences were observed between MM cell

lines and B-lymphocytes, as well as between RPMI 8226 siRNA lamin A/C and RPMI 8226 scrRNA. **B** – RPMI 8226 display increased intrachromosomal distance between CT 9 and CT 22, compared to B-lymphocytes. Lamin A/C downregulation did not alter intrachromosomal distance between CT 9 and CT 22 in PRMI 8226. **C** – MM cell lines display increased intrachromosomal distance compared to B-lymphocytes of CT 11 and CT 14. Lamin A/C downregulation did not alter intrachromosomal distance of CT 11 an CT 14 in RPMI 8226. **D** - MM cell lines display increased intrachromosomal distance compared to B-lymphocytes of CT 4 and CT 14. Lamin A/C downregulation did not alter intrachromosomal distance of CT 4 and CT 14 in RPMI 8226. **E** - MM cell lines display increased intrachromosomal distance compared to B-lymphocytes of CT 16 and CT 14. Lamin A/C downregulation did not alter intrachromosomal distance of CT 16 and CT 14 in RPMI 8226. Data expressed as non-linear regression. *$p < 0.05$ and ***$p < 0.001$.

6.6. Gene expression analysis in RPMI 8226 with downregulation of Lamin A/C using siRNA

Changes of chromosome positions has been associated with alterations of gene expression (see introduction). Analysis of chromosome territories in RPMI 8226 with downregulation of lamin A/C using siRNA (96 hours) showed alterations of chromosome positions, compared to scrRNA. Therefore, to analyse the impacts of lamin A/C downregulation on gene expression, related to changes on chromosome position, I performed quantitative polymerase chain reaction (qPCR) of genes involved in MM pathogeneses. Figure 12A shows up regulation ($p<0.05$) of B-cell maturation antigen (*BCMA*) gene placed on chromosome 16, Cyclin D1 (*CCND1*) gene placed on chromosome 11, proto-oncogene c-Maf (*MAF*) gene placed on chromosome 16, Mucosa-associated lymphoid tissue lymphoma translocation protein 1 (*MALT 1*) gene placed on chromosome 18 and B-cell lymphoma 3 (*BCL3*) gene placed on chromosome 19, in RPMI 8226 with downregulation of lamin A/C (72 hours) using siRNA compared to scrRNA (72 hours). Figure 12B shows all genes I investigated, their chromosome position, and chromosome territory movement of RPMI 8226 with downregulation of lamin A/C (96 hours) using siRNA compared to scrRNA.

Figure 12 – Gene expression analysis of RPMI 8226 with downregulation of Lamin A/C using siRNA

A

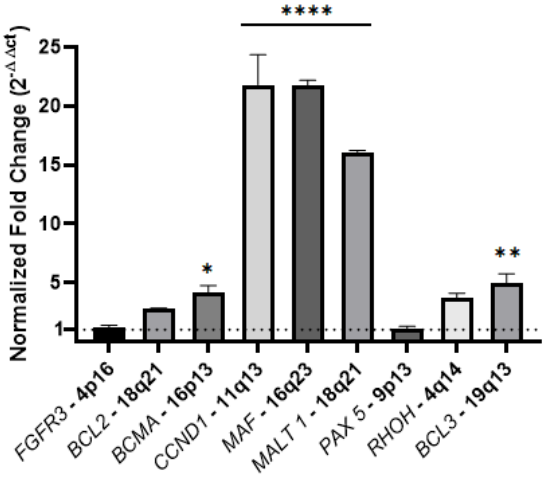

B

Genes	Gene Position	CT movement after lamin A/C downregulation
FGFR3	4p16	CT4 P → C
BCL2	18q21	CT18 P → C
BCMA	16p13	CT16 P → C
CCND1	11q13	CT11 P → C
MAF	16q23	CT16 P → C
MALT 1	18q21	CT18 P → C
PAX 5	9p13	CT9 P → C
RHOH	4p14	CT4 P → C
BCL3	19q13	None

P – Nuclear Periphery, **C** – Nuclear center, → Movement.

Figure 12. **A** – Gene expression analysis of PRMI 8226 with downregulation of lamin A/C using siRNA (72 hours). Upregulation of *BCMA*, *CCND1*, *MAF*, *MALT 1* and *BCL3* genes were observed, compared to scrRNA. The expression of targeted genes was normalized by housekeeping gene (*HBB)*, as indicated by the dashed line. **B –** Genes involved in multiple myeloma pathogenesis, their chromosome position, and chromosome territory intermingle of RPMI 8226 with downregulation of lamin A/C (96 hours) using siRNA compared to scrRNA. Data expressed as mean ± SD. * $p < 0.05$ and *** $p < 0.001$. P – Nuclear periphery, C – Nuclear center, → Movement.

6.7. Analysis of λ light-chain production in RPMI 8226 with downregulation of Lamin A/C using siRNA

Production of antibodies called M-protein is characteristic of MM disease. Several articles describe the role of M-protein on MM pathophysiology (see introduction). Therefore, to evaluate whether lamin A/C downregulation would impact M-protein production, I performed a western blot analysis of λ light-chain proteins, secreted by RPMI 8226. Figure 13A shows immunoblot of RPMI 8226 (Ctrl), RPMI 8226 scramble RNA (96 hours) and RPMI 8226 siRNA lamin A/C (96 hours). Figure 13B shows λ light-chain proteins analysis of RPMI 8226, RPMI 8226 scrRNA and RPMI 8226 siRNA. No statistical differences were observed between the groups analysed. Data expressed as mean ± SD.

Figure 13 – M-proteins analysis of RPMI 8226 with downregulation of Lamin A/C using siRNA.

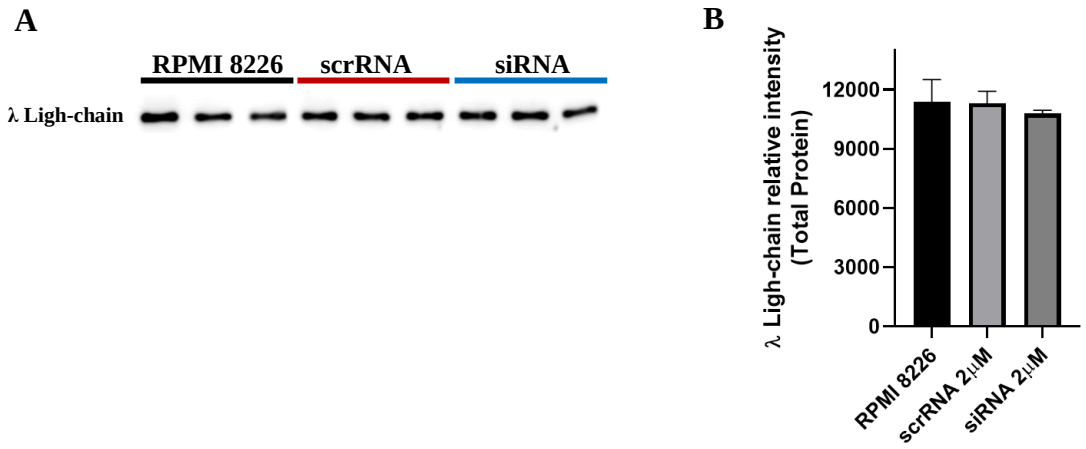

Figure 13. **A** – Wester blot (100 µg of protein) of λ light-chain proteins in RPMI 8226 (96 hours), RPMI 8226 scrRNA (96 hours) and RPMI 8226 with downregulation of lamin A/C using siRNA (96 hours). **B** - λ light-chain protein analysis of RPMI 8226, RPMI 8226 scrRNA (96 hours) and RPMI 8226 with downregulation of lamin A/C using siRNA (96 hours). No statistical differences were observed between groups analysed. λ light-chain protein intensity was normalized by total protein concentration, stained with ponceau S. Data expressed as mean ± SD.

6.8. Quantitative super resolution analysis of chromatin organization in RPMI 8226 with downregulation of Lamin A/C using siRNA

Lamin A/C is a key protein regulating chromatin structure and organization in human cells. After showing that downregulation of lamin A/C leads to changes on chromosome position, I further investigated the chromatin compaction status. Therefore, to analyse chromatin organization in RPMI 8226 after downregulation of lamin A/C using siRNA and the scrambled RNA, I performed quantitative super resolution analysis of chromatin structures and chromatin poor spaces. Figure 14A illustrates chromatin organization (white signals) in RPMI 8226 siRNA lamin A/C from 24 to 96 hours, as well as scrRNA. Dark signals were quantified as DNA-poor interchromatin spaces, as shown in RPMI 8226 siRNA lamin A/C as well as scrRNA (Figure 14A). Figure 14B shows granulometry analysis, which measures differences in the DNA-structure at submicron size. In the X- axis we can observe the diameter of DNA structures in µm while the Y-axis shows the frequency distribution of the single cell analysis (Figure 14B). In the zoomed right graph, we can observe decrease of chromatin structures diameter in RPMI 8226 siRNA lamin A/C in 24 hours and 48 hours, compared to scrRNA (Figure 14B). However, in 72 and 96 hours we can observe increased chromatin structures diameter in RPMI 8226 siRNA lamin A/C, compared to scrRNA (Figure 14B). Figure 14C shows dark granulometry analysis, which measures differences in the DNA-poor structures at submicron size. In the zoomed right graph, we can observe decrease of DNA-poor structures diameter in RPMI 8226 siRNA lamin A/C in 24 hours and 48 hours, compared to scrRNA (Figure 14C). However, in 72 and 96 hours we can observe increased DNA-poor structures diameter in RPMI 8226 siRNA lamin A/C, compared to scrRNA (Figure 14C). The two-sided, two-sample Kolmogorov-Smirnov (KS) test was used to analyse differences between RPMI 8226 siRNA and scrRNA.

Figure 14– Quantitative super resolution analysis of chromatin organization in RPMI 8226 with downregulation of Lamin A/C using siRNA

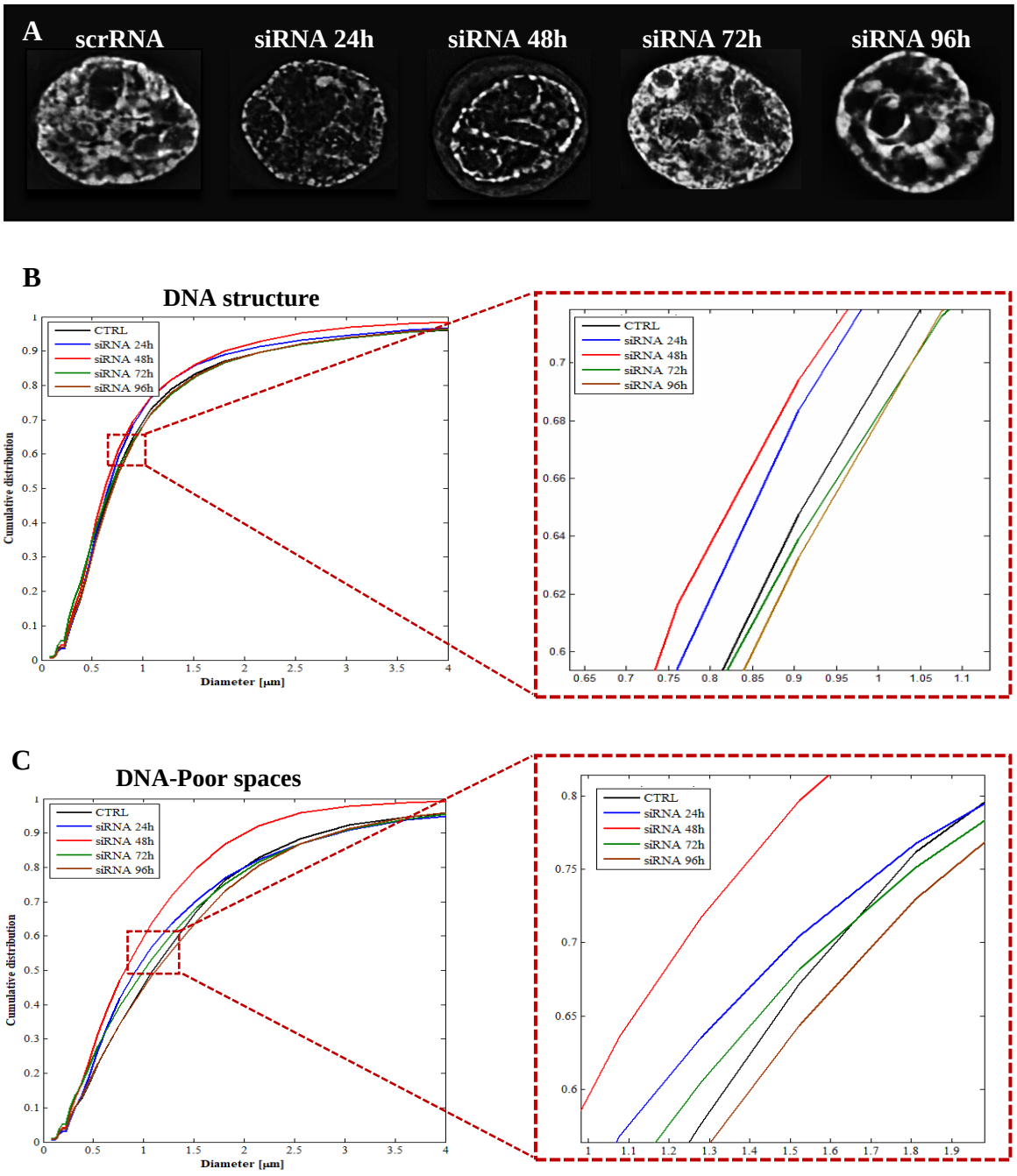

Figure 14. **A** – DNA staining (DAPI) of RPMI 8226 with downregulation of lamin A/C using siRNA and RPMI 8226 with scrRNA. **B** – Quantitative analysis of DNA structures in RPMI 8226 with downregulation of lamin A/C using siRNA and RPMI 8226 with scrRNA. Decreases in chromatin signal diameters were observed at 24 and 48 (p<0.01) hours after siRNA treatment, while increases in chromatin signal diameter were found at 72 and 96 (p<0.01) hours

after siRNA treatment, compared to scrRNA. **C** – Quantitative analysis of DNA-poor structures in RPMI 8226 with downregulation of lamin A/C using siRNA, and RPMI 8226 with scrRNA. Decreases in DNA-poor signal diameters were observed at 24 and 48 hours after siRNA treatment, while increases in DNA-free signal diameter were found at 72 and 96 hours after siRNA transduction, compared to scrRNA. Data expressed as non-linear regression.

6.9. Lamin A/C downregulation in RPMI 8226 using shRNA

Transient downregulation of lamin A/C using siRNA leads to heterogeneous protein depletion, as previously showed here. Stable protein downregulation would unravel the effects of prolonged lamin A/C downregulation to chromosome territories. Therefore, to evaluate the effects of lamin A/C downregulation on chromosome territories and cell viability, I performed a stable downregulation of lamin A/C using a short hairpin RNA (shRNA), and non target shRNA as control. Figure 15 shows western blot of lamin A/C in RPMI 8226 one week after shRNA treatment, 2 weeks after, 2.5 weeks and 3 weeks, α-tubulin was used as house keeping protein. We can observe that after 1 week of shRNA treatment, lamin A/C protein was downregulated, compared to non-target shRNA. However, lamin A/C levels returned to basal production over time. Three weeks after shRNA treatment, I observed a complete protein recovery (Figure 15).

Figure 15– Lamin A/C downregulation in RPMI 8226 using shRNA

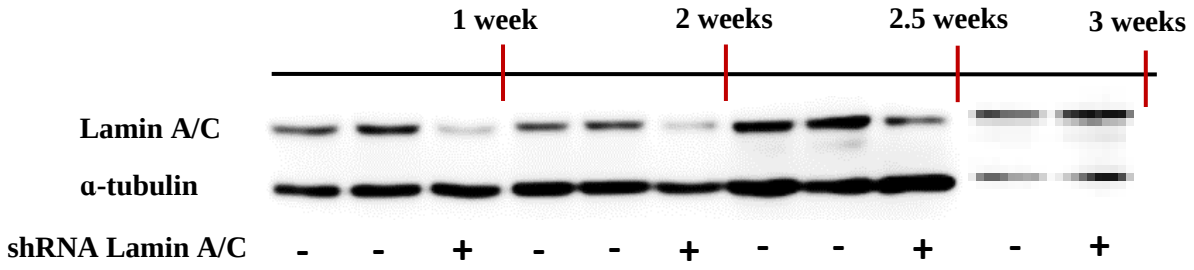

Figure 15. Wester blot (30µg of protein) of lamin A/C in RPMI 8226 with downregulation of lamin A/C using shRNA. Downregulation of lamin A/C is shown 1 week after shRNA treatment. Lamin A/C protein levels recovers over time as observed after 3 weeks of shRNA treatment.

6.10. Lamin A/C knockout in RPMI 8226 using CRISPR Cas9

To evaluate whether lamin A/C depletion would induce cell death in RPMI 8226, I performed lamin A/C knockout mediated through CRISPR Cas9 system. Figure 16A shows double positive cells for Cas 9 tagged with green fluorescent proteins (GFP) and small guide RNA (sgRNA) tagged with blue florescence protein (BFP) for *LMNA* gene. In figure 16B, we can observe western blot analysis of lamin A/C in RPMI 8226 double positive cells (GFP+/BFP+). No differences in lamin A/C protein were observed between RPMI 8226 double positive, compared to RPMI 8226 GFP+ (Figure 16B). α-tubulin was used as housekeeping protein. Figure 16C shows cell viability analysis of RPMI 8226 double positive cells compared to RPMI 8226 GPF +, using trypan blue exclusion assay. No statistical differences were observed between RPMI double positive cells and RPMI 8226 GFP+ (Figure 16C). Overall, I could not observe any effects of lamin A/C knockout in RPMI 8226 due to methodology limitations of our constitutive CRISPR Cas9 system.

Figure 16– Lamin A/C knockout in RPMI 8226 using CRISPR Cas9

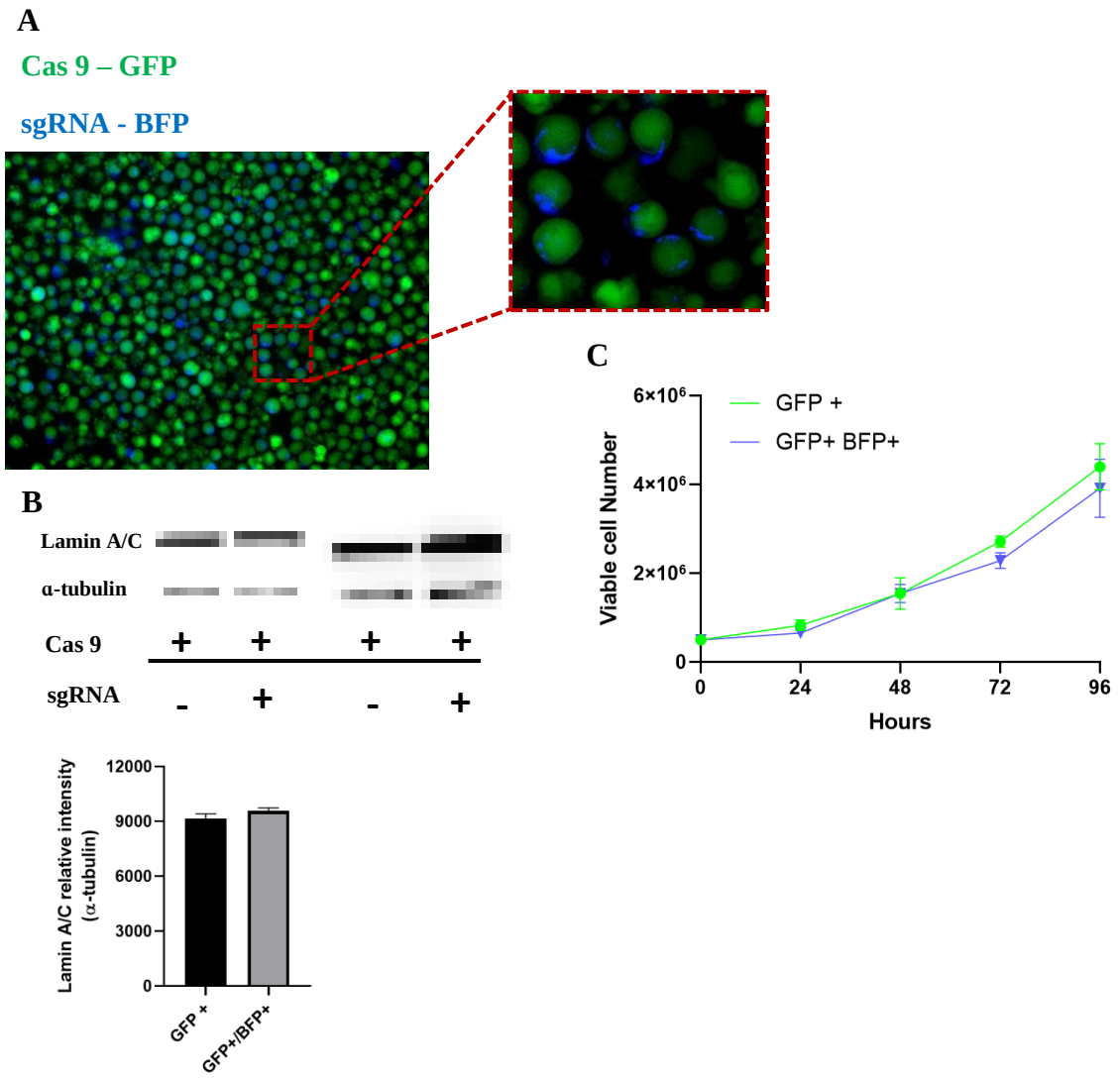

Figure 16. **A** – RPMI 8226 double positive cells for Cas9 (GFP) and sgRNA (BFP). **B** – Western blot of lamin A/C in RPMI 8226 GFP+/BFP+ and RPMI 8226 GFP+. No differences were observed in lamin A/C protein levels between RPMI GFP+/BFP+ and RPMI 8226 GFP+. **C** – Cell viability analysis of RPMI 8226 GFP+/BFP+ and RPMI 8226 GFP+. No differences in cell viability were observed between RPMI GFP+/BFP+ and RPMI 8226 GFP+. Data expressed as mean ± SD.

7. DISCUSSION

MM treatment has shown improved outcomes in the past years, although, MM remains an incurable disease. The discovery of new therapeutical targets remains a major focus in MM. In preliminary data we observed that lamin A/C was overexpressed in 10 primary treatment naïve MM patient's samples. Therefore, I sought to investigate if lamin A/C downregulation would induce cell death and the role of lamin A/C in maintenance of genomic architecture, specifically regarding chromosome organization. The investigation was focused on the effects of lamin A/C downregulation to chromosome organization, MM cell viability, gene expression, λ light chain production, and chromatin structure.

Analysis of lamin A/C protein levels in MM cell lines (MM.1R and RPMI 8226), using immunostaining and western blot showed that RPMI 8226 overexpress lamin A/C compared to MM.1R. Moreover, lamin A/C peripheral structures could be observed in RMPI 8226, while only few cells show lamin A/C expression in MM.1R. Heterogeneous gene expression was demonstrated in MM cells lines and was associated with changes in MM cell phenotype (Harding et al., 2018, Bagratuni et al., 2019, Bong et al., 2022). Moreover, heterogeneous gene expression has been implicated in differences in treatment response and resistance in MM (Harding et al., 2018, Bagratuni et al., 2019, Bong et al., 2022). Furthermore, report of lamin A/C in Hodgkin's Lymphoma shows heterogeneous lamin A/C patterns, which may reflect differences in lamin A/C expression between Hodgkin's Lymphoma cells (Contu et al., 2018). Changes in lamin A/C expression according to disease stages have also been reported, which may account for different levels of lamin A/C expression related to cell origin (Roth et al., 2010, Hutchison et al., 2014, Bell et al., 2016). Additionally, lamin A/C expression profile and implications of lamin A/C variability in MM phenotype have not been addressed to date.

Transient lamin A/C downregulation with siRNAs showed up to 80% lamin A/C inhibition in RPMI 8226 from 48 to 96 hours. Moreover, immunofluorescence analysis of

RPMI 8226 after siRNA treatment revealed that only a few cells maintained lamin A/C expression after 96 hours. However, I could observe that simultaneous transduction of two siRNAs did not increase lamin A/C downregulation. Reports of protein downregulation in MM using siRNA has shown similar downregulation efficiency (up to 50% downregulation in 24 hours) (Peng et al., 2020, Soma et al., 2022). Moreover, studies of lamin A/C downregulation, in cancer cells, have shown heterogeneous lamin A/C disruption, leading to cells with remaining lamin A/C and cells with complete protein suppression (Chaturvedi et al., 2012, Roncato et al., 2021). This result highlights the importance of single cell imaging analysis, which reveals variations in protein downregulation after siRNA treatment.

Cell viability analysis of lamin A/C downregulation in RPMI 8226, using trypan blue exclusion assay and MTT showed no statistical differences between siRNA and scrRNA. Literature lacks reports of transient downregulation of lamin A/C in MM and consequences in cell viability. However, studies in prostate cancer cell lines as well as cervical cancer shows that downregulation of lamin A/C by siRNA also has no effect in cell viability (Guo et al., 2010, Salus et al, 2022). In contrast, downregulation of lamin A/C in circulating tumor cells causes cell death through decrease of resistance to sheer stress forces of the blood stream (Mitchell et al., 2015). Moreover, downregulation of lamin A/C using shRNA in prostate cancer cell lines showed decrease in cell colony formation, cellular migration, and invasion (Kong et al., 2012). Therefore, studies with focus in tumor progression events such as migration and invasion would address the effects of lamin A/C downregulation to late stages of MM development characterized by an increase in circulating tumor cells in blood stream, as called extramedullary plasmacytoma (Zhu et al., 2021).

Chromosome territory analysis of normal B-lymphocytes and MM cell lines revealed altered chromosome position in MM. Many reports in cancer cells have shown altered nuclear architecture related to tumorigenesis process and cancer aggressiveness (Marella et al., 2009,

Bisht et al., 2022, Lima et al., 2022). Studies using patients derived MM samples shows altered chromosome position of CT 4, 9, 11, 14, and 18 (Sathitruangsak et al., 2017). Moreover, gene expression profile analysis of MM patient samples shows that genes placed on altered CT present aberrant expression that may promote MM progression (Broyl et al., 2010, Chen et al., 2022). Therefore, this supports a role of chromosome position in myeloma progression. In this study, we also observe that CT varies within MM cells lines, which most chromosomes that are placed towards nuclear center in MM.1R, are located in the nuclear periphery in RPMI 8226. Many reports on cancer cell lines have shown several differences of gene expression and cell phenotype between cell lines of same disease origin (Harding et al., 2018, Bagratuni et al., 2019, Bong et al., 2022). Furthermore, alteration of nuclear proteins (Emerin, Lamina associated proteins, Lamin B receptor protein, lamin A/C) expression has been corelated to altered chromosome territories (Kinney et al., 2018, Pradhan et al., 2018, Shevelyov et al., 2019, Vivante et al., 2019). Here, I show that expression of lamin A/C is different among MM.1R and RPMI 8226. Furthermore, many studies report the role of lamin A/C in attaching chromatin to nuclear periphery, mostly mediating gene repression (Solovei et al., 2013, Shevelyov et al., 2018). Overall, I suggest that differences in CT between MM cell lines, used in this study, correlate with the heterogeneous lamin A/C expression.

Chromosome territory analysis also revealed that MM cell lines display an altered intrachromosomal distance, compared to normal B-lymphocytes. In summary, MM.1R and RPMI 8226 present an increased intrachromosomal distance for CT 9 and 22 (only RPMI 8226), CT 4 and 14, CT 11 and 14 and CT 14 and 16, while in normal B-lymphocytes the distance between those chromosome pairs is shorter. Several publications have shown that chromosome neighborhood relationship accounts for increased frequency of chromosome translocation (Hakim et al., 2012, Balajee et al., 2018, Barwick et al., 2019). Studies using B-lymphocytes revealed that upon exposure to radiation, the frequency of chromosome

translocation was inversely correlated to chromosome proximity (Balajee et al., 2018). Mouse models of plasmacytoma also corroborates with increased chromosome translocation regarding chromosome proximity (Righolt et al., 2011). Therefore, chromosome proximity would facilitate translocation events to occur, which may play a major role in myelomagenesis. Regarding the increased intrachromosomal distance reported here for MM cell lines, I suggest that chromatin architecture would influence the distance between chromosomes. Some studies report that in MM, plasma cells display increased nuclear size according to gains of chromosome numbers (Seili-Bekafigo et al., 2013, Li et al., 2018, Snyers et al., 2018). Others have reported that chromosome territory volume is also increased in MM (Sathitruangsak et al., 2017). Furthermore, analysis of chromatin structure using super resolution microscopy revealed that MM have a decondensed chromatin structure even in pre symptomatic stages (MGUS) (Sathitruangsak et al., 2015). Therefore, increase chromosome number, increase CT volume and a decondensed chromatin state might play a role in increasing intrachromosomal distance reported here for MM cell lines.

Down regulation of lamin A/C in RPMI 8226 using siRNA altered the chromosome position of CT 4, 9, 11, 14, 16, 18 and 22, compared to scrRNA. Overall, all chromosomes investigated move towards the nuclear center as an effect of lamin A/C downregulation. It is worth mentioning that single cell analysis in combination with co-immuno FISH of lamin A/C and chromosome territories was the key for determining CT alterations upon lamin A/C downregulation, as limitations of siRNA technology led to heterogeneous single cell protein downregulation. Reports on lamin A/C and high-order nuclear architecture shows that lamin A/C is essential for chromatin attachment to peripheral located nuclear lamina and organization of chromosomes by binding chromatin in nucleoplasm (Solovei et al., 2013, Naetar et al., 2017, Shevelyov et al., 2018). Furthermore, studies of lamin A/C disruption have shown to increase chromatin dynamics and changes of CT position (De Vos et al., 2010, Bronshtein et al., 2016,

Ranade et al., 2019). Therefore, our results corroborate with the idea that downregulation of lamin A/C increases chromatin dynamics, thus affecting chromosome position. The impact of increased chromatin dynamics regarding CTs overlapping and possible consequences for chromosome translocations and rearrangements were not investigated here. However, the intrachromosomal distance of chromosome pairs used in this study was not affected by downregulation of lamin A/C, which suggests that lamin A/C downregulation would not modulate intrachromosomal distance between chromosomes.

Analysis of gene expression in RPMI 8226 after siRNA treatment (72 hours) shows up-regulation of *CCND1, BCMA*, *MAF*, *MALT 1* and *BCL3* genes, compared to scrRNA (72 hours). Those genes are placed on chromosomes 11, 16, 18 and 19 respectively. The same chromosomes showed altered CT position after lamin A/C downregulation. Reports on chromatin architecture as gene expression modulators states that genes placed on nuclear center have increased transcription rate, compared to genes placed on nuclear periphery (Chen et al., 2018). Therefore, movements of CT to nuclear center may induce up regulation of gene expression. Furthermore, attachment of genes to the nuclear Lamina through lamina associated domains (LADs) represents a powerful mechanism of gene repression (Chen et al., 2018, Lochs et al., 2019, Wong et al., 2021). Reports of lamin A/C disruption shows increase overall gene expression by lacking chromatin binding to nuclear Lamina (Dubik and Mai, 2020). Thus, increased gene expression reported here may be related to decreased chromatin interaction with nuclear lamina. In addition, lamin A/C also interacts with gene promoters and histones, mediating indirect gene expression regulation (Dubik and Mai, 2020). Downregulation of lamin A/C induces lamin A/C dissociation from gene promoters, increasing protomers availability for transcriptional machinery and histone modifications in studies using adipocytes (Lund et al., 2013). Furthermore, open chromatin state has been associated with increased gene transcription (Kikutake et al., 2022). Therefore, downregulation of lamin A/C may increase

chromatin permissiveness to the transcriptional process, which may trigger alterations on gene expression.

Expression of *CCND1, MAF* and *BCL3* in MM cells have been associated with enhanced cell cycle progression (stimulating MM cell growth), increase survival and resistance to chemotherapy (Hurt et al., 2004, Brenne et al., 2009, Sewify et al., 2014, Jiang et al., 2022, Jiang et al., 2022). While expression of *BCMA* and *MALT 1* is correlated to activation of NF-κB pathway, which also promotes MM cell growth and cell survival (Otsuyama et al., 2008, Demchenko et al., 2010, Tai et al., 2016, Vrábel et al., 2019). Furthermore, inhibition of NF-κB pathway has shown to decrease MM cell growth (Jourdan et al., 2007). Up-regulation of the genes reported in this study could be related to the processes regarding lamin A/C downregulation and changes on high-order chromatin architecture as previously discussed, or it can reflect a mechanism of resistance to lamin A/C downregulation, once we did not observe changes on growth rate of RPMI 8226 (siRNA-lamin A/C), compared to scrRNA using cell counting and indirect measure of cell viability by MTT assay.

Production of immunoglobulins by MM cells is a characteristic marker of MM disease and it is associated with the end organ damage observed in MM (Hemminki et al., 2021, Sadaf et al., 2022). Analysis of λ light chain production of RPMI 8226 siRNA (96 hours) did not show any statistical differences compared to scrRNA, despite movements of CT14 to nuclear center. Modulation of immunoglobulin production would be great value as supportive therapy to MM patients by preventing multiple organs failure. Future research needs to address new strategies to decrease immunoglobulin production by MM cells.

Investigations of chromatin structure and chromatin free spaces in PRMI 8226 siRNA lamin A/C (24 to 96 hours) shows alterations of chromatin state as results of increased chromatin dynamics. It was observed that downregulation of lamin A/C increases chromatin

condensation in 24 and 48 hours, followed by chromatin decondensation in 72 and 96 hours, compared to scrRNA. Increase chromatin dynamics can be attributed to downregulation of lamin A/C as reported by others (Dubik and Mai, 2020). Chromatin decondensation may reflex lamin A/C recovery, due to limitations of transient protein downregulation using siRNA. Although reports on chromatin analysis using super resolution microscopy in MM derived patient' samples show that MM present with an overall open chromatin state, impacts of lamin A/C or other proteins downregulation was not investigated to date (Sathitruangsak et al., 2015). Therefore, I am the first to report that lamin A/C downregulation induces chromatin rearrangement in MM. Furthermore, increase chromatin dynamics and an open chromatin state could correlate with the up-regulated genes reported here.

Constitutive downregulation of lamin A/C in RPMI 8226 using shRNA was performed in order to determine possible effects to chromosome territories and cell viability in MM. Downregulation of 50% of lamin A/C was observed in the first week after cell selection using puromycin. Lamin A/C returned to basal expression levels after 3.5 weeks in regular conditions of cell culture. Therefore, no other investigations were performed using the shRNA RPMI 8226 cells. Furthermore, the mechanism of lamin A/C recovery after transduction with shRNA could not be addressed in this study.

Lamin A/C knockout using CRISPR Cas9 was used to determine effects of lamin A/C disruption to chromosome territories and cell viability in MM. RPMI 8226 was transfected to express both Cas 9 (GFP) protein and small guide RNAs (BFP) for *LMNA* gene. After cell sorting using flow cytometry, no differences were observed on lamin A/C protein levels as well as cell viability on double positive cells (GFP+/BFP+). CRISPR Cas9 current limitations includes high frequency of off targets regarding binding of sgRNA to different genomic areas (Zhang et al., 2015, Albadri et al., 2017, Uddin et al., 2020). Furthermore, as hypothesized in

this study, lamin A/C knock out is lethal to MM. Loss of knock-out cell population before cell sorting could interfere with selecting lamin A/C knock out cells.

8. Summary and Conclusions

Lamin A/C is required for the maintenance of chromosome territories and regulation of different cellular processes related to cell migration, invasion, nuclear structure, DNA-damage responses, and gene expression. Our preliminary data shows that lamin A/C is overexpressed in 10 primary treatment naïve MM patient' samples. Therefore, I sought to investigate the role of lamin A/C in MM, specifically the effects of lamin A/C downregulation to chromosome territories organization, cell viability, and gene expression.

In this study I was able to show that MM cell lines display an heterogenous expression of lamin A/C protein. Lamin A/C expression may correlate with MM disease development and cell phenotype. Future studies will determine if lamin A/C can be used as a MM biomarker.

Altered chromosome position was reported here, among MM cells lines in comparison to normal B-lymphocytes. Altered chromosome territories among MM cells lines were attributed to differences in lamin A/C expression. Moreover, altered chromosome territories have been associated to the tumorigenic process. Therefore, CT may play a role on myelomagenesis. Furthermore, intrachromosomal distances of chromosome pairs here analysed revealed that normal B-lymphocytes display smallest distance between chromosomes, compared to MM cell lines. Increased chromosome proximity in B-lymphocytes facilitates translocation events to occur, which may explain why MM present a variety of chromosome translocations and support the role of CT in myelomagenesis.

Downregulation of lamin A/C using siRNA have consequences in chromosome positioning, gene expression and chromatin state. Chromosome territories intermingled to nuclear center in RPMI 8226 siRNA lamin A/C, reflecting the key role of lamin A/C in

organizing genome architecture in MM. Increased gene expression of specific genes as an effect of lamin A/C depletion or indirectly related to CT intermingle to nuclear center was suggested. Furthermore, increased gene expression of cell survival pathways may reflect a possible resistance mechanism in MM as changes on cell viability was not observed in this study for RPMI 8226 siRNA lamin A/C. Analysis of chromatin state in RPMI 8226 siRNA lamin A/C shows that chromatin and DNA-poor spaces starts to condensate (24 to 48 hours), followed by chromatin decondensation (72 to 96 hours). Lamin A/C plays a key role binding chromatin site and organizing chromatin into the nuclear architecture. I concluded that its downregulation led to changes on chromatin state, reversed by protein rescue, as result of siRNA limitations.

Lamin A/C downregulation using shRNA could not provide stable lamin A/C knockdown. Furthermore, use of CRISPR Cas9 could not determine if lamin A/C knockout would induce MM cell death. Limitations regarding stability of protein knockdown and protein knockout may take place in this study. RPMI 8226 restored lamin A/C expression over time, this was attributed as a potential mechanism of resistance of MM. Regarding lamin A/C knockout, our CRISPR Cas9 model was not able to disrupt lamin A/C protein levels or if disruptive effect had happened cells could not maintain their integrity and died consequently.

Overall, this study provides new insight into the role of lamin A/C as genome architecture modulator and its role on chromosome territories maintenance in MM. Future studies needs to determine if stable downregulation no lamin A/C or its knockout would induce MM cells death.

9. Limitations and Future Directions

The effects of transient lamin A/C downregulation using siRNA to chromosome territories, gene expression and cell viability were addressed in this study. However, limitations of siRNA technology led us to a heterogeneous cell population that was still expressing lamin A/C. The development of stable lamin A/C downregulation using shRNA would overcome this issue. However, complete protein recovery after 3-4 weeks of shRNA treatment was observed, which suggests a MM cell defence mechanism against lamin A/C downregulation. The disruption of lamin A/C using CRISPR Cas9 was not achieved successfully in this study once no decreases in lamin A/C protein levels were observed. Usage of inducible CRISPR Cas9 system would better addresses whether lamin A/C knock out is affecting cell viability in MM. The inducible CRISPR model makes possible to control the time of the genetic alteration, which facilitates the investigation of any possible effects of lamin A/C disruption to MM cells (Sun et al., 2019, Lundin et al., 2020).

Analysis of lamin A/C expression in MM patient samples in different stages of MM (MGUS and SMM) would address the role of lamin A/C in MM progression. Moreover, downregulation of lamin A/C in patient derived MM cells (MGUS, SMM and MM) would better determine the effects of lamin A/C disruption according to MM development *in vitro*. Furthermore, xenograft mouse models using patients derived MM cells (in different stages of development) would unravel the effects of lamin A/C downregulation *in vivo*. Furthermore, analysis of gene expression and chromosome position using *in situ* RNA-FISH would address the relationship between chromosome position and gene expression regulation in different stages of MM development.

10. Supplementary Figures

Figure S1 – Whole chromosome painting probes validation in metaphase spreads of MM.1R

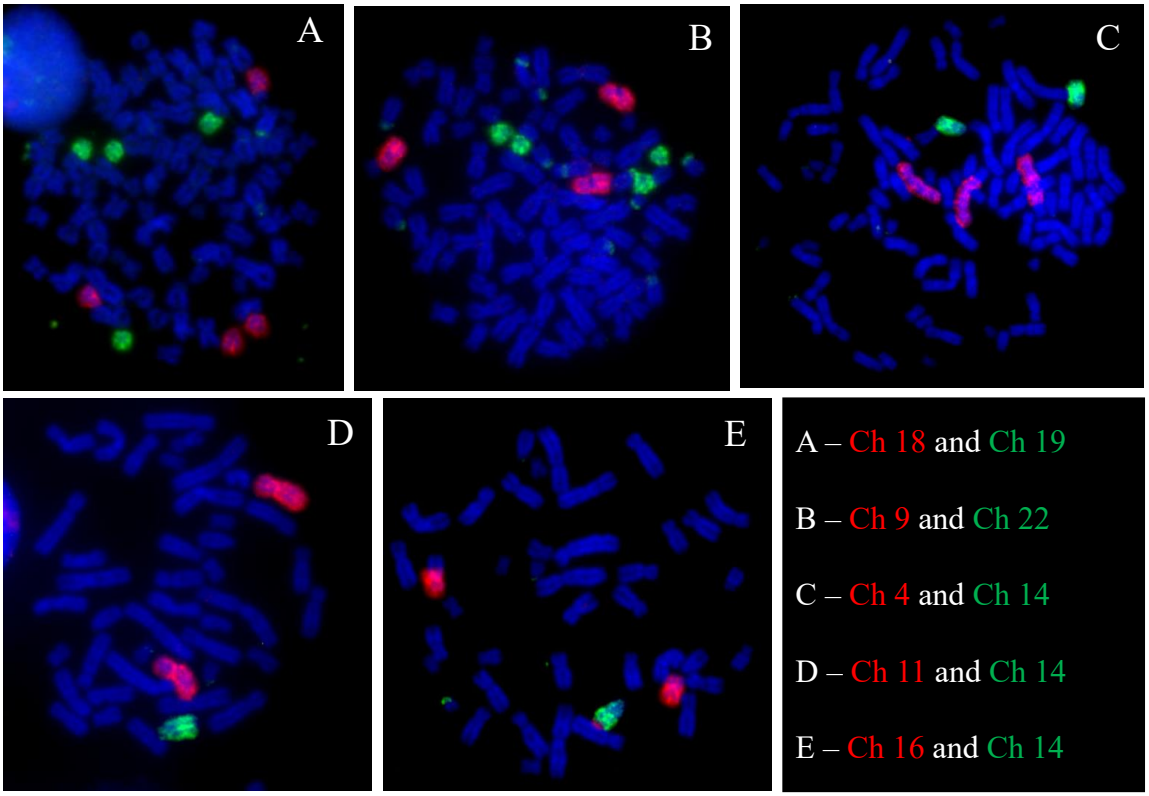

Figure S1. **A** – E Whole chromosome painting probes validation in metaphase spreads of MM.1R. **A** – Chromosomes 18 (red) and 19 (green). **B** – Chromosomes 9 (red) and 22 (green). **C** – Chromosomes 4 (red) and 14 (green). **D** – Chromosomes 11 (red) and 14 (green). **E** – Chromosomes 16 (red) and 14 (green). Ch – Chromosomes.

Figure S2 – Co-immune 3D FISH of RPMI 8226 Validation

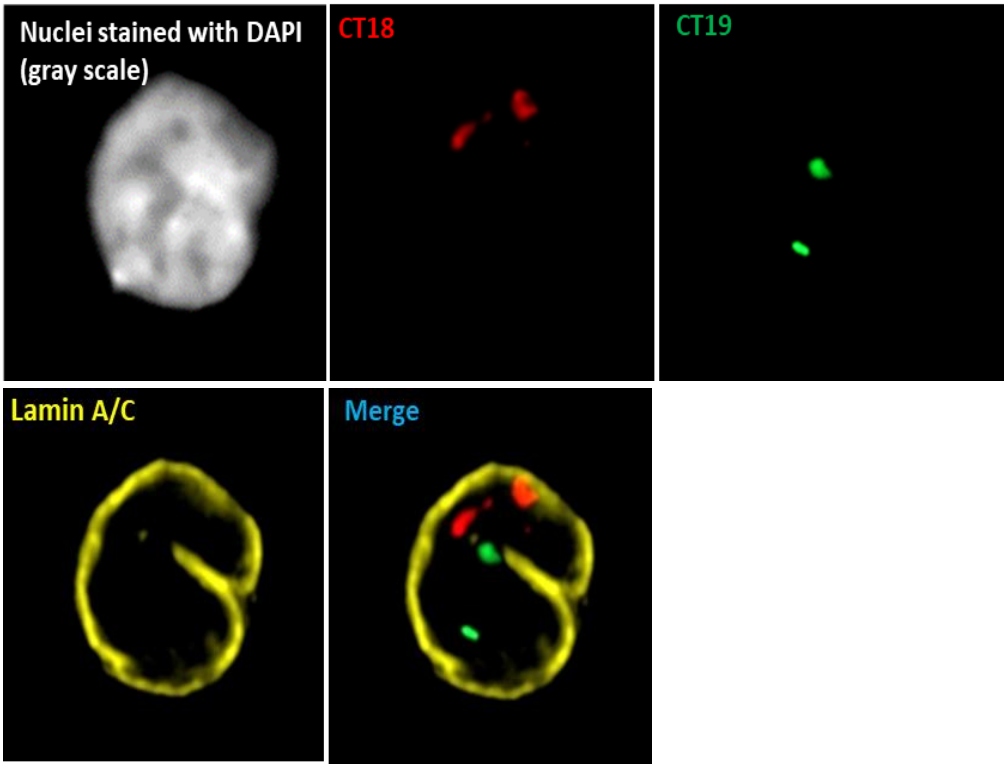

Figure S2. Co-immune 3D FISH of RPMI 8226. Chromosomes territories 18 (Red - Cy3) and chromosome territories 19 (Green – FITC). Lamin A/C is labeled with Cy5 (Yellow). Co-immune FISH was used to select RPMI 8226 cells that do not show lamin A/C expression after siRNA downregulation.

11. REFERENCES

Abdallah, Nadine, et al. "Cytogenetic abnormalities in multiple myeloma: association with disease characteristics and treatment response." Blood cancer journal 10.8 (2020): 1-9.

ACHIM, Camelia, et al. "kidney disease in multiple myeloma–clinical features and diagnosis." Proc. Rom. Acad., Series B, 2021, 23(3), p. 237–244

Adkins, Nicholas L., Meagan Watts, and Philippe T. Georgel. "To the 30-nm chromatin fiber and beyond." Biochimica et Biophysica Acta (BBA)-Gene Structure and Expression 1677.1-3 (2004): 12-23.

Aktas Samur, Anil, et al. "Deciphering the chronology of copy number alterations in Multiple Myeloma." Blood cancer journal 9.4 (2019): 1-10.

Al Hamed, Rama, et al. "Current status of autologous stem cell transplantation for multiple myeloma." Blood cancer journal 9.4 (2019): 1-10.

Albadri, Shahad, Filippo Del Bene, and Céline Revenu. "Genome editing using CRISPR/Cas9-based knock-in approaches in zebrafish." Methods 121 (2017): 77-85.

Al-Saaidi, Rasha, and Peter Bross. "Do lamin A and lamin C have unique roles?." Chromosoma 124.1 (2015): 1-12.

An, Gang, et al. "t (11; 14) multiple myeloma: a subtype associated with distinct immunological features, immunophenotypic characteristics but divergent outcome." Leukemia Research 37.10 (2013): 1251-1257.

Anderson, Kenneth C. "Lenalidomide and thalidomide: mechanisms of action—similarities and differences." Seminars in Hematology. Vol. 42. WB Saunders, 2005.

Ashby, Cody, et al. "Chromoplexy and chromothripsis are important prognostically in myeloma and deregulate gene function by a range of mechanisms." Blood 134 (2019): 3767.

Bagratuni, Tina, et al. "Toll-like receptor 4 activation promotes multiple myeloma cell growth and survival via suppression of the endoplasmic reticulum stress factor chop." Scientific reports 9.1 (2019): 1-12.

Balajee, Adayabalam S., et al. "Investigation of spatial organization of chromosome territories in chromosome exchange aberrations after ionizing radiation exposure." Health physics 115.1 (2018): 77-89.

Banaszkiewicz, Małgorzata, et al. "New biomarkers of ferric management in multiple myeloma and kidney disease-associated anemia." Journal of Clinical Medicine 8.11 (2019): 1828.

Barwick, Benjamin G., et al. "Multiple myeloma immunoglobulin lambda translocations portend poor prognosis." Nature communications 10.1 (2019): 1-13.

Bell, Emily S., and Jan Lammerding. "Causes and consequences of nuclear envelope alterations in tumour progression." European journal of cell biology 95.11 (2016): 449-464.

Berezney, Ronald. "Regulating the mammalian genome: the role of." Advances in enzyme regulation 42 (2002): 39.

Bergsagel, P. Leif, and W. Michael Kuehl. "Chromosome translocations in multiple myeloma." Oncogene 20.40 (2001): 5611-5622.

Bisht, Madhoolika, et al. "Distinct chromosome territory organization and dynamics in cancer cells." Biophysical Journal 121.3 (2022): 476a.

Bolli, Niccolo, et al. "Analysis of the genomic landscape of multiple myeloma highlights novel prognostic markers and disease subgroups." Leukemia 32.12 (2018): 2604-2616.

Bolli, Niccolò, et al. "Genomic patterns of progression in smoldering multiple myeloma." Nature communications 9.1 (2018): 1-10.

Bolzer, Andreas, et al. "Three-dimensional maps of all chromosomes in human male fibroblast nuclei and prometaphase rosettes." PLoS biology 3.5 (2005): e157.

Bong, Ivyna Pau Ni, et al. "Gene expression profiling and in vitro functional studies reveal RAD54L as a potential therapeutic target in multiple myeloma." Genes & Genomics (2022): 1-10.

Boyd, Kevin D., et al. "Mapping of chromosome 1p deletions in myeloma identifies FAM46C at 1p12 and CDKN2C at 1p32. 3 as being genes in regions associated with adverse survival." Clinical cancer research 17.24 (2011): 7776-7784.

Branco, Miguel R., and Ana Pombo. "Intermingling of chromosome territories in interphase suggests role in translocations and transcription-dependent associations." PLoS biology 4.5 (2006): e138.

Brenne, Anne-Tove, et al. "High expression of BCL3 in human myeloma cells is associated with increased proliferation and inferior prognosis." European journal of haematology 82.5 (2009): 354-363.

Brenner, Darren R., et al. "Projected estimates of cancer in Canada in 2022." CMAJ 194.17 (2022): E601-E607.

Bridoux, Frank, et al. "Management of acute kidney injury in symptomatic multiple myeloma." Kidney International 99.3 (2021): 570-580.

Brito, Jose LR, et al. "MMSET deregulation affects cell cycle progression and adhesion regulons in t (4; 14) myeloma plasma cells." haematologica 94.1 (2009): 78.

Broers, J. L., et al. "Dynamics of the nuclear lamina as monitored by GFP-tagged A-type lamins." Journal of cell science 112.20 (1999): 3463-3475.

Broers, Jos LV, et al. "Both lamin A and lamin C mutations cause lamina instability as well as loss of internal nuclear lamin organization." Experimental cell research 304.2 (2005): 582-592.

Bronshtein, I., et al. "Loss of lamin A function increases chromatin dynamics in the nuclear interior." Nature communications 6.1 (2015): 1-9.

Bronshtein, Irena, et al. "Exploring chromatin organization mechanisms through its dynamic properties." Nucleus 7.1 (2016): 27-33.

Broyl, Annemiek, et al. "Gene expression profiling for molecular classification of multiple myeloma in newly diagnosed patients." Blood, The Journal of the American Society of Hematology 116.14 (2010): 2543-2553.

Brünnert, Daniela, et al. "Novel cell line models to study mechanisms and overcoming strategies of proteasome inhibitor resistance in multiple myeloma." Biochimica et biophysica acta (BBA)-molecular basis of disease 1865.6 (2019): 1666-1676.

Bruno, Benedetto, et al. "European Myeloma Network perspective on CAR T-Cell therapies for multiple myeloma." Haematologica 106.8 (2021): 2054.

Bustoros, Mark, et al. "Genomic profiling of smoldering multiple myeloma identifies patients at a high risk of disease progression." Journal of Clinical Oncology 38.21 (2020): 2380.

Campbell, Bruce CV, et al. "Endovascular therapy for ischemic stroke with perfusion-imaging selection." New England Journal of Medicine 372.11 (2015): 1009-1018.

Capo-Chichi, Callinice D., et al. "Lamin A/C deficiency is an independent risk factor for cervical cancer." Cellular Oncology 39.1 (2016): 59-68.

Cavo, Michele, et al. "Bortezomib with thalidomide plus dexamethasone compared with thalidomide plus dexamethasone as induction therapy before, and consolidation therapy after,

double autologous stem-cell transplantation in newly diagnosed multiple myeloma: a randomised phase 3 study." The Lancet 376.9758 (2010): 2075-2085.

Cejalvo, María J., and Javier de la Rubia. "Which therapies will move to the front line for multiple myeloma?." Expert Review of Hematology 10.5 (2017): 383-392.

Chang, Pearl, et al. "Computational methods for assessing chromatin hierarchy." Computational and structural biotechnology journal 16 (2018): 43-53.

Chapman, Michael A., et al. "Initial genome sequencing and analysis of multiple myeloma." Nature 471.7339 (2011): 467-472.

Chaturvedi, Pankaj, Richa Khanna, and Veena K. Parnaik. "Ubiquitin ligase RNF123 mediates degradation of heterochromatin protein 1α and β in lamin A/C knock-down cells." (2012): e47558.

Chen, D., et al. "Bortezomib as the first proteasome inhibitor anticancer drug: current status and future perspectives." Current cancer drug targets 11.3 (2011): 239-253.

Chen, Shiwei, et al. "A lamina-associated domain border governs nuclear lamina interactions, transcription, and recombination of the Tcrb locus." Cell reports 25.7 (2018): 1729-1740.

Chen, Yan-Ting, et al. "Prognostic gene expression analysis in a retrospective, multinational cohort of 155 multiple myeloma patients treated outside clinical trials." International Journal of Laboratory Hematology 44.1 (2022): 127-134.

Chen, Yu, et al. "Mapping 3D genome organization relative to nuclear compartments using TSA-Seq as a cytological ruler." Journal of Cell Biology 217.11 (2018): 4025-4048.

Chng, W. J., et al. "IMWG consensus on risk stratification in multiple myeloma." Leukemia 28.2 (2014): 269-277.

Chng, W. J., et al. "Prognostic factors for hyperdiploid-myeloma: effects of chromosome 13 deletions and IgH translocations." Leukemia 20.5 (2006): 807-813.

Chretien, Marie-Lorraine, et al. "Understanding the role of hyperdiploidy in myeloma prognosis: which trisomies really matter?." Blood, The Journal of the American Society of Hematology 126.25 (2015): 2713-2719.

Chüeh, Anderly C., et al. "ATF3 repression of BCL-XL determines apoptotic sensitivity to HDAC inhibitors across tumor types." Clinical Cancer Research 23.18 (2017): 5573-5584.

Collins, Shauna M., et al. "Elotuzumab directly enhances NK cell cytotoxicity against myeloma via CS1 ligation: evidence for augmented NK cell function complementing ADCC." Cancer Immunology, Immunotherapy 62.12 (2013): 1841-1849.

Contu, Fabio, et al. "Distinct 3D structural patterns of lamin A/C expression in Hodgkin and Reed-Sternberg cells." Cancers 10.9 (2018): 286.

Corre, Jill, Nikhil Munshi, and Hervé Avet-Loiseau. "Genetics of multiple myeloma: another heterogeneity level?." Blood, The Journal of the American Society of Hematology 125.12 (2015): 1870-1876.

Cremer, Thomas, and Christoph Cremer. "Chromosome territories, nuclear architecture and gene regulation in mammalian cells." Nature reviews genetics 2.4 (2001): 292-301.

Cremer, Thomas, and Marion Cremer. "Chromosome territories." Cold Spring Harbor perspectives in biology 2.3 (2010): a003889.

D'Agostino, Mattia, and Noopur Raje. "Anti-BCMA CAR T-cell therapy in multiple myeloma: can we do better?." Leukemia 34.1 (2020): 21-34.

de Castro, Inês J., et al. "Altered nuclear architecture in blood cells from Huntington's disease patients." Neurological Sciences 43.1 (2022): 379-385.

De Vos, Winnok H., et al. "Increased plasticity of the nuclear envelope and hypermobility of telomeres due to the loss of A–type lamins." Biochimica et Biophysica Acta (BBA)-General Subjects 1800.4 (2010): 448-458.

Demchenko, Yulia N., et al. "Classical and/or alternative NF-κB pathway activation in multiple myeloma." Blood, The Journal of the American Society of Hematology 115.17 (2010): 3541-3552.

Dimopoulos, Meletios A., et al. "Carfilzomib and dexamethasone versus bortezomib and dexamethasone for patients with relapsed or refractory multiple myeloma (ENDEAVOR): a randomised, phase 3, open-label, multicentre study." The Lancet Oncology 17.1 (2016): 27-38.

Dissanayaka, D. W. V. N., et al. "Oral manifestations of systemic amyloidosis, an aid to diagnosis of multiple myeloma-report of two cases." Brazilian Journal of Otorhinolaryngology 88 (2022): 146-149.

Dittmer, Travis A., and Tom Misteli. "The lamin protein family." Genome biology 12.5 (2011): 1-14.

Dubik, Niina, and Sabine Mai. "Lamin A/C: Function in normal and tumor cells." Cancers 12.12 (2020): 3688.

Fonseca, Rafael, et al. "Deletions of chromosome 13 in multiple myeloma identified by interphase FISH usually denote large deletions of the q arm or monosomy." Leukemia 15.6 (2001): 981-986.

Fonseca, Rafael, et al. "International Myeloma Working Group molecular classification of multiple myeloma: spotlight review." Leukemia 23.12 (2009): 2210-2221.

Foster, Clare R., et al. "Lamins as cancer biomarkers." Biochemical Society Transactions 38.1 (2010): 297-300.

Foster, Clare R., et al. "The role of Lamin A in cytoskeleton organization in colorectal cancer cells: a proteomic investigation." Nucleus 2.5 (2011): 434-443.

Furukawa, Yusuke, and Jiro Kikuchi. "Molecular basis of clonal evolution in multiple myeloma." International Journal of Hematology 111.4 (2020): 496-511.

Galiová, Gabriela, et al. "Chromatin changes induced by lamin A/C deficiency and the histone deacetylase inhibitor trichostatin A." European journal of cell biology 87.5 (2008): 291-303.

Georgakopoulou, Rebecca, et al. "Occupational Exposure and Multiple Myeloma Risk: An Updated Review of Meta-Analyses." Journal of Clinical Medicine 10.18 (2021): 4179.

Gertz, Morie A., et al. "Clinical implications of t (11; 14)(q13; q32), t (4; 14)(p16. 3; q32), and-17p13 in myeloma patients treated with high-dose therapy." Blood 106.8 (2005): 2837-2840.

Goldman-Mazur, Sarah, et al. "A multicenter retrospective study of 223 patients with t (14; 16) in multiple myeloma." American journal of hematology 95.5 (2020): 503-509.

Guo, Shutao, et al. "Enhanced gene delivery and siRNA silencing by gold nanoparticles coated with charge-reversal polyelectrolyte." ACS nano 4.9 (2010): 5505-5511.

Hakim, Ofir, et al. "DNA damage defines sites of recurrent chromosomal translocations in B lymphocytes." Nature 484.7392 (2012): 69-74.

Han, Zhijun, et al. "Diploid genome architecture revealed by multi-omic data of hybrid mice." Genome research 30.8 (2020): 1097-1106.

Hansen, Anders S. "CTCF as a boundary factor for cohesin-mediated loop extrusion: evidence for a multi-step mechanism." Nucleus 11.1 (2020): 132-148.

Hansen, Vincent L., et al. "An expanded treatment protocol of panobinostat plus bortezomib and dexamethasone in patients with previously treated myeloma." Clinical Lymphoma Myeloma and Leukemia 18.6 (2018): 400-407.

Harabula, Izabela, and Ana Pombo. "The dynamics of chromatin architecture in brain development and function." Current opinion in genetics & development 67 (2021): 84-93.

Harding, Taylor, Jessica Swanson, and Brian Van Ness. "EZH2 inhibitors sensitize myeloma cell lines to panobinostat resulting in unique combinatorial transcriptomic changes." Oncotarget 9.31 (2018): 21930.

Harizanova, Jana, Cheryl Taylor-Kashton, and Sabine Mai. "Summary of the quantitative analyses of the three-dimensional distribution of chromosomes in mouse cells." Cancer Research 68.9_Supplement (2008): 809-809.

Hemminki, Kari, et al. "Epidemiology, genetics and treatment of multiple myeloma and precursor diseases." International Journal of Cancer 149.12 (2021): 1980-1996.

Hurt, Elaine M., et al. "Overexpression of c-maf is a frequent oncogenic event in multiple myeloma that promotes proliferation and pathological interactions with bone marrow stroma." Cancer cell 5.2 (2004): 191-199.

Hutchison, Christopher J. "Do lamins influence disease progression in cancer?." Cancer Biology and the Nuclear Envelope (2014): 593-604.

Ikegami, Kohta, et al. "Phosphorylated lamin A/C in the nuclear interior binds active enhancers associated with abnormal transcription in progeria." Developmental cell 52.6 (2020): 699-713.

Jiang, Qiuyun, et al. "Targeting the oncogenic transcription factor c-Maf for the treatment of multiple myeloma." Cancer Letters (2022): 215791.

Jiang, Yuwen, et al. "The prognostic role of cyclin D1 in multiple myeloma: a systematic review and meta-analysis." Technology in Cancer Research & Treatment 21 (2022): 15330338211065252.

Jin, Yi, et al. "Active enhancer and chromatin accessibility landscapes chart the regulatory network of primary multiple myeloma." Blood, The Journal of the American Society of Hematology 131.19 (2018): 2138-2150.

Jourdan, Michel, et al. "Targeting NF-κB pathway with an IKK2 inhibitor induces inhibition of multiple myeloma cell growth." British journal of haematology 138.2 (2007): 160-168.

Kaweme, Natasha Mupeta, Geoffrey Joseph Changwe, and Fuling Zhou. "Approaches and challenges in the management of multiple myeloma in the very old: future treatment prospects." Frontiers in Medicine 8 (2021): 180.

Keats, Jonathan J., et al. "In multiple myeloma, t (4; 14)(p16; q32) is an adverse prognostic factor irrespective of FGFR3 expression." Blood, The Journal of the American Society of Hematology 101.4 (2003): 1520-1529.

Khalyfa, Ahamed, Alessandra C. Carrillo, and Yhana Chavis. "An Unusual Presentation of Multiple Myeloma: A 71-Year-Old Female With a Single Lytic Lesion of Her Appendicular Skeleton." Cureus 14.5 (2022).

Kikutake, Chie, and Mikita Suyama. "Pan-cancer analysis of mutations in open chromatin regions and their possible association with cancer pathogenesis." *Cancer Medicine* (2022).

Kinney, Nicholas Allen, Igor V. Sharakhov, and Alexey V. Onufriev. "Chromosome–nuclear envelope attachments affect interphase chromosome territories and entanglement." Epigenetics & chromatin 11.1 (2018): 1-18.

Kloosterman, Wigard P., Jan Koster, and Jan J. Molenaar. "Prevalence and clinical implications of chromothripsis in cancer genomes." Current opinion in oncology 26.1 (2014): 64-72.

Kong, Lu, et al. "Lamin A/C protein is overexpressed in tissue-invading prostate cancer and promotes prostate cancer cell growth, migration and invasion through the PI3K/AKT/PTEN pathway." Carcinogenesis 33.4 (2012): 751-759.

Kong, Lu, et al. "Lamin A/C protein is overexpressed in tissue-invading prostate cancer and promotes prostate cancer cell growth, migration and invasion through the PI3K/AKT/PTEN pathway." Carcinogenesis 33.4 (2012): 751-759.

Kortüm, K. Martin, et al. "Targeted sequencing of refractory myeloma reveals a high incidence of mutations in CRBN and Ras pathway genes." Blood, The Journal of the American Society of Hematology 128.9 (2016): 1226-1233.

Kotla, Venumadhav, et al. "Mechanism of action of lenalidomide in hematological malignancies." Journal of hematology & oncology 2.1 (2009): 1-10.

Kozubek, Stanislav, et al. "The topological organization of chromosomes 9 and 22 in cell nuclei has a determinative role in the induction of t (9, 22) translocations and in the pathogenesis of t (9, 22) leukemias." Chromosoma 108.7 (1999): 426-435.

Krejcik, Jakub, et al. "Daratumumab depletes CD38+ immune regulatory cells, promotes T-cell expansion, and skews T-cell repertoire in multiple myeloma." Blood, The Journal of the American Society of Hematology 128.3 (2016): 384-394.

Kuhn, Deborah J., et al. "Potent activity of carfilzomib, a novel, irreversible inhibitor of the ubiquitin-proteasome pathway, against preclinical models of multiple myeloma." Blood, The Journal of the American Society of Hematology 110.9 (2007): 3281-3290.

Kumar, Shaji K., Francis K. Buadi, and S. Vincent Rajkumar. "Pros and cons of frontline autologous transplant in multiple myeloma: the debate over timing." Blood, The Journal of the American Society of Hematology 133.7 (2019): 652-659.

Kuroda, Masahiko, et al. "Alteration of chromosome positioning during adipocyte differentiation." Journal of cell science 117.24 (2004): 5897-5903.

Kyle, Robert A., et al. "Long-term follow-up of monoclonal gammopathy of undetermined significance." New England journal of medicine 378.3 (2018): 241-249.

Kyle, Robert A., et al. "Review of 1027 patients with newly diagnosed multiple myeloma." Mayo Clinic Proceedings. Vol. 78. No. 1. Elsevier, 2003.

Lagrue, K.; Carisey, A.; Morgan, D.J.; Chopra, R.; Davis, D.M. Lenalidomide augments actin remodeling and

Landgren, Ola, et al. "Monoclonal gammopathy of undetermined significance (MGUS) consistently precedes multiple myeloma: a prospective study." Blood, The Journal of the American Society of Hematology 113.22 (2009): 5412-5417.

Laubach, Jacob P., et al. "Panobinostat for the treatment of multiple myeloma." Clinical cancer research 21.21 (2015): 4767-4773.

Li, Tian-Neng, et al. "Intrahepatic hepatitis B virus large surface antigen induces hepatocyte hyperploidy via failure of cytokinesis." The Journal of pathology 245.4 (2018): 502-513.

Lima, Matheus Fabiao de, et al. "Chromosome Territories in Hematological Malignancies." Cells 11.8 (2022): 1368.

Ling, Silvia CW, et al. "Response of myeloma to the proteasome inhibitor bortezomib is correlated with the unfolded protein response regulator XBP-1." Haematologica 97.1 (2012): 64.

Liu, Dan, and Lin-Li Lv. "New understanding on the role of proteinuria in progression of chronic kidney disease." Renal Fibrosis: Mechanisms and Therapies (2019): 487-500.

Lochs, Silke JA, Samy Kefalopoulou, and Jop Kind. "Lamina associated domains and gene regulation in development and cancer." Cells 8.3 (2019): 271.

Lohr, Jens G., et al. "Widespread genetic heterogeneity in multiple myeloma: implications for targeted therapy." Cancer cell 25.1 (2014): 91-101.

Lonial, Sagar, et al. "Elotuzumab therapy for relapsed or refractory multiple myeloma." New England Journal of Medicine 373.7 (2015): 621-631.

Lonial, Sagar, et al. "Monoclonal antibodies in the treatment of multiple myeloma: current status and future perspectives." Leukemia 30.3 (2016): 526-535.

Lonial, Sagar, Lawrence H. Boise, and Jonathan Kaufman. "How I treat high-risk myeloma." Blood, The Journal of the American Society of Hematology 126.13 (2015): 1536-1543.

lowers NK-cell activation thresholds. Blood 2015, 126, 50–60.

Lu, Shin-Yu, et al. "The status of jaw lesions and medication-related osteonecrosis of jaw in patients with multiple myeloma." Journal of the Formosan Medical Association 120.11 (2021): 1967-1976.

Lund, Eivind, et al. "Lamin A/C-promoter interactions specify chromatin state–dependent transcription outcomes." Genome research 23.10 (2013): 1580-1589.

Lundin, Anders, et al. "Development of an ObLiGaRe doxycycline inducible Cas9 system for pre-clinical cancer drug discovery." Nature communications 11.1 (2020): 1-16.

Maes, Ken, et al. "In anemia of multiple myeloma, hepcidin is induced by increased bone morphogenetic protein 2." Blood, The Journal of the American Society of Hematology 116.18 (2010): 3635-3644.

Mahy, Nicola L., Paul E. Perry, and Wendy A. Bickmore. "Gene density and transcription influence the localization of chromatin outside of chromosome territories detectable by FISH." The Journal of cell biology 159.5 (2002): 753-763.

Malyavantham, Kishore S., et al. "Identifying functional neighborhoods within the cell nucleus: Proximity analysis of early S-phase replicating chromatin domains to sites of transcription, RNA polymerase II, HP1γ, matrin 3 and SAF-A." Journal of cellular biochemistry 105.2 (2008): 391-403.

Malyavantham, Kishore S., et al. "Spatio-temporal dynamics of replication and transcription sites in the mammalian cell nucleus." Chromosoma 117.6 (2008): 553-567.

Mangan, Hazel, and Brian McStay. "Human nucleoli comprise multiple constrained territories, tethered to individual chromosomes." Genes & development 35.7-8 (2021): 483-488.

Manier, Salomon, et al. "Genomic complexity of multiple myeloma and its clinical implications." Nature reviews Clinical oncology 14.2 (2017): 100-113.

Marella, Narasimharao V., et al. "Cell type specific chromosome territory organization in the interphase nucleus of normal and cancer cells." Journal of cellular physiology 221.1 (2009): 130-138.

Martin, Lorri D., et al. "Differential nuclear organization of translocation-prone genes in nonmalignant B cells from patients with t (14; 16) as compared with t (4; 14) or t (11; 14) myeloma." Genes, Chromosomes and Cancer 52.6 (2013): 523-537.

Maura, Francesco, et al. "Genomic landscape and chronological reconstruction of driver events in multiple myeloma." Nature communications 10.1 (2019): 1-12.

Maura, Francesco, et al. "Role of AID in the temporal pattern of acquisition of driver mutations in multiple myeloma." Leukemia 34.5 (2020): 1476-1480.

Mayer, Robert, et al. "Common themes and cell type specific variations of higher order chromatin arrangements in the mouse." BMC cell biology 6.1 (2005): 1-22.

Menè, Paolo, et al. "Light Chain Cast Nephropathy in Multiple Myeloma: Prevalence, Impact and Management Challenges." International Journal of Nephrology and Renovascular Disease 15 (2022): 173.

Mewborn, Stephanie K., et al. "Altered chromosomal positioning, compaction, and gene expression with a lamin A/C gene mutation." PloS one 5.12 (2010): e14342.

Mitchell, Michael J., et al. "Lamin A/C deficiency reduces circulating tumor cell resistance to fluid shear stress." American Journal of Physiology-Cell Physiology 309.11 (2015): C736-C746.

Mohty, Mohamad, et al. "The effects of bortezomib on bone disease in patients with multiple myeloma." Cancer 120.5 (2014): 618-623.

Moreau, Philippe, et al. "Bortezomib plus dexamethasone versus reduced-dose bortezomib, thalidomide plus dexamethasone as induction treatment before autologous stem cell transplantation in newly diagnosed multiple myeloma." Blood, The Journal of the American Society of Hematology 118.22 (2011): 5752-5758.

Moreau, Philippe, Michel Attal, and Thierry Facon. "Frontline therapy of multiple myeloma." Blood, The Journal of the American Society of Hematology 125.20 (2015): 3076-3084.

Morgan, Gareth J., Brian A. Walker, and Faith E. Davies. "The genetic architecture of multiple myeloma." Nature Reviews Cancer 12.5 (2012): 335-348.

Murase, Takayuki, et al. "Plasma cell myeloma positive for t (14; 20) with relapse in the central nervous system." Journal of Clinical and Experimental Hematopathology (2019): 19011.

Naetar, Nana, Simona Ferraioli, and Roland Foisner. "Lamins in the nuclear interior− life outside the lamina." Journal of cell science 130.13 (2017): 2087-2096.

Nakaya, Aya, et al. "Impact of CRAB symptoms in survival of patients with symptomatic myeloma in novel agent era." Hematology reports 9.1 (2017).

Neuse, Carl Jannes, et al. "Genome instability in multiple myeloma." Leukemia 34.11 (2020): 2887-2897.

Nijhof, I. S., et al. "Upregulation of CD38 expression on multiple myeloma cells by all-trans retinoic acid improves the efficacy of daratumumab." Leukemia 29.10 (2015): 2039-2049.

Nijhof, Inger S., et al. "CD38 expression and complement inhibitors affect response and resistance to daratumumab therapy in myeloma." Blood, The Journal of the American Society of Hematology 128.7 (2016): 959-970.

Nozaki, Tadasu, et al. "Dynamic organization of chromatin domains revealed by super-resolution live-cell imaging." Molecular cell 67.2 (2017): 282-293.

Ordoñez, Raquel, et al. "Chromatin activation as a unifying principle underlying pathogenic mechanisms in multiple myeloma." Genome research 30.9 (2020): 1217-1227.

Orlowski, Robert Z., et al. "Phase III (IMROZ) study design: Isatuximab plus bortezomib (V), lenalidomide (R), and dexamethasone (d) vs VRd in transplant-ineligible patients (pts) with newly diagnosed multiple myeloma (NDMM)." (2018): TPS8055-TPS8055.

Osmanagic-Myers, Selma, Thomas Dechat, and Roland Foisner. "Lamins at the crossroads of mechanosignaling." Genes & development 29.3 (2015): 225-237.

Otsuyama, Ken-ichiro, et al. "Biological Significance of Constitutive NF-κB Activity Levels in Human Myeloma Cell Lines." (2008): 5144-5144.

Oudet, P., M. Gross-Bellard, and P. Chambon. "Electron microscopic and biochemical evidence that chromatin structure is a repeating unit." Cell 4.4 (1975): 281-300.

Padala, Sandeep Anand, et al. "Epidemiology, staging, and management of multiple Myeloma." Medical Sciences 9.1 (2021): 3.

Palumbo, Antonio, et al. "Personalized therapy in multiple myeloma according to patient age and vulnerability: a report of the European Myeloma Network (EMN)." Blood, The Journal of the American Society of Hematology 118.17 (2011): 4519-4529.

Palumbo, Antonio, et al. "Revised international staging system for multiple myeloma: a report from International Myeloma Working Group." Journal of clinical oncology 33.26 (2015): 2863.

Peng, Yue, et al. "IGF-1 promotes multiple myeloma progression through PI3K/Akt-mediated epithelial-mesenchymal transition." Life sciences 249 (2020): 117503.

Peric-Hupkes, D., and B. van Steensel. "Role of the nuclear lamina in genome organization and gene expression." Cold Spring Harbor symposia on quantitative biology. Vol. 75. Cold Spring Harbor Laboratory Press, 2010.

Piekarowicz, Katarzyna, et al. "The effect of the lamin A and its mutants on nuclear structure, cell proliferation, protein stability, and mobility in embryonic cells." Chromosoma 126.4 (2017): 501-517.

Pinto, Vanessa, et al. "Multiple myeloma: Available therapies and causes of drug resistance." *Cancers* 12.2 (2020): 407.

Pradhan, Roopali, Devika Ranade, and Kundan Sengupta. "Emerin modulates spatial organization of chromosome territories in cells on softer matrices." Nucleic acids research 46.11 (2018): 5561-5586.

Privalov, Peter L., and Colyn Crane-Robinson. "Forces maintaining the DNA double helix and its complexes with transcription factors." Progress in Biophysics and Molecular Biology 135 (2018): 30-48.

Prokocimer, Miron, Ayelet Margalit, and Yosef Gruenbaum. "The nuclear lamina and its proposed roles in tumorigenesis: projection on the hematologic malignancies and future targeted therapy." Journal of structural biology 155.2 (2006): 351-360.

Puckelwartz, Megan J., Frederic FS Depreux, and Elizabeth M. McNally. "Gene expression, chromosome position and lamin A/C mutations." Nucleus 2.3 (2011): 14342-29.

Qiang, Ya-Wei, et al. "MAF protein mediates innate resistance to proteasome inhibition therapy in multiple myeloma." Blood, The Journal of the American Society of Hematology 128.25 (2016): 2919-2930.

Rajkumar, S. Vincent. "Multiple myeloma: 2018 update on diagnosis, risk-stratification, and management." American journal of hematology 93.8 (2018): 1091-1110.

Rajkumar, S. Vincent. "Multiple myeloma: Every year a new standard?." Hematological oncology 37 (2019): 62-65.

Ranade, Devika, et al. "Lamin A/C and Emerin depletion impacts chromatin organization and dynamics in the interphase nucleus." BMC Molecular and Cell Biology 20.1 (2019): 1-20.

Rassner, Michael, et al. "Dapsone-Induced Hemolytic Anemia in Multiple Myeloma: Case Report of Various Differential Diagnoses." Clinical Lymphoma, Myeloma and Leukemia 20.11 (2020): e821-e825.

Rauschert, Ines, et al. "Promoter hypermethylation as a mechanism for Lamin A/C silencing in a subset of neuroblastoma cells." PLoS One 12.4 (2017): e0175953.

Reagan, Michaela R., et al. "Dynamic interplay between bone and multiple myeloma: emerging roles of the osteoblast." Bone 75 (2015): 161-169.

Reddy, K. L., et al. "Transcriptional repression mediated by repositioning of genes to the nuclear lamina." Nature 452.7184 (2008): 243-247.

Redwood, Abena B., et al. "A dual role for A-type lamins in DNA double-strand break repair." Cell cycle 10.15 (2011): 2549-2560.

Richardson, Paul G., et al. "A phase 2 study of bortezomib in relapsed, refractory myeloma." New England Journal of Medicine 348.26 (2003): 2609-2617.

Righolt, Christiaan H., et al. "Translocation frequencies and chromosomal proximities for selected mouse chromosomes in primary B lymphocytes." Cytometry Part A 79.4 (2011): 276-283.

Roncato, Francesco, et al. "Reduced lamin A/C does not facilitate cancer cell transendothelial migration but compromises lung metastasis." Cancers 13.10 (2021): 2383.

Roschke, Anna V., and Ester Rozenblum. "Multi-layered cancer chromosomal instability phenotype." Frontiers in oncology 3 (2013): 302.

Rosiñol, Laura, et al. "Superiority of bortezomib, thalidomide, and dexamethasone (VTD) as induction pretransplantation therapy in multiple myeloma: a randomized phase 3 PETHEMA/GEM study." Blood, The Journal of the American Society of Hematology 120.8 (2012): 1589-1596.

Roth, Udo, et al. "Differential expression proteomics of human colorectal cancer based on a syngeneic cellular model for the progression of adenoma to carcinoma." Proteomics 10.2 (2010): 194-202.

Sadaf, Humaira, et al. "Multiple myeloma etiology and treatment." Journal of Translational Genetics and Genomics 6.1 (2022): 63-83.

Sakthivel, Kunnathur Murugesan, and Poonam Sehgal. "A novel role of lamins from genetic disease to cancer biomarkers." Oncology reviews 10.2 (2016).

Salus, Griffin J., Marija Strojanova, and Christopher M. Heaphy. "Lamin A/C Downregulation Alters Prostate Cancer Cellular Phenotypes." The FASEB Journal 36 (2022).

Samur, Mehmet Kemal, et al. "Genome-wide somatic alterations in multiple myeloma reveal a superior outcome group." Journal of Clinical Oncology 38.27 (2020): 3107.

Sanborn, Adrian, et al. "Chromatin Extrusion Explains Key Features of Loop and Domain Formation in Wild-type and Engineered Genomes." The FASEB Journal 30 (2016): 588-1.

San-Miguel, Jesús F., et al. "Panobinostat plus bortezomib and dexamethasone versus placebo plus bortezomib and dexamethasone in patients with relapsed or relapsed and refractory multiple myeloma: a multicentre, randomised, double-blind phase 3 trial." The lancet oncology 15.11 (2014): 1195-1206.

Sathitruangsak, Chirawadee, et al. "Distinct and shared three-dimensional chromosome organization patterns in lymphocytes, monoclonal gammopathy of undetermined significance and multiple myeloma." International Journal of Cancer 140.2 (2017): 400-410.

Sathitruangsak, Chirawadee, et al. "Quantitative superresolution microscopy reveals differences in nuclear DNA organization of multiple myeloma and monoclonal gammopathy of undetermined significance." Journal of Cellular Biochemistry 116.5 (2015): 704-710.

Schaefer, L. H., D. Schuster, and H. Herz. "Generalized approach for accelerated maximum likelihood based image restoration applied to three-dimensional fluorescence microscopy." Journal of microscopy 204.2 (2001): 99-107.

Schmidt, Timothy M., and Natalie S. Callander. "Progress in the management of smoldering multiple myeloma." Current hematologic malignancy reports 16.2 (2021): 172-182.

Schoenfelder, Stefan, et al. "The pluripotent regulatory circuitry connecting promoters to their long-range interacting elements." Genome research 25.4 (2015): 582-597.

Sehgal, Nitasha, et al. "Reorganization of the interchromosomal network during keratinocyte differentiation." Chromosoma 125.3 (2016): 389-403.

Seili-Bekafigo, Irena, et al. "Myeloma cell morphology and morphometry in correlation with clinical stages and survival." Diagnostic Cytopathology 41.11 (2013): 947-954.

Sewify, Eman M., et al. "Cyclin D1 amplification in multiple myeloma is associated with multidrug resistance expression." Clinical Lymphoma Myeloma and Leukemia 14.3 (2014): 215-222.

Shaban, Haitham A., Roman Barth, and Kerstin Bystricky. "Formation of correlated chromatin domains at nanoscale dynamic resolution during transcription." Nucleic acids research 46.13 (2018): e77-e77.

Shah, Nina, et al. "B-cell maturation antigen (BCMA) in multiple myeloma: rationale for targeting and current therapeutic approaches." Leukemia 34.4 (2020): 985-1005.

Shaughnessy, John. "Amplification and overexpression of CKS1B at chromosome band 1q21 is associated with reduced levels of p27 Kip1 and an aggressive clinical course in multiple myeloma." Hematology 10.sup1 (2005): 117-126.

Shevelyov, Y. Y., and S. V. Ulianov. "Role of nuclear lamina in gene repression and maintenance of chromosome architecture in the nucleus." Biochemistry (Moscow) 83.4 (2018): 359-369.

Shevelyov, Yuri Y., and Sergey V. Ulianov. "The nuclear lamina as an organizer of chromosome architecture." Cells 8.2 (2019): 136.

Siegel, D. S., et al. "Vorinostat in combination with lenalidomide and dexamethasone in patients with relapsed or refractory multiple myeloma." Blood cancer journal 4.2 (2014): e182-e182.

Singh, Mayank, et al. "Lamin A/C depletion enhances DNA damage-induced stalled replication fork arrest." Molecular and cellular biology 33.6 (2013): 1210-1222.

Snyers, Luc, et al. "LEM4/ANKLE-2 deficiency impairs post-mitotic re-localization of BAF, LAP2α and LaminA to the nucleus, causes nuclear envelope instability in telophase and leads to hyperploidy in HeLa cells." European Journal of Cell Biology 97.1 (2018): 63-74.

Soler-Vila, Paula, et al. "Hierarchical chromatin organization detected by TADpole." Nucleic acids research 48.7 (2020): e39-e39.

Solovei, Irina, et al. "LBR and lamin A/C sequentially tether peripheral heterochromatin and inversely regulate differentiation." Cell 152.3 (2013): 584-598.

Soma, Emi, et al. "Successful Incorporation of Exosome-Capturing Antibody-siRNA Complexes into Multiple Myeloma Cells and Suppression of Targeted mRNA Transcripts." Cancers 14.3 (2022): 566.

Srivastava, Luv Kishore, et al. "Spatial distribution of lamin A/C determines nuclear stiffness and stress-mediated deformation." Journal of cell science 134.10 (2021): jcs248559.

Stewart, A. K., et al. "A practical guide to defining high-risk myeloma for clinical trials, patient counseling and choice of therapy." Leukemia 21.3 (2007): 529-534.

Sun, H.B.; Shen, J.; Yokota, H. Size-Dependent Positioning of Human Chromosomes in Interphase Nuclei. Biophys. J. 2000, 79,184–190.

Sun, Ning, et al. "Development of drug-inducible CRISPR-Cas9 systems for large-scale functional screening." BMC genomics 20.1 (2019): 1-15.

Sung, Hyuna, et al. "Global cancer statistics 2020: GLOBOCAN estimates of incidence and mortality worldwide for 36 cancers in 185 countries." CA: a cancer journal for clinicians 71.3 (2021): 209-249.

Sunkara, Krishna P., et al. "Functional relevance of SATB1 in immune regulation and tumorigenesis." Biomedicine & Pharmacotherapy 104 (2018): 87-93.

Suzuki, Kazuhito, Kaichi Nishiwaki, and Shingo Yano. "Treatment strategies considering micro-environment and clonal evolution in multiple myeloma." Cancers 13.2 (2021): 215.

Tai, Yu-Tzu, et al. "APRIL and BCMA promote human multiple myeloma growth and immunosuppression in the bone marrow microenvironment." Blood, The Journal of the American Society of Hematology 127.25 (2016): 3225-3236.

Talamo, Giampaolo, et al. "Beyond the CRAB symptoms: a study of presenting clinical manifestations of multiple myeloma." Clinical Lymphoma Myeloma and Leukemia 10.6 (2010): 464-468.

Tanabe, H., et al. "Inter-and intra-specific gene-density-correlated radial chromosome territory arrangements are conserved in Old World monkeys." Cytogenetic and genome research 108.1-3 (2005): 255-261.

Tanabe, Hideyuki, et al. "Non-random radial arrangements of interphase chromosome territories: evolutionary considerations and functional implications." Mutation Research/Fundamental and Molecular Mechanisms of Mutagenesis 504.1-2 (2002): 37-45.

Uddin, Fathema, Charles M. Rudin, and Triparna Sen. "CRISPR gene therapy: applications, limitations, and implications for the future." Frontiers in oncology 10 (2020): 1387.

Usmani, S.Z.; Lonial, S. Novel Drug Combinations for the Management of Relapsed/Refractory Multiple Myeloma. Clin. Lymphoma Myeloma Leukemia 2014, 14, S71–S77.

van de Donk, Niels WCJ, et al. "Clinical efficacy and management of monoclonal antibodies targeting CD38 and SLAMF7 in multiple myeloma." Blood, The Journal of the American Society of Hematology 127.6 (2016): 681-695.

van Sluis, Marjolein, et al. "NORs on human acrocentric chromosome p-arms are active by default and can associate with nucleoli independently of rDNA." Proceedings of the National Academy of Sciences 117.19 (2020): 10368-10377.

Vivante, Anat, et al. "Chromatin dynamics governed by a set of nuclear structural proteins." Genes, Chromosomes and Cancer 58.7 (2019): 437-451.

Vrábel, Dávid, Luděk Pour, and Sabina Ševčíková. "The impact of NF-κB signaling on pathogenesis and current treatment strategies in multiple myeloma." Blood reviews 34 (2019): 56-66.

Walker, Brian A., et al. "APOBEC family mutational signatures are associated with poor prognosis translocations in multiple myeloma." Nature communications 6.1 (2015): 1-11.

Wang, Audrey S., et al. "Tissue specific loss of A-type lamins in the gastrointestinal epithelium can enhance polyp size." Differentiation 89.1-2 (2015): 11-21.

Wegel, Eva, and Peter Shaw. "Gene activation and deactivation related changes in the three-dimensional structure of chromatin." Chromosoma 114.5 (2005): 331-337.

Williams, Ruth RE. "Transcription and the territory: the ins and outs of gene positioning." Trends in Genetics 19.6 (2003): 298-302.

Wong, Xianrong, et al. "Mapping the micro-proteome of the nuclear lamina and lamina-associated domains." Life science alliance 4.5 (2021).

Wood, Ashley M., et al. "TRF2 and lamin A/C interact to facilitate the functional organization of chromosome ends." Nature communications 5.1 (2014): 1-9.

Xie, Ying, et al. "Proteasome inhibitor induced SIRT1 deacetylates GLI2 to enhance hedgehog signaling activity and drug resistance in multiple myeloma." Oncogene 39.4 (2020): 922-934.

Xu, Hongxia, et al. "Exosome-transmitted PSMA3 and PSMA3-AS1 promote proteasome inhibitor resistance in multiple myeloma." Clinical Cancer Research 25.6 (2019): 1923-1935.

Yakovchuk, Peter, Ekaterina Protozanova, and Maxim D. Frank-Kamenetskii. "Base-stacking and base-pairing contributions into thermal stability of the DNA double helix." Nucleic acids research 34.2 (2006): 564-574.

Yee, Andrew J., and Noopur S. Raje. "Panobinostat and multiple myeloma in 2018." The oncologist 23.5 (2018): 516-517.

Yellapantula, Venkata, et al. "Correction: Comprehensive detection of recurring genomic abnormalities: a targeted sequencing approach for multiple myeloma." Blood cancer journal 10.1 (2020): 1-1.

Yu, Miao, et al. "SnapHiC: a computational pipeline to identify chromatin loops from single-cell Hi-C data." Nature methods 18.9 (2021): 1056-1059.

Zagouri, Flora, et al. "Hypercalcemia remains an adverse prognostic factor for newly diagnosed multiple myeloma patients in the era of novel antimyeloma therapies." European journal of haematology 99.5 (2017): 409-414.

Zangari, Maurizio, et al. "Response to bortezomib and activation of osteoblasts in multiple myeloma." Clinical Lymphoma and Myeloma 7.2 (2006): 109-114.

Zhang, Xiao-Hui, et al. "Off-target effects in CRISPR/Cas9-mediated genome engineering." Molecular Therapy-Nucleic Acids 4 (2015): e264.

Zhang, Xiaomei, and Yonggang Lv. "Suspension state increases reattachment of breast cancer cells by up-regulating lamin A/C." Biochimica et Biophysica Acta (BBA)-Molecular Cell Research 1864.12 (2017): 2272-2282.

Zhu, Xiaoli, et al. "Extramedullary plasmacytoma: long-term clinical outcomes in a single-center in China and literature review." Ear, Nose & Throat Journal 100.4 (2021): 227-232.

Zhu, Yuan Xiao, et al. "Identification of cereblon-binding proteins and relationship with response and survival after IMiDs in multiple myeloma." Blood, The Journal of the American Society of Hematology 124.4 (2014): 536-545.

Zinchenko, A.; Berezhnoy, N.V.; Chen, Q.; Nordenskiöld, L. Compaction of Single-Molecule Megabase-Long Chromatin under the Influence of Macromolecular Crowding. Biophys. J. 2018, 114, 2326–2335.